Recycling of Ti6Al4V swarf into Powder feedstock for Additive Manufacturing: Towards Achieving Sustainable Development Goals

A thesis submitted in the partial fullfilment of the requirement for the award of degree of

MASTER OF ENGINEERING

in

PRODUCTION ENGINEERING

THAPAR INSTITUTE

OF ENGINEERING & TECHNOLOGY

(Deemed to be University)

Submitted by

Sahil Dhiman

(801985007)

Under the Supervision of

Dr. Ravinder Singh Joshi
(Assistant Professor, Department of Mechanical Engineering)

Dr. Sachin Singh
(Assistant Professor, Department of Mechanical Engineering)

Dr. Vinod Kumar
(Associate Professor, Department of Mechanical Engineering)

MECHANICAL ENGINEERING DEPARTMENT

THAPAR INSTITUTE OF ENGINEERING & TECHNOLOGY, PATIALA (PUNJAB), INDIA

July, 2021

CANDIDATE'S DECLARATION

I, **Sahil Dhiman** hereby declares that the work presented in the thesis entitled **"Recycling of Ti6Al4V swarf into Powder feedstock for Additive Manufacturing: Towards Achieving Sustainable Development Goals"** in partial fulfilment of the requirements for the award of the degree of Master of Engineering and submitted to **Department of Mechanical Engineering, Thapar Institute of Engineering and Technology, Patiala** is an authentic record of the work carried out by me during a period from May 2020 to June 2021 under the supervision of **Dr. Ravinder Singh Joshi**, **Dr. Sachin Singh**, and **Dr. Vinod Kumar**.

The matter presented in this thesis has not been submitted by me for the award of any other degree of this or any other university/institute.

SAHIL DHIMAN

This is to certify that the above statement made by the candidate is correct to the best of my knowledge and the final viva-voce examination has been held on **19 July 2021**.

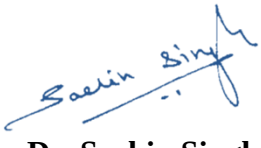

Dr. Ravinder Singh Joshi	**Dr. Vinod Kumar**	**Dr. Sachin Singh**
Assistant Professor *Department of Mechanical Engineering* *Thapar Institute of Engineering and Technology, Patiala* *(Punjab) India*	*Associate Professor* *Department of Mechanical Engineering* *Thapar Institute of Engineering and Technology, Patiala* *(Punjab) India*	*Assistant Professor* *Department of Mechanical Engineering* *Thapar Institute of Engineering and Technology, Patiala* *(Punjab) India*

Dedicated to all the people who left without saying goodbye to their loved ones and to all the families who have suffered loss due to the Covid-19 pandemic.

ACKNOWLEDGEMENT

The author takes this opportunity to express his deep sense of gratitude to his supervisors Dr. Ravinder Singh Joshi, Dr. Sachin Singh, and Dr. Vinod Kumar. They have been a great source of inspiration during the author's tenure at Thapar Institute of Engineering and Technology (TIET), Patiala. The author would have never completed this research work without their help. They generously provided the author with their time, resources, and valuable inputs. Without their timely monitoring of the author's research work and efforts to arrange facilities and equipment for the conduct of research work, it would have been impossible to complete this thesis in the present form. The author thank them for the confidence they had shown in his abilities, as well as, for granting autonomy to the author to pursue ideas become an independent researcher.

The author is highly thankful to Dr. Tarun Kumar Bera (Professor and Head, Department of Mechanical Engineering, TIET Patiala) for providing administrative infrastructure and access to equipments for the conduct of experimentation. The author is highly indebted to all the faculty members of the Department of Mechanical Engineering, TIET Patiala for their help and support.

Outside the TIET Patiala campus, the author gratefully acknowledges the support from Prof. Harpreet Singh (Professor, Indian Institute of Technology Ropar) for providing insights to the waste utilization concept. The author is grateful to Dr. Simranpreet Singh Gill (Associate Professor, Department of Mechanical Engineering, Beant College of Engineering and Technology, Gurdaspur) for helping in improving the quality of the manuscripts. He has been extremely supportive and ever-ready to extend his help to the author for any kind of work. The author is highly grateful to Dr. Malkeet Singh (Research Scholar, Indian Institute of Technology Ropar) for providing hands-on experience with various machines. The author feels great elation in expressing thanks to Dr. Sarabjeet Singh Sidhu (Associate Professor, Department of Mechanical Engineering, Sardar Beant Singh State University, Gurdaspur) for his constant support and motivation. The author is grateful to the following people for their support: Mr. Lalit Kumar (in charge, mechanical workshop, TIET, Patiala) for his guidance in the experimental work;

ACKNOWLEDGEMENT

Mr. Mohammed Bin Zacharia K (National Institute of Technology, Warangal) for his help with life cycle assessment; Dr. Mirzi Betasolo (Senior Lecturer, Department of Civil Engineering, Papua New Guinea University of Technology, Papua New Guinea) for her guidance to identify the non-technical barriers; Dr. Rakesh Kumar (Professor, Academy of Scientific and Innovative Research (AcSIR), CSIR-National Metallurgical Laboratory (Jamshedpur), India) for providing insights to the waste utilization using ball milling process; Willie Doaemo (Researcher, Department of Civil Engineering, Papua New Guinea University of Technology, Papua New Guinea) for help with the waste management concepts.

The author is highly obliged and thankful to his colleagues and very close friends, Mr. Sachin, Mr. Harshit Vij, and Mr. A Tank for their persistent advice, moral support, and valuable assistance during the entire research work.

The author would like to express his sense of sacrosanctity and gratitude for his beloved grandparents, mother Smt. Amita Dhiman and his father Sh. Madan Mohan Dhiman. The author is highly grateful to his sister Ms. Krishma Dhiman for her moral support during the course of this work. Above all, the author is highly indebted to Intelligence of Existence who blessed him with support, opportunities, and fortitude at every stage of this work.

The author is aware that the COVID-19 was declared a global pandemic before the start of the research work. During his stay at the campus, the author followed all the protocols as suggested by the TIET, Ministry of Health and Family Welfare -Government of India, and World Health Organization to stop the spread of the coronavirus.

Place: Thapar Institute of Engineering and Technology, Patiala

Date: 12 July 2021 **Sahil Dhiman**

ABSTRACT

The United Nations Development Programme (UNDP) listed responsible consumption and production as the 12th sustainable development goal. The efficient management of our shared natural resources and the way we dispose of toxic waste and pollutants are important targets to achieve this goal. Encouraging industries, businesses, and consumers to recycle and reduce waste is equally important as is supporting developing countries to move towards more sustainable patterns of consumption. One such waste originates from titanium (Ti) processing industries.

Ti alloys especially Ti6Al4V (Ti64) have a variety of applications in the avionics and biomedical industry by virtue of their unique properties like high strength, lightweight, extraordinary corrosion resistance, and the ability to withstand extreme temperatures. In the quest to obtain various shapes and sizes of Ti64 components, predominately subtractive machining is employed which produces a significant volume of machining scrap in the form of swarf. Ti alloys being high-value materials, there is an urgent need to develop sustainable technologies to recycle the swarf. The high surface-to-weight ratio in addition to the presence of coolant, dust, and tool impurities makes conventional recycling of swarf economically unviable.

The present study proposes multi-stage ball milling (BM) based sustainable technology to recycle Ti64 swarf into powder feedstock that can further be used as raw material for additive manufacturing (AM). Ti64 swarf was collected, cleaned, and ball-milled in an in-house designed and fabricated tumbler ball mill. In addition to bulk powder properties (flowability and spreadability) evaluation, the developed powder was characterised for particle size, morphology, hardness, and crystalline phases. Finally, the power was used as raw material for direct metal laser sintering (DMLS) to examine its suitability for AM.

It was found that the 25 mm diameter balls resulted in the largest powder particle size change followed by 12.5 mm and 6.25 mm diameter balls. Near-spherical morphology of Ti64 powder particles having the size of 40-200 µm was obtained after 18 h of BM. The flowability and the spreadability analyses of the powder proved its suitability for utilization in AM process. Experiment results show that proper melting of

the prepared powder takes place at 1000 mm/s scanning speed and 310 W laser power during the DMLS process.

The sustainability of the proposed process was analysed using a comparative life cycle assessment (LCA). It was found that the proposed method consumed less energy (~ 59 %), has low eco-cost (~ 82 %), and has less GWP (~ 68 %) as compared to the GA and thus, has the potential to produce powders with regulated characteristics from Ti64 swarf.

LIST OF PUBLICATIONS & AWARDS

Refereed Journals

1. **A Framework for Effective and Clean Conversion of Machining Waste into Metal Powder Feedstock for Additive Manufacturing**

   Sahil Dhiman, Ravinder Singh Joshi, Sachin Singh, Simranpreet Singh Gill, Harpreet Singh, Rakesh Kumar, Vinod Kumar
   Cleaner Engineering and Technology (Elsevier), ***(Online: https://bit.ly/3hjscwS)***

2. **Recycling of Ti6Al4V Machining Swarf into Additive Manufacturing Feedstock Powder to Realise Sustainable Recycling Goals**

   Sahil Dhiman, Ravinder Singh Joshi, Sachin Singh, Simranpreet Singh Gill, Harpreet Singh, Rakesh Kumar, Vinod Kumar
   Journal of Cleaner Production (Elsevier), (revision under review)

3. **Non-technical Barriers to the use of Recycled Metal Powders: A case of Ti6Al4V**

   Sahil Dhiman, Ravinder Singh Joshi, Sachin Singh, Simranpreet Singh Gill, Harpreet Singh, Rakesh Kumar, Vinod Kumar
   (in manuscript)

International conferences

4. **Solid-state Recycling of Ti6Al4V Swarf into Powder Feedstock for Additive Manufacturing**

   Sahil Dhiman, Simranpreet Singh Gill, Ravinder Singh Joshi, Sachin Singh, Harpreet Singh
   8th International and 29th National All India Manufacturing Technology, Design and Research Conference (AIMTDR), 09 - 11 Dec 2021

Awards

1. Received **Swachhta Saarthi Fellowship 2021** for the thesis project work by the *Office of the Principal Scientific Adviser to the Government of India* under the "**Waste to Wealth**" Mission.

CONTENTS

LIST OF TABLES

LIST OF FIGURES

CHAPTER 1

INTRODUCTION

1.1. BACKGROUND

To achieve the goal of sustainable manufacturing, the industries need to aim for processes that utilize less energy, emit fewer gases, and generate less waste in comparison to the conventional manufacturing techniques [1]. At the intermediate and importantly at the last stage of product life cycle, the waste should be managed using waste management hierarchy to bring sustainability to the entire process [2]. Metal cutting by conventional subtractive machining methods is an essential process throughout engineering design and manufacturing industries [3]. Conventional subtractive machining techniques are widely used to produce engineering components to meet the current technological demand [4]. The versatility of these machining processes has significantly increased efficiency and reduced production cost in recent times [5]. However, these manufacturing techniques apart from producing high-quality parts lead to the generation of scrap in the form of machining chips (MCs) [6]. The scrap generated during the product manufacture stage impacts the environment in several direct and indirect ways [7]. Widespread social awareness resulted in tighter legislation being introduced in order to minimize the ill effects of recycling of MCs [8]. One such obligation proposed is the recycling of MCs thereby converting them to reusable form. Relatively low production cost and ability to fulfil the needs of modern societies are some of the major advantages of MCs recycling [9].

In comparison to the new materials, recycled materials serve lower costs of processing right from the beginning of the product life cycle to the end product [10]. Therefore, conventional recycling of MCs thereby converting them to raw material in the form of billets with or without melting has become popular. Metal loss due to oxidation [11], increase in labour, and energy cost [12] are the major disadvantages associated with conventional recycling methods [13]. To overcome the shortcomings of conventional recycling methods like melting in the furnace [14] followed by casting [15], direct recycling methods of MCs have been recently explored [16]. Direct conversion methods (DCMs) implies the recycling modes that require less energy input compared to

conventional recycling methods [17]. The DCMs use MCs directly generated from the machining process. Based upon the process used, DCMs can be broadly categorized into four categories viz. melting, forging, extrusion, and the possible combination of these processes [18]. Specifically, DCMs include compression, spark plasma sintering [19], hot extrusion [20], friction-stir consolidation [21], equal channel angular pressing [22], cold pressing [23] and laser melting [24]. There are many advantages of DCMs of recycling MCs that include cost-saving, energy-saving, and environmental protection by reducing the emission of harmful gases [25]. However, problems such as poor surface topography and inferior mechanical characteristics (**Fig. 1.1)** of the parts fabricated with DCMs are inherited from the used raw material (MCs) [26]. The deformation in such components occurs through the weak interface present at the chips interface due to the improper binding of chips even at the high pressure and temperature [27]. In addition to this, the energy consumption during these processes is still considerable, which cannot be ignored. A high amount of energy is consumed to generate the required force for the direct conversion of large-sized chips into briquettes [28].

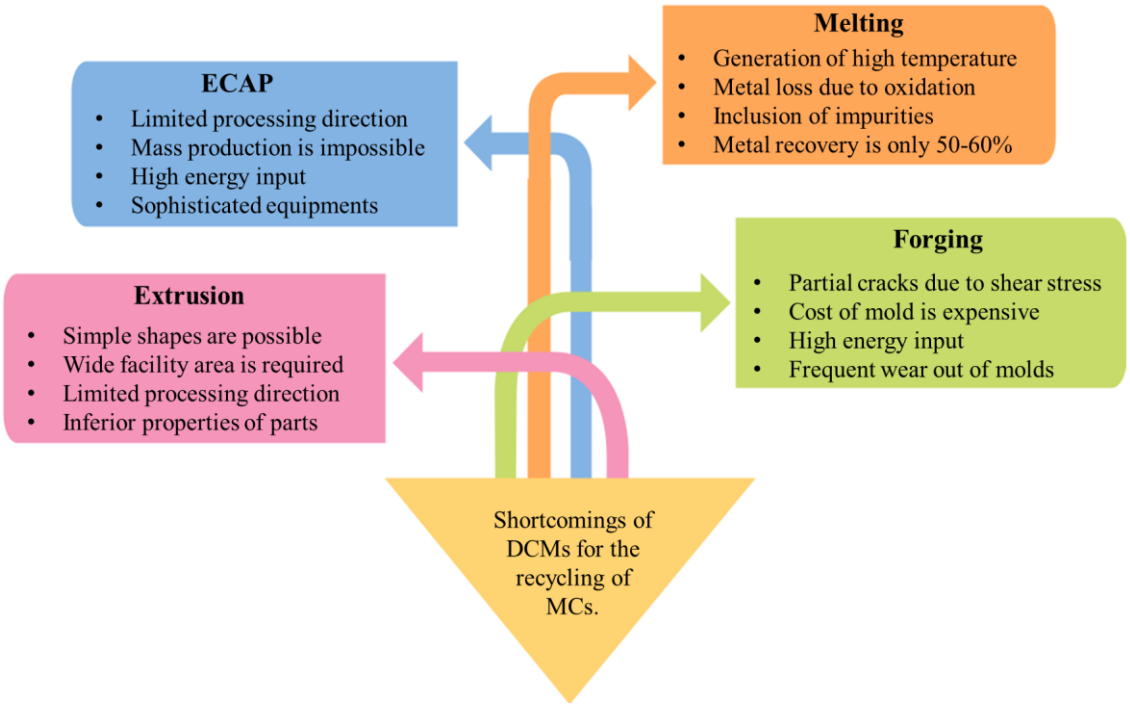

***Fig. 1.1** Shortcomings associated with the recycling of machining chips by direct conversion and conventional recycling methods*

Fig. 1.2 compares the performance of conventional melting of MCs and DCMs based on sustainability parameters. It is evident that the conventional melting of MCs is

not a good alternative. This is due to the high environmental impact related to the emission of harmful greenhouse gases, and metal oxides. These gases have the potential to affect the health of living beings and thus, conventional melting is not a viable solution to tackle MCs. On the other hand, DCMs convert MCs to briquettes that are easy to handle and post-process. Although materials like Al, Mg, and Cu can easily be processed by DCMs due to the consumption of less processing force, the materials like Ti and alloys, Ni and alloys, and other super alloys are difficult to process due to the high force requirement owing to the nature of the material. The high force usually breaks the die component of the system and hence is not a desired processing method for such materials. The blend of these limitations makes these methods of recycling MCs unsustainable. Hence, there is a need to develop either new technologies or innovative use of already existing technologies for sustainable and clean recycling of MCs.

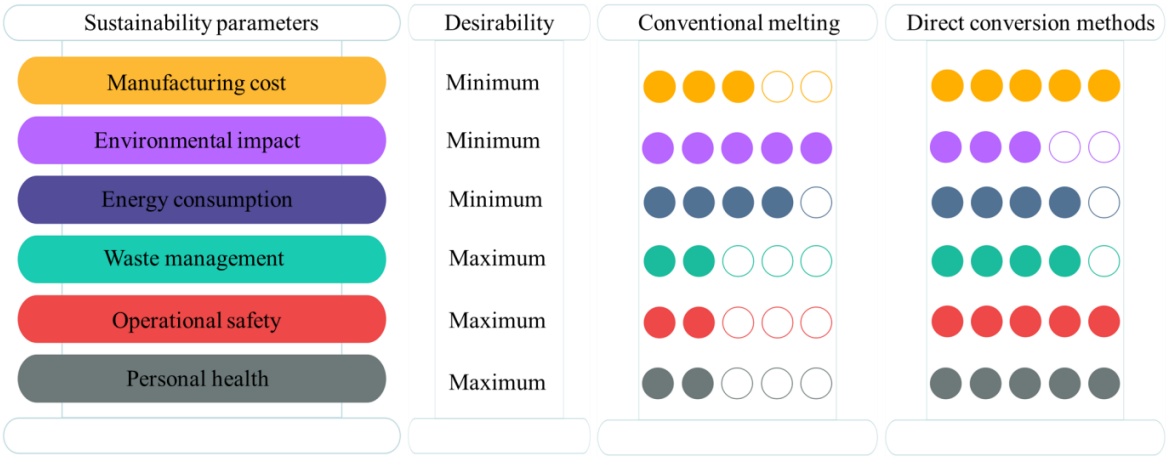

Fig. 1.2 *Performance comparison of machining chips recycling by conventional melting and direct conversion methods based on sustainability parameters.*

1.2. CURRENT SCENARIO OF MACHINING CHIPS RECYCLING

MCs have the potential to be converted into raw material for producing new engineering products. It is calculated that MCs constitute a large percentage (13.7% aluminium and 14.6% steel) of the waste generated from all the manufacturing processes globally [29]. On the other hand, if we compare the share of titanium (a difficult-to-machine material), it is estimated as 55% of the total input material gets converted into MCs (National data of US) [30] as evident from **Fig. 1.3**. By virtue of its low weight-to-strength ratio, titanium is widely used in the aviation sector. It generates a large amount of waste due to the complex geometry of components being made by employing various machining

processes. Recycling such materials has a significant impact on overall material cost. The circular economy emphasizes sustainable material usage that can only be achieved by reducing the formation of machining scrap.

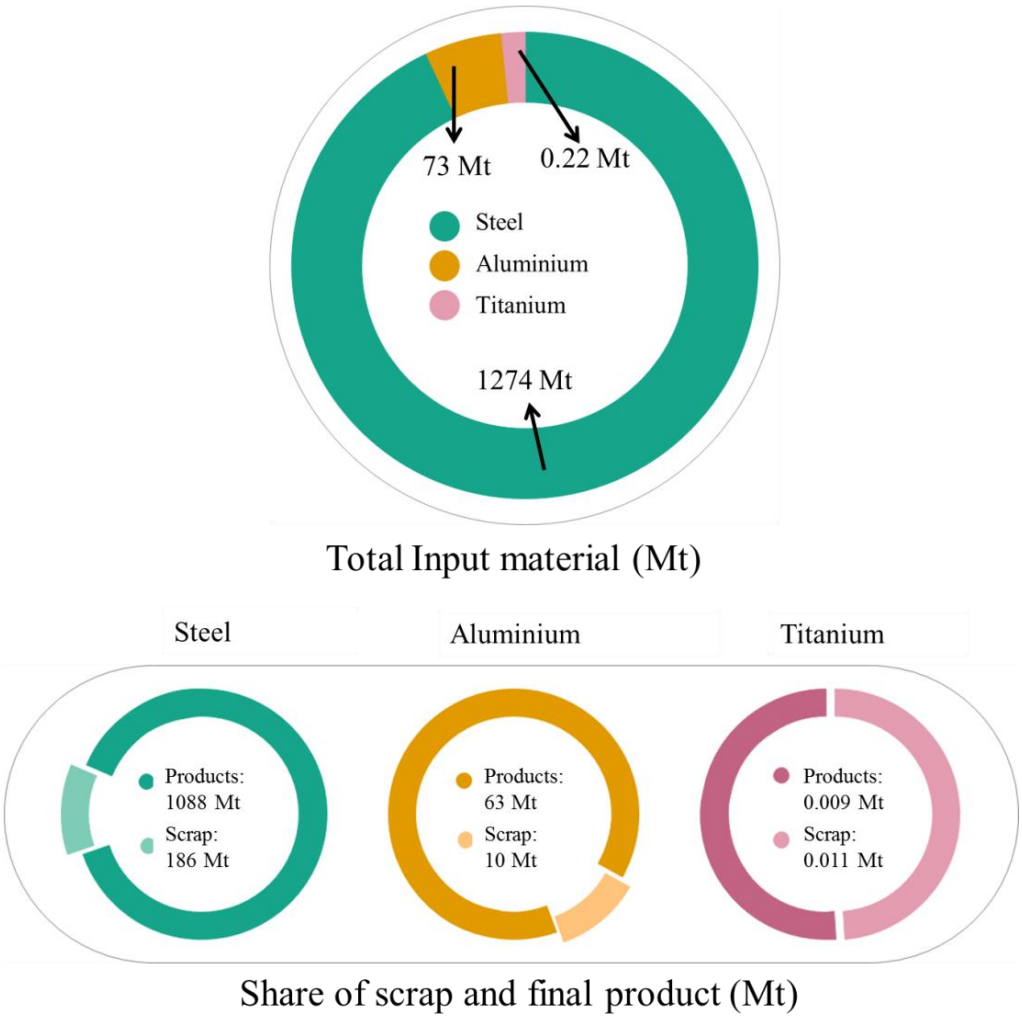

Fig. 1.3 *Machining scrap share of aluminium, steel, and titanium (Globally) {redrawn from [29]and [30]}.*

In the absence of any sustainable technology, presently majority of the industries recycling the MCs use DCMs. Due to the ongoing concerns over the environment, many companies are involved in MCs recycling and produce briquettes for further handling or processing. Usually, briquetting is a product of recycled MCs through DCMs. **Table 1.1** lists the major industrial players that recycle MCs by various DCMs. However, the briquettes do not have any direct end-use as such due to the high porosity and insufficient binding. Thus, post-processing or secondary melting is required [31]. These shortcomings limited the use of DCMs of recycling thereby generating the need for newer recycling technologies.

Table 1.1 *List of companies involved in recycling machining chips using direct conversion methods.*

S.No.	Company	Recycling material	Output (kg/hr)	Type of process	Briquette size (mm)	Ref.
1	RUF Briquetting systems	Al, SS, Cu, Bronze, Brass	50-5,000	Forging	60x40 – 150x120; Ø60-150	[32]
2	PPALLMANN industries	Al, Cu, Mg	150-1,280	Extrusion	L210; Ø60	[33]
3	WEIMA	Al, SS	50-300	Extrusion	70x70-150x60; Ø50	[34]
4	WEIMA	Al, SS, Cu, Brass	400-6,000	Forging	150x60-340x340	[34]
5	NEDERMAN	Al, SS, CI	100-800	Forging	L110; Ø60-80	[35]
6	STANSZ	Al, SS	85-1375	Forging	Ø65-225	[36]
7	SIMOLIN WATER & ENERGY LTD	Al, SS, Cu, Brass	300-5,000	Forging	Ø70-220	[37]
8	CO.MA.FER MACCHINE	Al, SS, CI, Cu, Brass, Bronze, Mg	50-2,000	Forging	Ø60-110	[38]
9	METSO	Al, SS, CI, Cu, Brass, Bronze	Up to 9,600	Forging	60x210-90x195;Ø140-210	[39]
10	EMI Inc.	Al, SS, CI, Cu, Brass	1,500-5,000	Forging	Ø100-170	[40]
11	ARS	Al, SS, CI, Cu, Brass	34-1,450	Forging	70x76-90x90	[41]
12	JOHN HARTAdvanced Manufacturing Technologies	Al, SS, CI, Cu, Brass, Ni alloy	45-230	Forging	63x40-72x40	[42]
13	PRAB	Al, SS, CI, Cu, Brass	57-2,268	Forging	Ø50-130	[43]
14	POSSTECH	Al, CI	200-550	Forging	Ø100	[44]
15	ANYANG	Al, CI, Brass	600-8,500	Forging	60x110-200x250; Ø90-220	[45]
16	AMADA	Al, SS, CI, Cu	60-120	Forging	Ø70-80	[46]

In recent times, there have been great efforts to develop an effective, versatile, efficient, reliable, and environmental-friendly 'Cleaner Recycling Technology' for the

recycling of MCs. One such alternate way-out is possible by converting the MCs into feedstock powder instead of briquettes. Thus produced feedstock powder can be used as raw material for the manufacturing variety of products by additive manufacturing (AM) and powder metallurgy (PM) technologies. In a recent study by [9], the recycling of MCs as feedstock material in AM was carried out by means of energy-intensive melting and solidification process techniques known as additive friction stir deposition (AFS-D). The results showed the potential to recycle MCs by feeding them directly into the AFS-D process and generating structurally sound deposition that can be used for point-of-need production particularly in the austere environment where multi-step processing of MCs is not possible due to prevailing shop floor limitations. Similar efforts were made to design a continuous recycling process. In an effort by [47] the potential of friction stir extrusion was presented and discussed. It was demonstrated that MCs could be recycled to produce filler wire for AM process by using a designed direct chip-recycling device. However, these techniques are only in their early phases of development and are not commercially available. In addition, as already discussed, materials like Ni alloys, Ti alloys, and stainless steel are not possible to process owing to their high resistance to deformation. Hence, there is a need to develop newer recycling technologies specifically for hard-to-machine alloys

One of the most suitable cleaner recycling methods investigated by many researchers is the breakdown of larger-size MCs into smaller sizes in the form of powder [48]. Depending upon the size of the chip powder (CP), the CP can be used as a raw material in various PM and AM processes [49]. However, to produce high-quality CP comparable to feedstock powder produced by conventional powder production techniques (CPPTs) like plasma rotating electrode process (PREP) [50], plasma atomization (PA), gas atomization (GA) [51], and other techniques like water atomization (WA) [52] is a challenging task. CPPTs include methods like PA and GA to produce near-spherical shaped powder as shown in **Fig. 1.4**. However, other methods like WA produce near-to-spherical morphology of powder. Thus, amongst the mentioned CPPTs, due to the controllable distribution of particle size and spherical morphology, the powder produced via GA is the most popular feedstock [53]. But it is imperative to mention here that the powder produced from the CPPTs needs a considerable amount of energy and hence increases the cost of the end product by several folds [54]. As a result, the CPPTs are economical only for mass production.

In addition to this, CPPTs are not feasible for powder production from a variety of alloys that are not commonly used due to the economic point of view of the processes. To overcome these shortcomings, ball milling (BM) has recently been explored as a viable solution for powder production from MCs. BM is a traditional powder-processing technique primarily used for reducing particle sizes [55]. During BM, the collusive impact interaction of balls with powder particles and walls of the closed container generates localized high pressure to reduce the particle size due to the mechanical impacts of the balls [56].

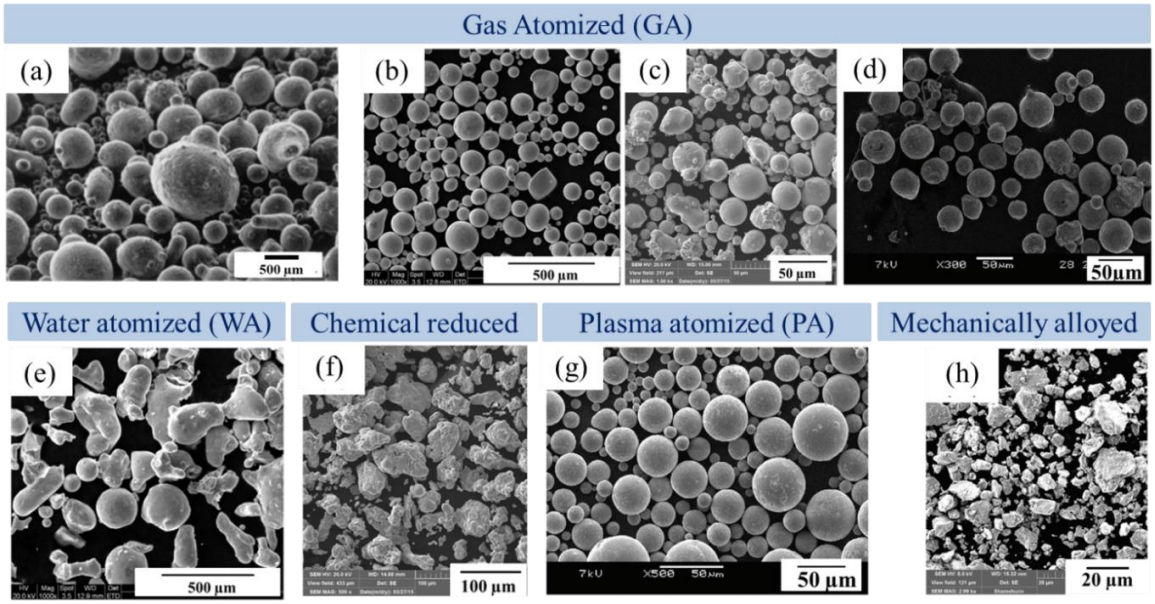

Fig. 1.4 *Morphology of powder used in metal-additive manufacturing obtained from different conventional powder production techniques. {(a) Ti–47Al–3Cr* [57]*; (b) 316L stainless steel* [58]*;(c) 316L stainless steel* [58]*; (d) inconel-718* [59]*; (e) Fe* [59]*; (f) Ti6Al4V* [59]*; (g) Ti–6Al–4V* [59]*; (h) Fe–18Cr–8Ni–12Mn–N* [59]*}.*

Absence of issues as mentioned for other conventional and DCMs, BM can be explored as a sustainable alternative for recycling of MCs [60]. Thus, this work presents a systematic review to suggest an alternate powder production technique focused on the recycling of MCs by BM. Firstly, the morphology of MCs best suitable for recycling is reviewed. Thereafter, the effect of BM parameters on the morphological, mechanical, and physical properties of the CP is evaluated. In addition, a comparison of the CP obtained by recycling of MCs is performed with commercially available powder produced by CPPTs.

1.4. ISSUES WITH CONVENTIONAL RECYCLING OF Ti6Al4V SWARF

Ti alloys are typically used in several applications ranging from avionics to biomedical owing to its exceptional properties such as high corrosion resistance, impact toughness, formability, weldability, and biocompatibility [61]. Ti is extracted through Kroll's process and the complexity of the process owes its high cost [62]. Moreover, machining of Ti alloys is comparatively difficult and results in generation of a considerable amount of waste in the form of swarf, turnings, hard waste, and agglomerated powder waste (**Fig. 1.5**). It is estimated that 55% of the total Ti alloy input material gets converted into machining waste (national data of US) [30] (**Fig. 1.5)**. Ti alloys being high-value materials, there is an urgent need to develop technologies to recycle this waste.

Conventionally, the swarf (size < 1000 mm) is recycled by going through various processes: crushing, centrifuge (oil recovery), thermal degreasing, melting in furnaces, and casting into ingots [30]. Amongst these, the most important process is melting, which is not a sustainable route owing to many limitations such as the use of water-cooled copper crucibles, use of energy-intensive vacuum arc melting furnaces, the requirement of vacuum, or/and inert environment [63]. Also, to achieve homogeneity of the recycled material, this process is only able to melt a small volume of the swarf otherwise multiple melting steps are required. It has been reported that metal recycling via such routes consumes > 6000 litres of water per metric ton of output [64]. On melting, swarf emits metallurgical smoke due to oxidation of impurities and some fraction of base metal [65]. Having a high value of global warming potential (GWP), this smoke is very harmful to the environment. All these issues collectively contribute to a permanent metal loss of 15-25 % which leads to the unsustainability of the entire process [66].

Few studies have been conducted with the aim to realize sustainable recycling of Ti64 swarf. [67] characterized the powder produced from Ti64 swarf using hydrogenation-dehydrogenation (HDH) process and utilized the same using cold spray technology. Likewise, [68] recycled the coarse Ti64 MCs into fine powder for PM via BM. Majority of the work explored the HDH process to recycle Ti64 MCs into powder using BM. But the HDH process itself is energy-intensive and it is hard to maintain specific temperature and pressure conditions during the process; also utilization of hydrogen in a controlled environment is itself a challenge [69].

The raw material for metal AM in the form of metal powder is generally produced using the GA technique [70]. In this process, the metal is made to melt at high temperatures using vacuum induction furnaces and atomized using a high jet of a pressurized (0.5 - 4 MPa) inert gas such as argon and nitrogen [71]. The price of consumables such as liquid nitrogen used to cool the melted powder, high purity raw material, and electricity is very high [72]. The raw material used in the GA process is freshly procured high purity billets of the concerned material [73]. This entire process is energy-intensive and only feasible for mass production [74]. Besides, the production of harmful metallurgical smoke during the melting of metal is not good for the onsite workers as well as the environment. Thus, GA process is not economical and environment friendly [51] and in turn, there is a requirement for the development of a clean powder production technique.

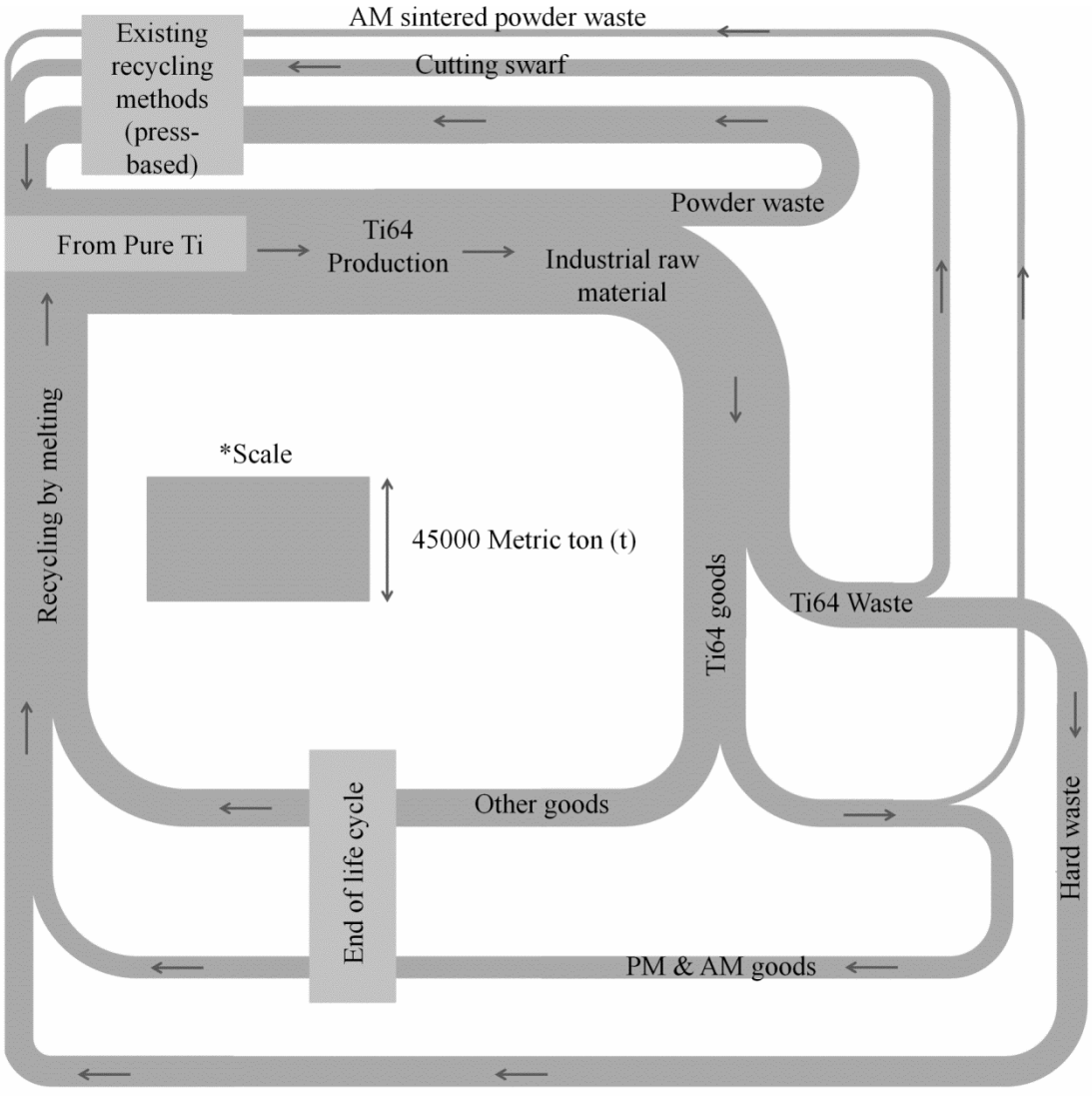

Fig. 1.5 *Ti6Al4V life cycle showing various recycling routes* [30].

1.5. BALL MILLING

BM is a process used to grind powders into fine particles and make a homogeneous mixture. This mixture of powder can be served as raw material for various metal-AM processes [75]. As an environment-friendly substitute for CPPTs, BM can be explored owing to its process competencies [76]. There are various forms of BM techniques depending upon the application but the basic principle is the same for all. It comprises a rotating (axially or radially) cylinder that is partially filled with balls made from hard materials like ceramic, stainless steel, or of the processing material (for high purity) as shown in **Fig. 1.6 (a)**. The cylinder is also partially filled with raw material that generally is non-homogeneous powder particles of larger size. The powder, which is trapped between the colliding surfaces (cylinder wall-ball contact surface, ball-ball contact surface) undergoes mechanical load under high strain rates. Due to this load, high mechanical stress is generated at the point of contact. The deformation induced by these stresses depends upon the intensity of the mechanical stresses and also on the morphology, arrangement, and properties of the particles (physical and chemical) [77]. Researchers classify the ball mills according to their mode of activity into two groups: direct and indirect. Rollers or mechanical shafts in the case of direct BM operate directly on the particles and transfer the kinetic energy. In the case of indirect BM, the kinetic energy is passed first to the body of the device, and then to the grinding media. They can be classified further into three types *viz*., tumbler ball mills [78], vibratory ball mills [79], and planetary mills [80] as shown in **Fig. 1.6 (a)** and explained below:

1. Tumbler mill: It consists of a circle, partly packed with revolving steel balls along its longitudinal axis [78]. The performance of the method in this sort of instrument depends primarily on the diameter of the device. Larger diameters generate higher fall height and therefore higher energy is transferred to the balls;
2. Vibratory mill: In the vibratory mill, the tank holding the steel balls and the grinding medium is shaken back and forth at strong vibration frequencies [81]. In this situation, the vibration strength and the density of the milling medium are significant considerations;
3. Planetary mill: In the planetary ball mill, the vessels are positioned on a spinning support disk in a planetary pump spinning on its axes [82]. Again, vessel size is an important parameter for process performance, since a higher distance allows higher kinetic energy and therefore produces stronger impacts [83];

4. Attritor mill: A shaft with arms or discs stir the media contributing to more effective use of energy in the BM process [84].

During the BM process, the thermal, shear, kinetic, and strain energy transforms powder particles by the change in their morphology and reduction in size via the solid-state deformation mechanism (by grinding the starting materials together). The impact force plays a significant role in powder refinement during the process [85]. The mechanism of refinement of ductile materials is followed by four stages as presented in **Fig. 1.6 (b)**.

1. Welding stage: The irregularly shaped powder particles get welded to themselves when they come in contact with each other under the high impact force of balls;
2. Squeezing stage: The morphology of welded powder particles changes into a sheet that gets thinner as the process progresses;
3. Fracturing stage: On the further continuation of impacts, the particles get fragmented into even smaller size and reaches the desired size range for metal-AM;
4. Dynamic stable stage: Further fragmentation of particles and intermixing to obtain a stable size range [86].

The morphology, size, and composition of MCs can be altered to the desired characteristics of the powder by controlling the BM process parameters [87].

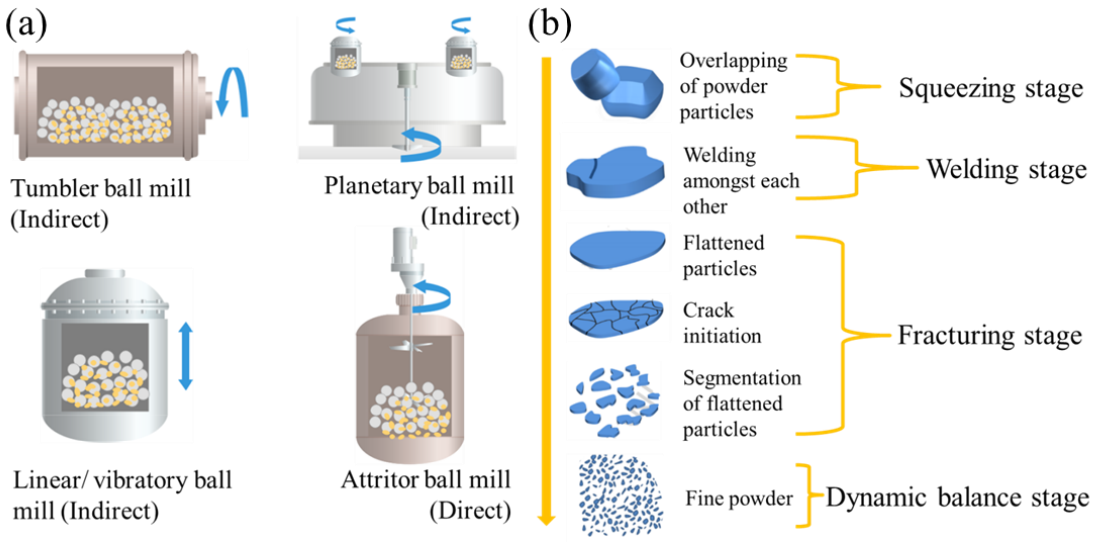

Fig. 1.6 *(a) Schematic of ball milling processes {redrawn from* [83]*}, (b) mechanism of powder particle size reduction in ball milling {redrawn from* [85] *and* [88] *}.*

CHAPTER 2

LITERATURE REVIEW

2.1. METHODOLOGY ADOPTED

A comprehensive literature review is performed to reveal the possibility of utilizing waste MCs by converting them into powder feedstock for metal-AM processes using BM. It is found that many authors performed studies related to BM of MCs but a comprehensive study on a larger scale still needs to be carried out. Thereafter, the process flow can also be proposed to provide an insight into the actual use of this technology on a large scale. The review process includes the following steps as depicted in **Fig. 2.1**.

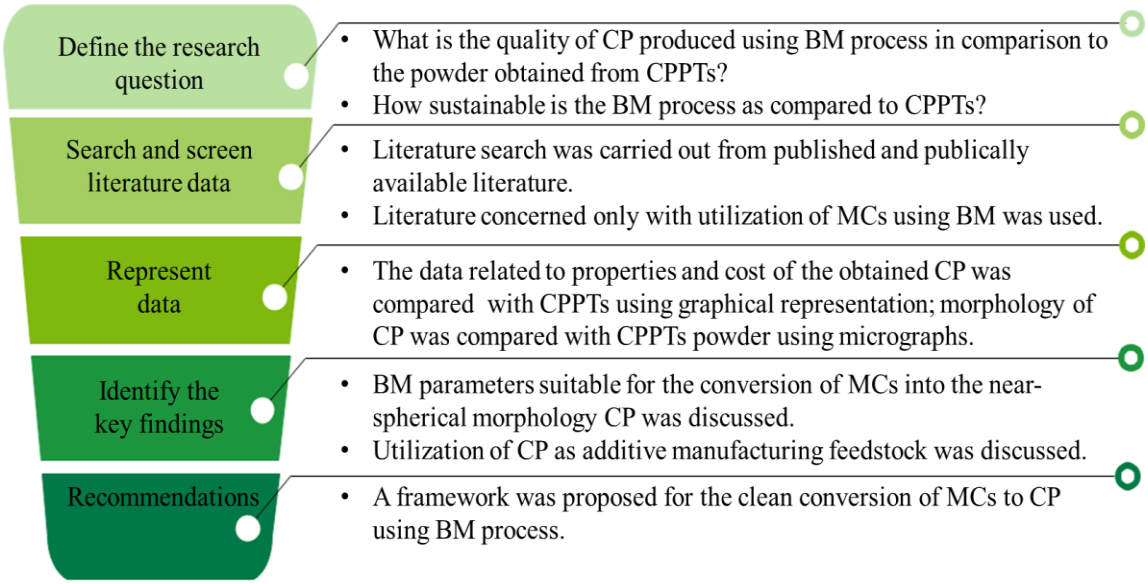

***Fig. 2.1** Methodology adopted for the literature review.*

The major part of the research is based on the quality assessment of produced CP using BM. Evaluation of produced powder is made on the economic aspects of the proposed process and compared with CPPTs. A literature search is carried out from published and publically available literature. Besides, data from relevant sources available on the internet is used for the powder cost comparison. The screening of the obtained literature is a major task to stay focused on answering the research questions. For the same, literature concerned only with the utilization of MCs using BM is used.

The data relating to the properties and morphology of the obtained CP of various materials is compared with powder obtained by GA (one of the most common CPPT) using graphical representation and micrographs. Further, the quality comparison of the obtained single track (single layer of powder deposited using laser/electron beam) using various AM technologies utilizing CP is presented. Finally, a framework based on BM technology is presented which suggests the plausible methodology for recycling MCs into CP from the generation stage to the final utilization stage.

2.2. SIZE AND MORPHOLOGY OF MACHINING CHIPS

The size and morphology of MCs derive the properties of the material mass obtained after the recycling process. Irrespective of the method of recycling used, it is always desirable to use the small and smooth MCs to make the recycling process sustainable by reducing energy consumption. But different machining processes end up producing a variety of sizes and shapes of MCs. Generated MCs have different morphology and sizes as per the manufacturing process, input parameters, and the type of tool used. Thus, it is imperative to investigate the types of process (machining) used to fabricate the components and hence the generation of MCs. **Fig. 2.2** shows the different types of MCs generated from various manufacturing processes. Conventional machining processes contribute hugely to MCs generation. These include turning [89], end-milling [20] drilling [90], stamping [91], grinding [92], and also non-conventional processes like laser cutting [93]. Primarily, the size and shape of the MCs are decided by machining parameters such as speed [94], feed rate [95], tool diameter [96], depth of cut [97], type of workpiece material [98], and machining environment or cutting fluid [99].

The MCs produced during grinding and laser cutting are appropriate for recycling without any pre-processing due to their smaller size. However, contamination of MCs with wheel impurities and high-temperature oxidation limited the use of these MCs for recycling purposes. Hence, the majority of the MCs that are available for recycling comes from other machining operations like turning, drilling, end-milling, and shaping. These processes generally produce comparatively large MCs that can be easily cleaned by washing and chemical treatments [100]. Consequently, there is a requirement for the breakdown of bigger-size MCs into smaller-size MCs so that they can effectively be used for recycling purposes. That is possible by either using some means to reduce the chip size during the machining process itself or post-machining. These provisions include:

1. Breakage of large-sized MCs into the smaller size during the machining processes by the use of chip breakers [101];
2. Using advanced manufacturing processes such as modulation-assisted machining which produces discrete MCs [102] in the size range from 1 mm to 50 µm (**Fig. 2.2**);
3. Mechanical shredding of already generated continuous large MCs [103].

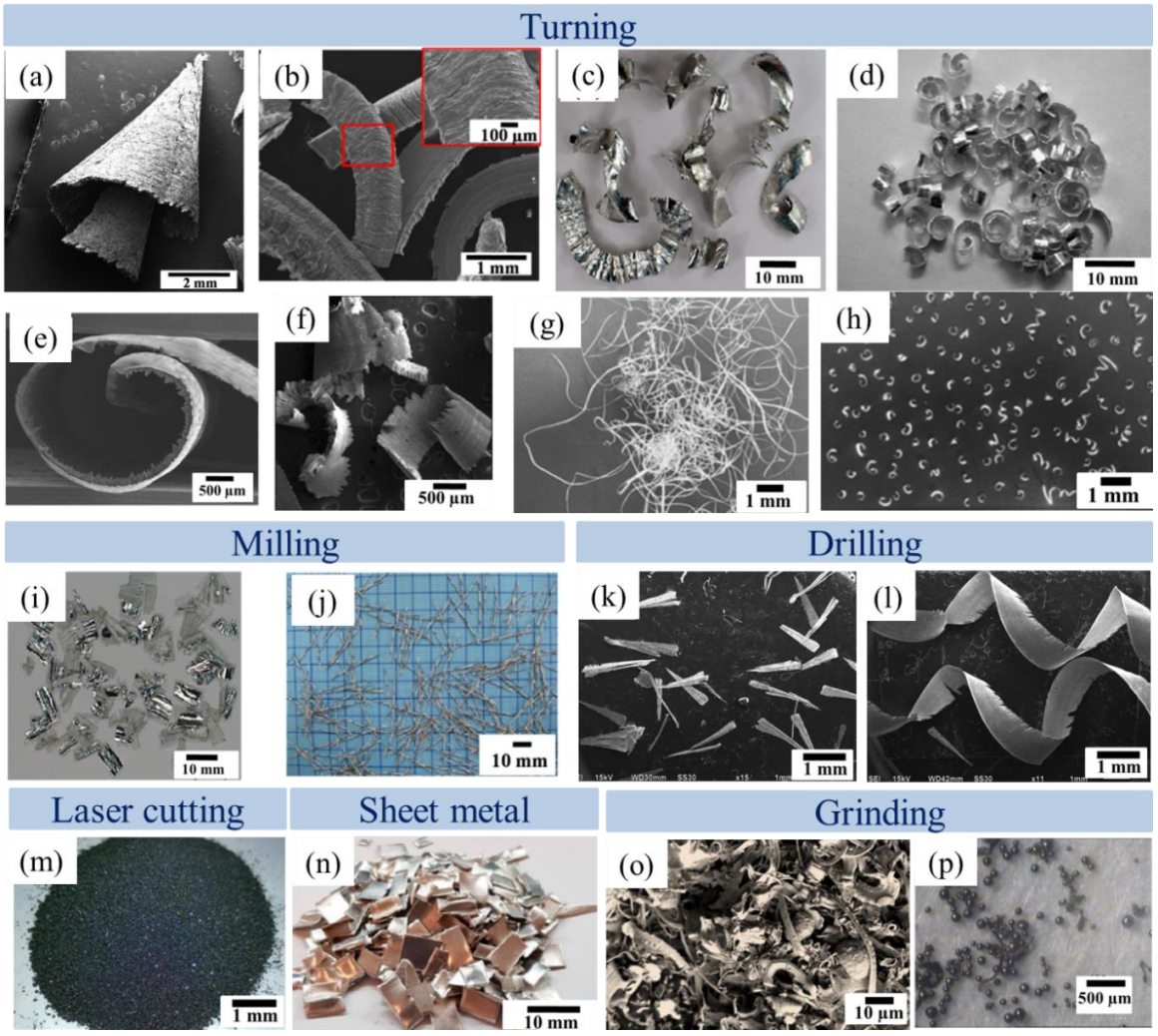

Fig. 2.2 *Type of machining chips generated during various manufacturing processes. {(a) grey cast iron* [104]*; (b) stainless steel* [105]*; (c) AA-6060 aluminium alloy [20]; (d) AZ31B magnesium alloy* [106]*; (e) Ti6Al4V* [107]*; (f) CuSn10 bronze* [108]*; (g) chips produced without chip breaker* [109]*; (h) aluminium chips produced with chips breaker on the turning tool* [109]*. (i) AA-6060 aluminium alloy [20]; (j) AC4CH aluminium alloy* [110]*; (k)stainless steel during modulation-assisted drilling* [90]*; (l) stainless steel during conventional drilling* [90]*;. (m) low carbon steel* [93]*; (n) AA1050 aluminium alloy [21]; (o)AISI 4340 steel* [111]*; (p) low alloy steel* [112]*}.*

In addition to the size of MCs, morphology plays an important role in deciding the effectiveness of recycling by reducing machine damage. Most of the machining

processes produce MCs of complex morphology with sharp irregular edges (**Fig. 2.3**). These cannot be processed directly for recycling as they can damage machinery in the subsequent stages due to their morphology and tangling behaviour [113]. Therefore, these MCs are subjected to mechanical shredding to reduce their size and making them relatively smooth. The morphology of the MCs before and after shredding by mechanical shredders can be observed in **Fig. 2.3**. It can be seen that the mechanical shredder breaks continuous MCs of various morphologies such as helical screw [114], long cylindrical screw [115], and short helix into discrete particles of irregular but homogeneous morphology. Horizontally or vertically mounted rotor-type shredders are commonly used for the size reduction of MCs [116]. Inside these shredders, the material is subject to complex stressing modes *viz.* tearing off of fragments, intense deformation, further deformation & compaction of the fragments, and compaction of the fragments until they have the homogeneous morphology [117]. Also, it is essential to mention that techniques like mechanical shredding increase the overall energy input to some extent, which is not desired [113]. But still, the total energy consumption is far less than that utilized in CPPTs like GA [118].

Thus, briefly, it can be said that the smaller the size of the MCs, easy and sustainable is recycling. Another aspect of machine damage can also be taken care of by the discrete nature of smaller MCs due to the homogeneousness of morphology.

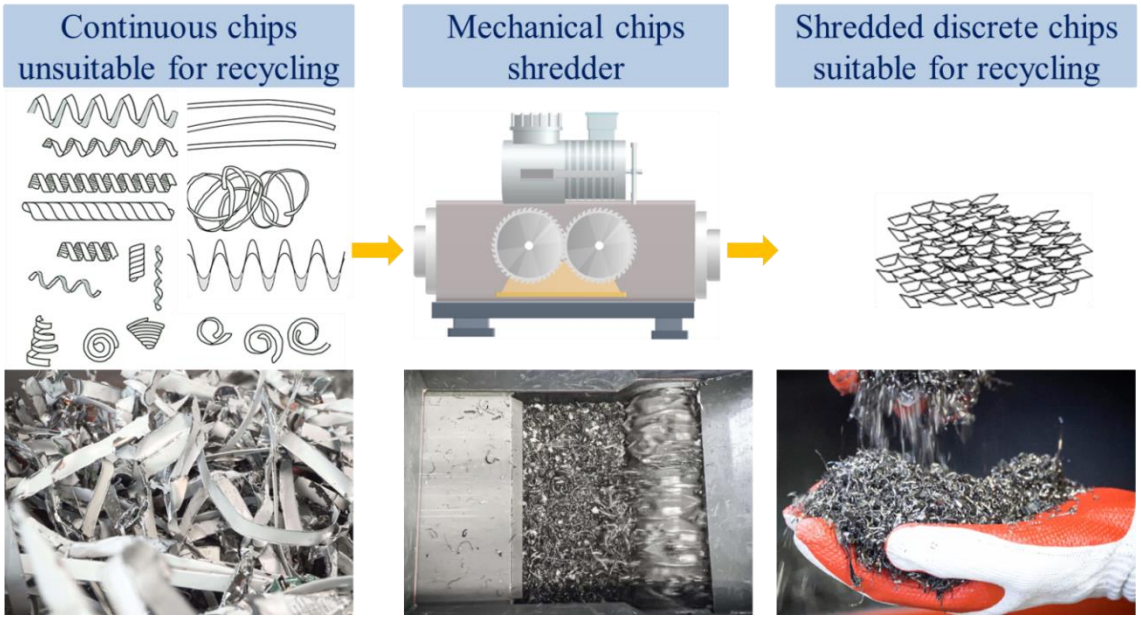

Fig. 2.3 *Chips shredder (roller type) and morphology of chips before and after mechanical shredding {redrawn from* [119]*}.*

2.3. BALL MILLING PARAMETERS

The effect of the BM parameters (listed in **Table 2.1**) on the obtained CP can be explained by studying the changes in intrinsic and extrinsic properties of the CP as the quality of the metal powder feedstock is generally assessed by these properties. Although the general effect of BM parameters on the quality of feedstock powder obtained is well explored and understood, the effects of some of the prominent BM parameters are still required to be explored. Intrinsic properties are mainly dependent on the structure and chemical composition of the material such as elemental composition [120], hardness [121], and microstructure [122]; on the other hand, extrinsic properties depends upon the structural defects or presence of avoidable chemical contaminants such as particle size distribution (PSD) [123], shape [124], and morphology of the powder [125]. In the actual environment, the metal powders are not 100% pure. Impurities of other metals are usually present. The overall chemical composition of powder ensures the quality of the part fabricated using AM. Thus, it is important to determine the same by various methods including micro, bulk, and surface analysis [126]. The hardness of a material depends on the material microstructure and is, therefore, a useful tool to examine the microstructural changes [127]. Due to the oxygen and moisture content, the intrinsic properties can be influenced and can reduce the mechanical properties of the part been fabricated [128]. The PSD of a powder is a list of values or a mathematical function that defines the relative amount, typically by mass, of particles present according to size [129]. Particle size and PSD have a significant effect on the behaviour of metal powders during their processing [130]. It is well accepted that the spherical morphology contributes to the required flowability due to the particle-particle friction [131]. Thus, spherical morphology is preferred due to enhanced flowability, easy layer spreading, and loose powder packing [132]. Hence, it is required to justify the quality of powder obtained from recycling MCs based on these properties.

As an environment-friendly substitute for CPPTs, the BM of MCs to produce powder feedstock is a promising method. Many authors explored the BM process and discussed the effects of various BM parameters on CP produced from MCs of different materials like stainless steel [49], aluminium [133], copper alloys [134], and titanium alloys [135]. The high-energy BM process was demonstrated as a sustainable way to reuse stainless steel MCs with the impurities of different materials (in this particular case- the addition of vanadium carbide (VC) for the development of a metal-carbide composite).

Table 2.1 *Important ball milling parameters that decide the final characteristics of the produced powder.*

S.No.	Parameter	Effect on powder characteristics	Ref.
1	Container material	It is an important factor as it defines the extent of the impact. A ductile material absorbs most of the impact energy and thus the residual impacts are not sufficient to change the morphology of particles.	[136]
2	Milling medium	The number of balls should be sufficiently high relative to the powder volume to have an acceptable effect on the powder.	[137]
3	Rotational speed	The rotational speed of the mill is an important factor. Higher the rotation speed, the higher is the energy transferred to the milling medium and hence powder. More precisely, with increased rotational speed, the effectiveness of the BM process increases.	[138]
4	Charge ratio	It is also called a ball to powder ratio (BPR). BPR estimates the powder transformation rate. Due to the increase in the number of successful impacts at higher BPR, the powder is easily processed.	[137]
5	Milling time	This parameter is important to accomplish a balanced stage between cold welding and the fracturing of particles.	[138]
6	Milling atmosphere	To prevent the powder from oxidation and contamination, milling is carried usually in argon, helium, or vacuum atmosphere depending on the reactivity of the powder being processed.	[139]
7	Vial filling volume	Around half of the vial, space is kept unfilled so that the balls can achieve adequate energy for the impacts.	[138]
8	Process control agents (PCA)	PCAs are organic compounds like stearic acid to control excessive cold welding.	[138]

Compared to the material without VC addition, the addition of VC to the BM process causes a more reduction in CP size. Moreover, the mathematical analysis revealed that the addition of VC as an impurity is the chief factor in the BM process followed by BPR, rotational speed, and milling time [140]. The morphology of powder is a significant factor in determining its quality. The shape and size of the particles produced at different milling times are presented in **Fig. 2.4**. It can also be perceived from **Fig. 2.4** that the morphology depends upon the milling time and the type of processing material. The BM of tungsten (W) powder revealed that with the BPR of 15:1, a high reduction in particle size was achieved in contrast to the BPR of 10:1 and 4:1 at a milling time of 60 h [88]. To assess the impact of ball size on CP particle size in BM, [105] conducted the experiments by varying ball diameters. The findings have shown that Ø20 mm balls bring down the particle size to micron range, while Ø6 mm balls efficiently alter the CP morphology to near-spherical.

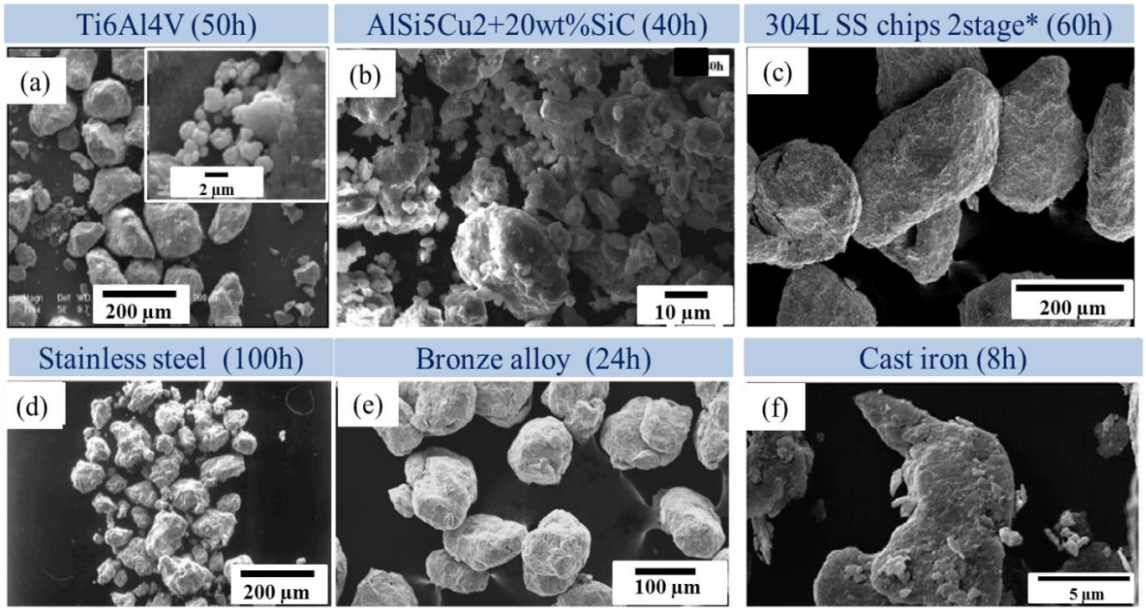

Fig. 2.4 *Scanning electron micrographs of chips powder of various materials produced at different milling times {(a)* [135]*, (b)* [133]*, (c) *2 stage ball milling first carried out with Ø 20 mm balls for 24hr and then Ø 6 mm balls for 36 h [49], (d)* [141]*, (e)* [142]*, (f)* [143]*}.*

Likewise, Hong et al. [144] conducted a study on CP production using BM and concluded that balls of large diameters are more effective for the conversion of aluminium foil MCs into the CP owing to the high impact energy associated with large diameters. It was also found that the intermediate stops (cause subsequent cooling) in the course of the BM process results in the production of finer powder as compared to the nonstop BM for 25 h. In their study, Canakci et al. [145] found that the average CP particle size of the AA7075 MCs decreased to 30 µm -100 µm after 10 h of BM. Results also showed that the critical milling time of 5 h is sufficient to modify irregular chip morphology (average size of 10 mm) into near-spherical powder morphology. After 10 h of BM, the particles of processed CP were about 286 times smaller than the initial MCs. Afshari et al. [146] used jet milling (JM) to produce tin-bronze (90% Cu and 10% Sn) CP from MCs. Investigations revealed that the pre-existing cracks on the MCs that were produced during the machining operation act as crack initiation sites during the fragmentation in JM. Besides, the propagation of cracks is hugely influenced by the existence of the delta phase in the microstructure of the tin-bronze alloy. If broadly categorized, there are two sizes of MCs reported in the literature used for the powder conversion using BM: 900 µm – 200 µm (**Fig. 2.5 (a)**) and 2000 µm -1000 µm (**Fig. 2.5 (b)**). The size reduction of CP varies differently with different materials. It can be

observed from **Fig. 2.5 (a)** that for materials like aluminum, bronze, and copper, 90% of the size reduction occurred in the first 20 h of BM. But on the other hand, for materials like titanium and stainless steel, the same percentage of reduction occurred after the first 50 h of BM [147] (**Fig. 2.5 (b)**).

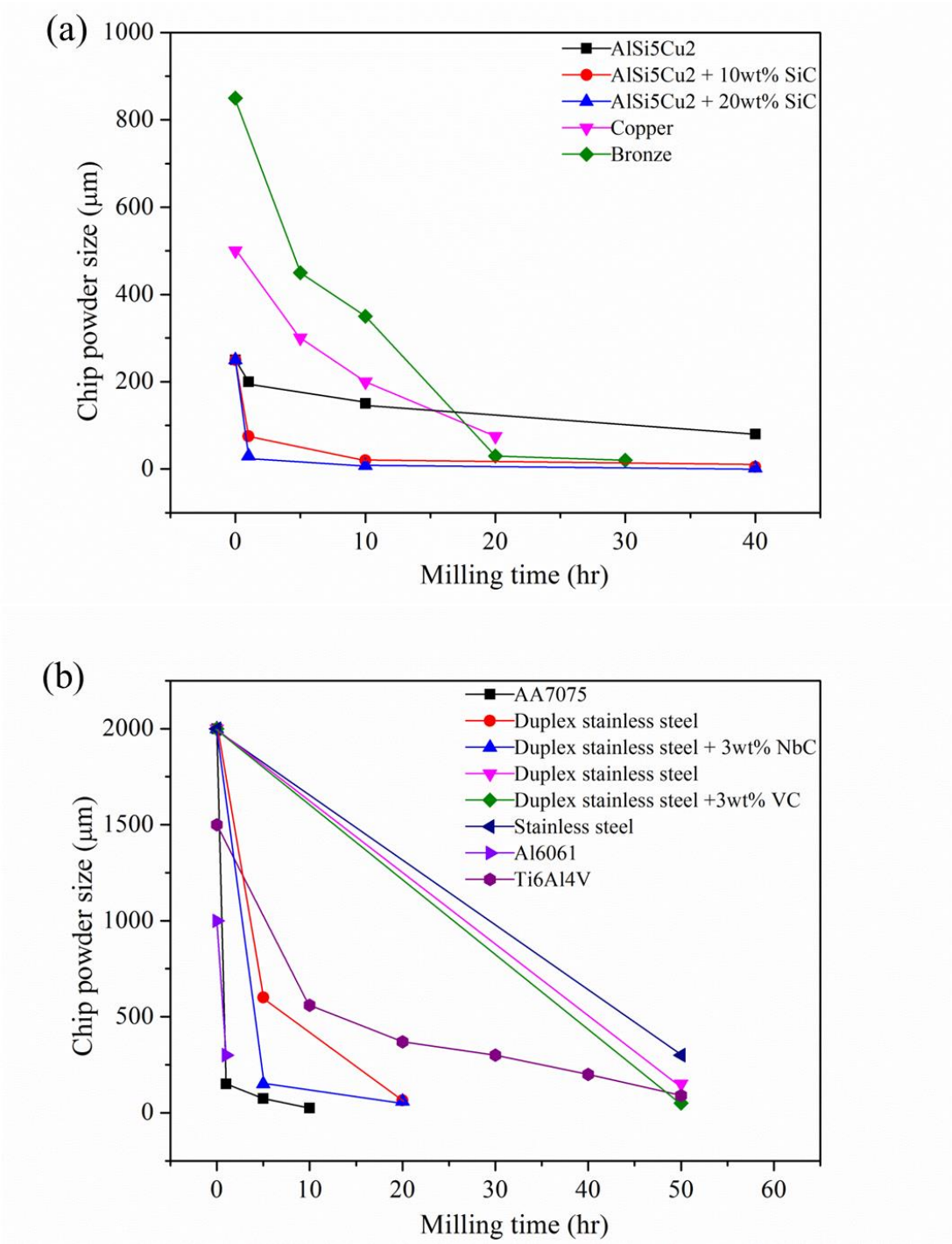

Fig. 2.5 *Effect of milling time on chip size of different materials, starting chip size- (a) 900 µm-200 µm, (b)2000 µm-1000 µm. {redrawn from: Aluminium alloys* [148], [145], *and* [133]*; Copper alloys* [142] *and* [134]*; Stainless steel* [149], [141], *and* [150]*; Titanium alloys* [135] *and* [151]*; for process parameters, refer* **Fig. 2.6***}.*

The effect of hardness of the CP particles is an important characteristic to predict the quality of the CP and the subsequent component made by it using AM. It was found that the hardness of the CP increases with the increase in milling time as can also be observed from **Fig. 2.6**. From **Fig. 2.6**, it can be perceived that the hardness of CP with the addition of impurities like SiC and Mg [133], increases rapidly during BM as compared to the pure CP (without any addition). BM of stainless steel (austenitic) MCs were explicitly studied and findings showed that BM resulted in martensite nanoscale phase formation in CP. Produced CP had a dual structure comprising of martensite and austenite phases with a value of microhardness twice that of the original MCs [141]. It can also be perceived from **Fig. 2.6** that post powder heat treatment reduces the overall hardness.

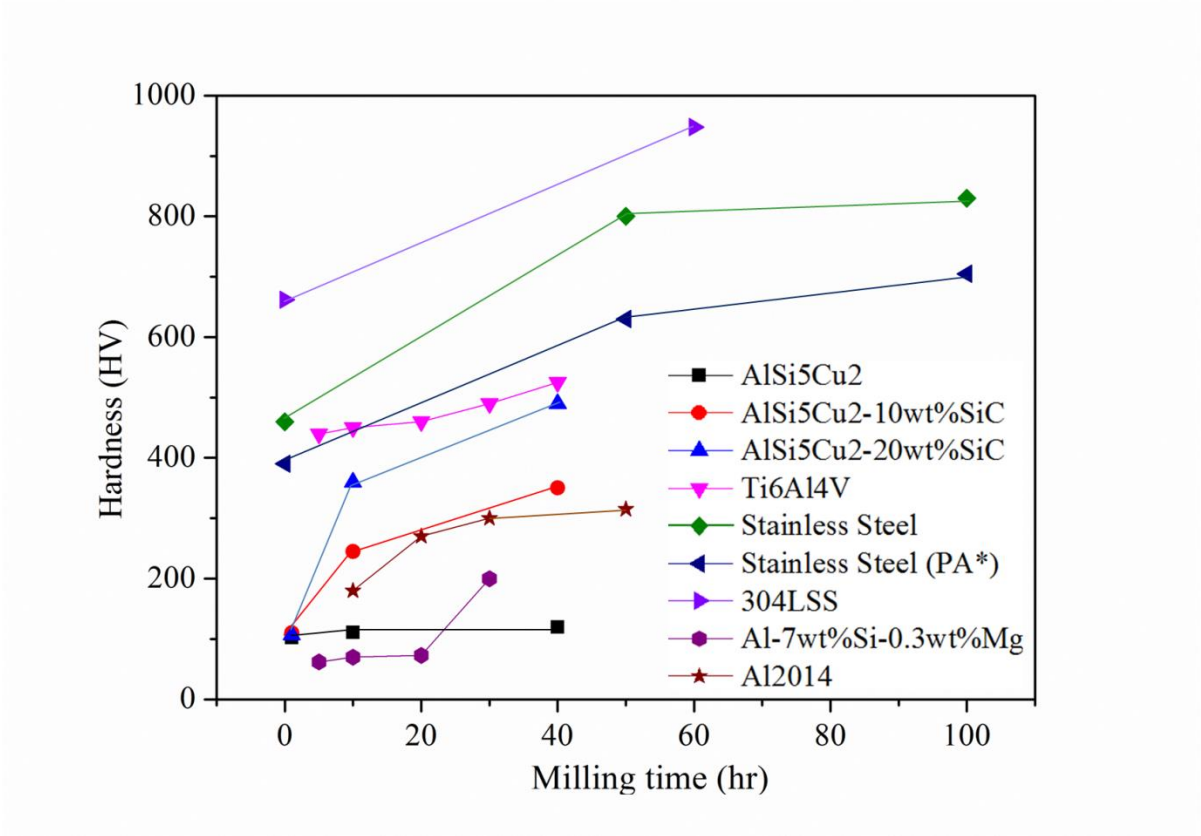

Fig. 2.6 *Effect of milling time on the hardness of chips powder of various materials.{redrawn from: At BPR-10:1; Ø 20 mm; rpm 200 for AlSiCu2* [133], *AlSiCu 2-10wt% SiC* [133], *AlSiCu 2-20wt% SiC* [133], *400 rpm for stainless Steel* [141], *stainless Steel PA** [141], *500 rpm for Ti6Al4V* [135], *304LSS [49]*, *Al-7wt%Si-0.3wt%Mg* [152], *Al2014* [153]*; all processes were carried in an argon atmosphere in planetary ball mill; * Post-treatment-Annealing for 1 h at 700 ºC}.*

Bulk properties such as flowability and spreadability [154] of metal powder are crucial to discuss due to their role in feedstock flow during electron beam melting (EBM) (powder is fed along with laser) and layer spread during selective laser melting (SLM) (single layer is melted) respectively [155]. Carney Funnel measurements of irregular Ti64 powder showed a decrease in the value of angle of repose by ~15 degrees after BM of 18 h [67]. This decrease is primarily due to the reduction of inter-particle friction during the flow of near-spherical particles [156]. Usually, in AM systems, the spherical powder is desired due to its enhanced bulk properties which assure the perfect flow or layer spread in comparison to non-spherical CP [157]. It has been reported that the irregular particles generate non-continuous melt pools keeping the same scanning parameters due to the uneven initial spread on the base plate. Because with the increase in particle size, the lesser powder particles were irradiated during laser scanning and the irradiance intensity distribution becomes inhomogeneous and hence results in improper melting [158].

Despite having many advantages, CP produced using BM has some drawbacks associated. Process inherited drawbacks such as contamination of metal powder due to the excessive wear of balls and cylinder; large milling time or less output limits its use at a small scale. Also, while processing several reactive metals like Ti and Al, the process should be optimised for a safe milling environment due to their high affinity towards oxygen and nitrogen [159]. Powder of such metals is highly reactive and can catch fire with sudden exposure to air leading to catastrophic damage. High energy BM can promote cold welding due to the ductile nature of such metals and alloys [77]. To avoid such issues, it is mandatory to use PCAs during BM. PCA such as heptane is usually preferred for Ti and its alloys due to the absence of oxygen in this chemical compound [160]. Many studies used cyclohexane which is more stable (closed ring structure) [161]. It is advisable to use organic PCAs in the presence of an inert atmosphere due to their flammable nature. Also, during BM of Fe and Ni-based alloys, a mixture of paraffin and stearin showed promising results by lowering the formation of respective oxides and cold welds between powders [162]. It can be observed from **Fig. 2.7** that with the milling time, the weight percentage of oxygen and nitrogen pickup has increased even with the use of different PCAs. However, this increased percentage is still near the standard value (0.22 wt% for oxygen and 0.06 wt% for nitrogen) [163]. Also, it can be observed that for

materials like stainless steel, the oxygen and nitrogen pickup is very less even after 60 h of BM without the use of any PCA [49].

The concentration of interstitial elements (mainly oxygen and nitrogen) regulates the final properties of the parts in AM. Once the powder is produced with a fixed concentration of interstitials, the next step is to control its percentage during the AM process. During an AM process, the powder interacts with a laser or electron beam, and the local temperature rises that melts the powder. This rise in temperature favours the formation of stable oxides. To maintain the balanced concentration of gases in the atmosphere, usually, the gas is vented out and the chamber is filled with selected gas such as argon. In a study by [164], argon gas was flushed during the SLM process and the desired oxygen content was obtained in parts produced. The differences in oxygen and nitrogen dissolution appeared to have little effect on the mechanical properties, which are already over passing that of conventionally processed stainless steel.

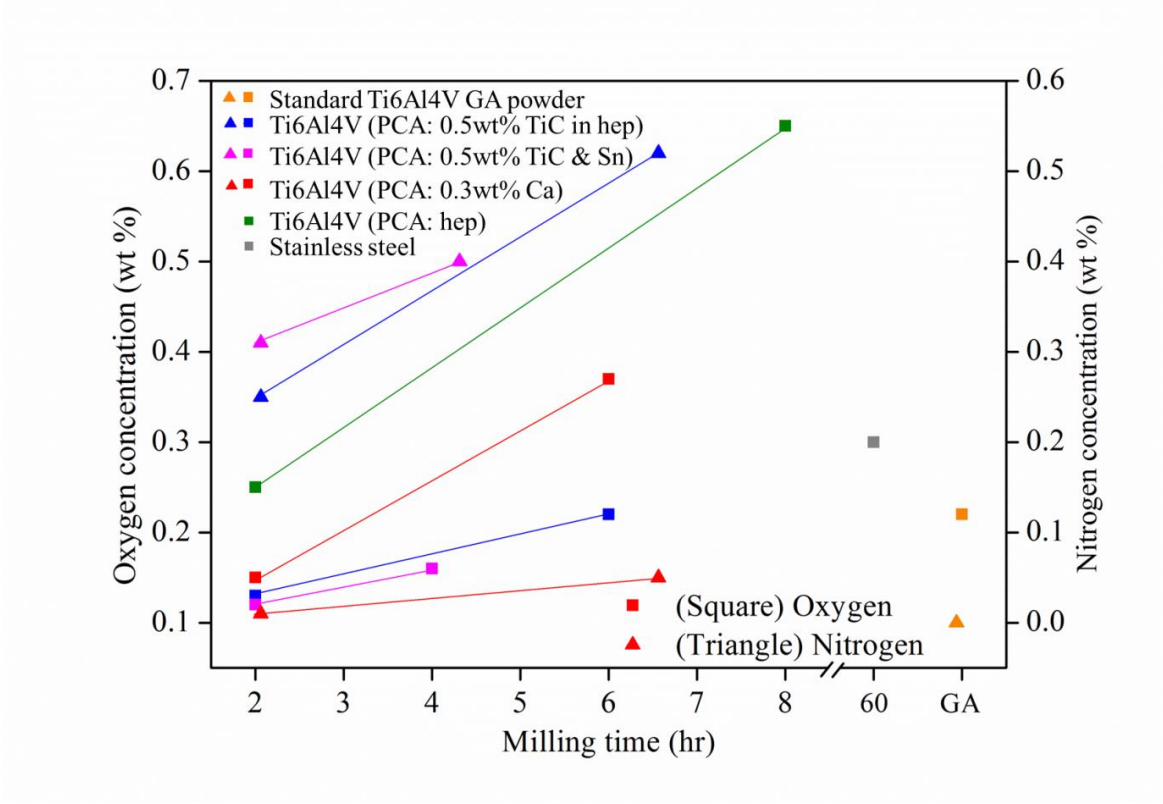

Fig. 2.7 *Effect of milling time on the oxygen and nitrogen pickup of different materials BM using process control agents, (a) Ti6Al4V (PCA: 0.5wt% TiC in heptane)* [165], *(b) Ti6AL4V (PCA: 0.5wt% TiC & Sn)* [165], *(c) Ti6AL4V (PCA: 0.3wt% Ca)* [166], *(d) Ti6AL4V (PCA: heptane)* [160], *(e) Stainless steel [49], Standard Ti6Al4V GA powder* [163].

BM as a powder production technique has shown a good capability of producing CP from the MCs with properties comparable to the powder produced from the CPPTs. To achieve this goal on a large scale towards the sustainable production of feedstock for metal-AM, many process parameters such as milling time, rotational speed, BPR, and ball diameter are needed to be regulated as per the requirement [167]. It was found from the literature that the ball diameter should be substantially larger than the largest size of the chip being BM. Also, the material of the ball should be tough enough to deform the MCs and not themselves due to the continuous impact action [168]. To avoid the contamination of media, the balls should be made of the same material being processed [169]. The spherical morphology of the powder particles is desirable for the proper flow and energy absorption during processing with PBF (powder bed fusion) AM processes. It was found that the BM carried out in different stages is a promising procedure for the production of near-spherical morphology of CP [49]. For converting stainless steel MCs (5 mm- 20 mm) into CP with a particle size of a few hundred microns, BM with Ø20 mm balls for 24 h was found effective. For the further reduction in the size of CP (40 µm-150 µm) and altering the morphology to near-spherical, BM with Ø6 mm for 36 h was found to be the best combination of parameters. This is attributable to the rise in the frequency of impacts arouse from the reduced diameter of the balls [49]. Due to the high deformation of the matrix during the making of CP composite, the presence of reinforcement particles makes the BM process fast [170]. The impacts are dissimilar due to the non-homogeneity of the milling material and hence results in higher deformation. Various authors to make a comparison with the BM technique also explored JM. It was found that the shape irregularity of JM powder was more in comparison to BM powder. The hardness enhancement in produced CP was found only 3% in the case of JM, while in the case of BM it reached 30%. Moreover, JM powder was free from oxides but the oxygen content in BM CP was found to be increased considerably [142]. However, JM is capable of particle size reduction in softer materials but to achieve a low range of particle size is still a challenging task; in this regard micro-BM under cold conditions can be a promising alternative [171].

Concisely it can be said that the ball diameter is a crucial parameter for the size reduction followed by BPR, rotational speed, and milling time. On the other hand,

morphology is regulated by milling time followed by ball diameter. However, the reduction in size and change in morphology is highly dependent on the type of material being processed. Thus, these parameters can be regulated as per the requirement and ensuring minimal BM time towards sustainable conversion. In addition, the selection of a suitable PCA is necessary to avoid the cold-welding (in the case of ductile metals) and interstitial elements pickup (in the case of reactive metals).

2.4. UTILIZATION OF BALL-MILLED CHIPS POWDER

Metal-AM allows the manufacturing of functional components layer-by-layer with high structural integrity at a low cost and is compatible with various materials, including biocompatible titanium alloys [158]. The range of particle sizes used in various AM techniques is different. For instance, for laser-based systems (direct metal laser sintering (DMLS), laser engineered net shaping (LENS), SLM), the suitable range is <60 µm and for electron beam-based systems, the suitable range is 50-150 µm [172]. BM produces powder in a wide range of sizes with varying milling parameters. For example, after 18h of BM of Ti64 MCs (starting from a chip of size ~600 µm), >60% of powder falls in the range 53-150 µm and only 10% of powder falls in the range 5-53 µm [173]. Thus, the total share of powder to be used in EBM systems is more, and hence, the applicability of CP is more. In this regard, single tracks of CP produced using BM were successfully deposited via LENS (**Fig. 2.8 (a)**) and it can be observed from **Fig. 2.8 (b, b1, c, c1)** that both the single tracks (using GA and BM powder) show consistency in melt pool for stainless steel [49]. In a similar study by [174], geometric characterization and surface morphology of SLM-fabricated single tracks of BM-produced tungsten powder were studied. It was revealed that the inhomogeneity of produced CP influences the Marangoni flow (transfer of mass across the interface between two fluids due to a surface tension gradient [174]) by causing the variability in the melt pool size (**Fig. 2.8 (f)**). Also, high powder absorption due to small particle sizes caused a more continuous and regular single-track [158]. In a comparative study by [131], it was found that the sphericity of the powder influence the product quality. Likewise, [175] used irregular powder in the range of 44-110 µm in the EBM system to fabricate bulk samples of Ti64. Large interconnected pores in the order of 200 µm were discovered near the top surface for the standard process conditions. During SLM, varying the powder size from D50=5.7 µm to D50=57.63, single tracks shows inhomogeneity at the same processing parameters

(**Fig. 2.8 (d, e)** [158]. In a study by [176], spherical Nb-37Ti-13Cr-2Al-1Si pre-alloyed powders were used to fabricate single tracks varying laser power (LP) and scanning speed (SS) via SLM. Continuous single tracks were achieved using an LP of 380 W and SS of 600 mm/s from different combinations of these parameters. For stainless steel (904L) powders with different particle sizes it was found that the most influencing parameter is the LP, and then, in order of decreasing importance, are the powder layer thickness, the SS, and, finally, the particle size [177]. On the other hand, the quality of the single tracks or fabricated part depends upon the energy density as it can be easily regulated for the combined effect of LP and SS, which are the two most important factors in most AM systems [178]. Hence, more optimization studies are a way for the high applicability of CP produced using BM.

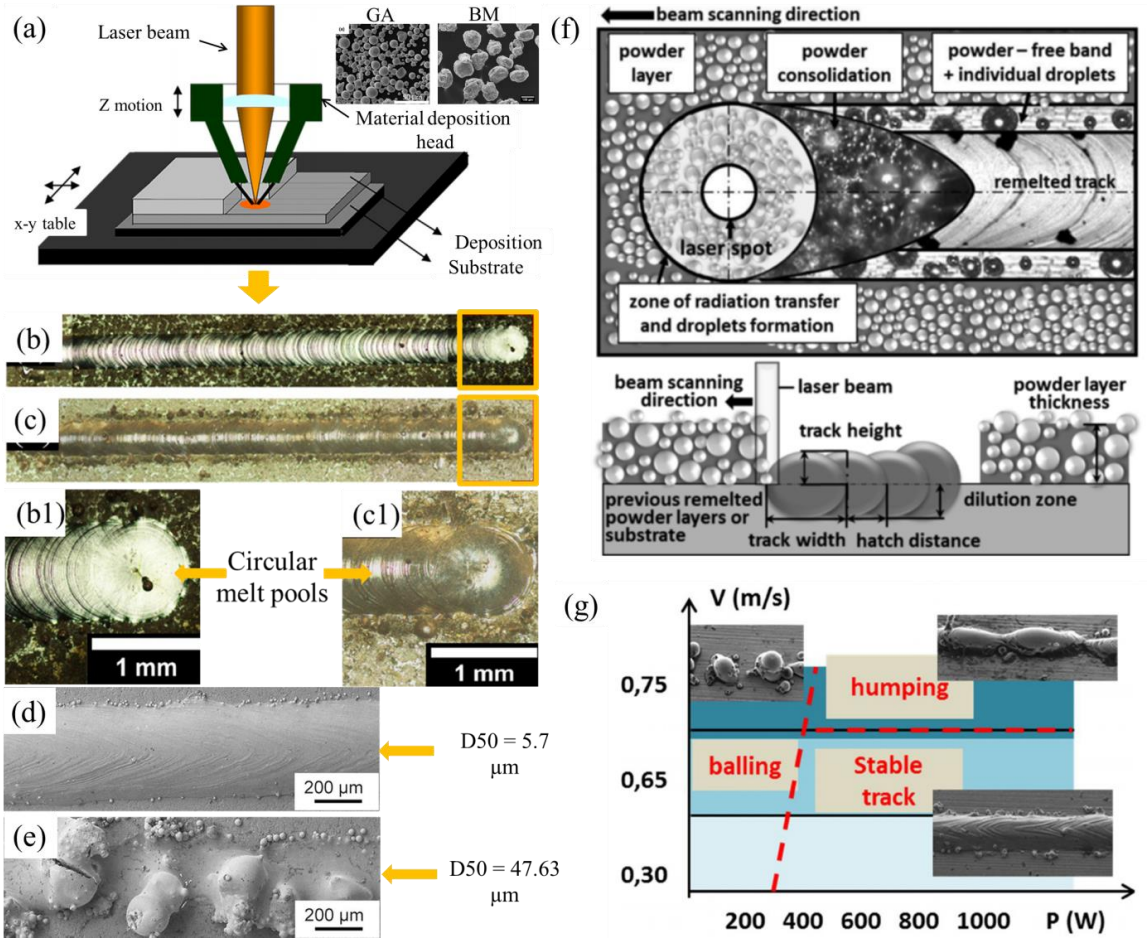

Fig. 2.8 *(a) Schematic of LENS process, (b,c) single tracks fabricated using LENS at a scanning speed of 1.7 cm/sec and laser power of 410 W using (b,b1) stainless steel gas atomised powder, (c,c1) stainless steel two-stage (Ø 20 mm balls for 24 h and then Ø 6 mm balls for 36 h) ball milled powder as feedstock [49], (d, e) single track of pure tungsten powder at laser power of 350 W and 200 mm/s at variable powder size* [158], *(f) Spatial scales of a single track and schematics of typical geometrical parameters*

during SLM process [179], *(g) variation of single track geometry of stainless steel varying laser power and scanning speed during SLM* [180].

From the existing studies, it can be briefed that to ensure the sound single tracks and full builds, the total energy density can be optimised by regulating the dominating parameters (SS and LP) against the size and morphology of CP particles (**Fig. 2.8 (g)**). As not much literature is available on the utilization of CP produced by BM in metal-AM, it is evident from the existing literature that its utilization is successful and can be implemented by ensuring the quality of CP against GA powder, which is considered as a standard reference being representative of CPPTs.

2.5. PROPERTIES OF THE PART FABRICATED USING CHIPS POWDER

The quality of the part fabricated by metal-AM is directly influenced by the characteristics of feedstock i.e., metal powder [181]. Disparities in feedstock characteristics can lead to uneven layer spread [182], inconsistent bulk density [183], increased defects [184], undesired mechanical properties [185], and poor surface finish [186]. In recent times, some investigators published their findings on the use of CP produced by BM of MCs. In a study by Mangour et al. [187], 316L–Ti–graphite mixed CP obtained using BM of MCs for 35-h were used as a feedstock in SLM. Fabricated single tracks showed refinement in microstructure owing to the addition of TiC as reinforcing particles. Amongst several parameters, applied total energy density was found to be decisive in determining the microstructure of the fabricated single tracks incorporating CP using SLM. Similarly, Costa et al. [188] investigated the recycling of grey cast iron MCs using BM and used it as an input raw material in the PM by the sintering process. The results revealed that for CP to reach a size range comparable to commercial powder feedstock can be achieved after 24 h of BM. Due to the irregular shape, the powder particles shows good connectivity under lower sintering pressures and are suitable for applications where internal porosity in the fabricated parts is required. Likewise, in a work by [105] single tracks were made from powders obtained by BM and GA separately via LENS using similar conditions. Single track using BM powder exhibits circular geometry and uniformity of melt pool, and uniform arrangement of consecutive melt pools, similar to the characteristics perceived in single tracks made using GA powder. The uniformity and geometry of the melt pool of the single tracks are significantly influenced by machining parameters and are important in determining the

properties of the fabricated part [189]. During both GA and BM powder use, the substrate surfaces were found to have a minimal difference in splatter and grain structure that defines the effectiveness of BM powder. Similarly, [104] prepared compacts from powder feedstock obtained by mixing commercial pure GA iron powder with BM iron powder. The compacts of the prepared powder were made and found to have suitable mechanical properties. [142] found that CP produced by JM is capable to produce sound compacts by PM technique. Moreover, it was revealed that on the increment in compaction pressure from 300 MPa to 700 MPa, sound compacts having a green density of 7-8 g/cm^3 can be produced.

Parts fabricated by BM-produced CP using AM and PM showed similar or even enhanced mechanical properties as fabricated by GA powder. This is due to the refinement of the microstructure during BM. Specifically, in AM, the sphericity of the powder can be compensated by regulating laser energy density to produce sound parts.

2.6. COST AND QUALITY ANALYSIS

Total mechanical energy spent in the BM process is utilized in various forms like sound energy, potential energy, thermal effects, electromagnetic effects, strain energy, chemical energy, structural rearrangement, amorphisation, and entropic contribution [190]. However, this total energy input in BM is significantly low in comparison to CPPTs due to the nature of the process, in which the material is melted to a temperature higher than its melting point. High purity inert gases like helium and argon are used to atomize the melted metal with the help of a high-pressure jet [73]. Also, the total cost associated with CPPTs comprises of cost of consumables (including energy), labour cost, and capital cost. But the yield can be ranged from 20-80% which is difficult to maintain and depends upon the scale of operation [74]. Thus, the cost comparison of the powder produced by both the CPPTs and BM techniques is important. It can be observed from **Table 2.2** that the cost of powder feedstock produced using CPPTs is quite high which is not economical for the manufacturing of products on a large scale [191]. Specifically for difficult-to-cut materials like titanium and Inconel, this cost is even higher owing to the high cost of the primary raw materials and high melting temperature.

Table 2.2 *Cost analysis of commercial gas atomized powder of various metals and alloys for metal-additive manufacturing.*

S.No.	Material	Cost of GA powder (US$ per Kg) [192]	GA cost inputs [193]
1	TiCP	350-600	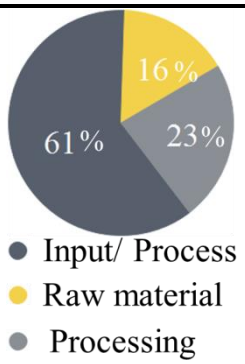
2	Hastelloy X (Ni-alloy)	48-102	
3	316L stainless steel	14-23	
4	CoCrMo	64-115	
5	Inconel-625	53-118	
6	Inconel-718	50-102	

To make a comparison of cost and the quality of GA and BM-produced powder feedstock, a rating from 1 to 5 is given to the associated parameters and is presented in **Fig. 2.9**. It can be perceived from **Fig. 2.9 (a)** that during BM, the primary raw material is machining waste (MCs), which is available at the cheapest cost contrary to the raw material used for CPPTs (**Table 2.2**). Alongside this, the machinery used in CPPTs is highly sophisticated and maintenance is expensive, contrary to the BM where simple machinery can fulfil the task [194]. In contrast, the morphology of the BM-produced CP is not perfectly spherical unlike those produced by CPPTs (**Fig. 2.9 (b)**). Thus, the reduction in the cost of powder production comes with inferior quality powder (in terms of morphology). Nevertheless, due to the sustainable nature of the process, it can still be further modified and explored to fulfil the shortcomings.

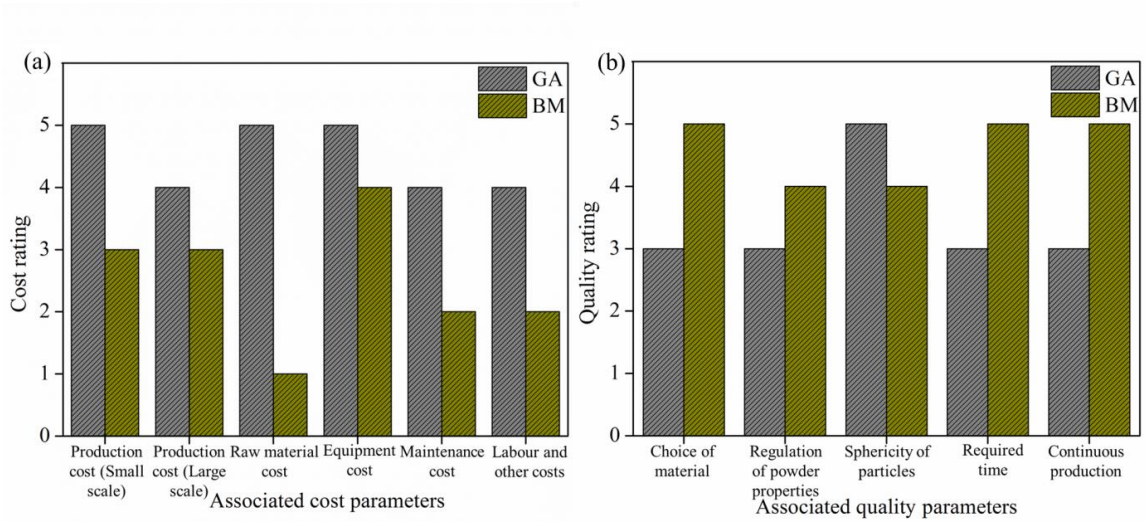

Fig. 2.9 *Comparison of powder feedstock produced using gas atomization and ball milling based on (a) cost, (b) quality; For the cost comparison, rating 1: least cost and*

5: highest cost; for quality comparison, rating 1: inferior quality and rating 5: superior quality.

2.7. CONCLUSIONS FROM LITERATURE REVIEW

The possibility of recycling MCs by converting them into powder feedstock via the BM process is reviewed. The major conclusions drawn are:

1. The type of MCs (material, size, and morphology) is a factor that is directly associated with the efficiency and economy of the recycling process using BM. As compared to conventional recycling (material loss 30-50%), the metal loss in the BM process ranges from 5-7%.
2. Milling time and ball diameter are the two influencing parameters that regulate the size and morphology of the produced CP by the BM process. Multistage BM shows promising results in obtaining the near-spherical morphology (70-90% sphericity) as the large diameter ball size effectively decreases the chip size and smaller-sized balls modify the morphology owing to the surge in the frequency of low force impacts.
3. The hardness of the BM-produced CP increases with an increase in the milling time due to phase transformations combined with other reinforcing mechanisms such as increased dislocation density and grain size refinement. Thus, by regulating milling time, the required properties of CP suitable for a particular material and application can be achieved.
4. The produced CP can be successfully used in AM techniques as a feedstock material due to their near-spherical morphology and superior properties as compared to the GA powder.

2.8. GAPS IN LITERATURE

Based on the literature survey conducted on the possibility of recycling MCs into powder feedstock, the following are the gaps found:

1. There are many studies on the recycling of stainless steel and aluminium MCs, but there is very little data reported on difficult-to-machine materials like Ti alloys and Ni-superalloys.
2. There is a lack of literature concerning the utilization of recycled powder of difficult-to-machine materials in additive manufacturing.

3. Despite the availability of data related to recycled metal powders, there is no mention of sustainability metrics of the same in the literature.

2.9. OBJECTIVES OF THE CURRENT STUDY

Based on the conclusions drawn from the literature survey conducted on the possibility of recycling MCs by converting them into powder feedstock via the BM process, the following objectives have been formulated for the current study:

1. The main objective of the study is to design a sustainable recycling technique/framework for Ti64 swarf by converting it into powder feedstock for additive manufacturing.
2. To obtain the chips powder using the proposed framework. Besides, to characterise the chips powder for particle size, morphology, hardness, and crystalline phases alongside to find the bulk powder properties (flowability and spreadability).
3. To find the optimised laser parameters (laser power and scanning speed) for proper melting of produced chips powder during direct metal laser sintering (DMLS) to examine its suitability for additive manufacturing.
4. Finally, to understand and compare the environmental impact of the proposed powder production framework with its conventional counterpart, gas atomization.

CHAPTER 3

EXPERIMENTAL TECHNIQUES AND PROCEDURES

3.1. PROPOSED FRAMEWORK BASED ON LITERATURE REVIEW

Based on the findings obtained from the literature review, a process for the successful conversion of MCs into CP using BM is hereby proposed and shown in **Fig. 3.1**. Expensive materials like titanium and inconel can be recycled by this method to contribute to the circular economy. Tool life is the regulating factor in machining and the least consideration is given to the quality of MCs produced [195]. Thus to enhance the tool life, different types of coolants are used [196]. After machining, coolant covers the chip surface and contaminates them. Moreover, due to the large surface area, this contamination is huge and can affect adversely the subsequent recycling stages and final product quality.

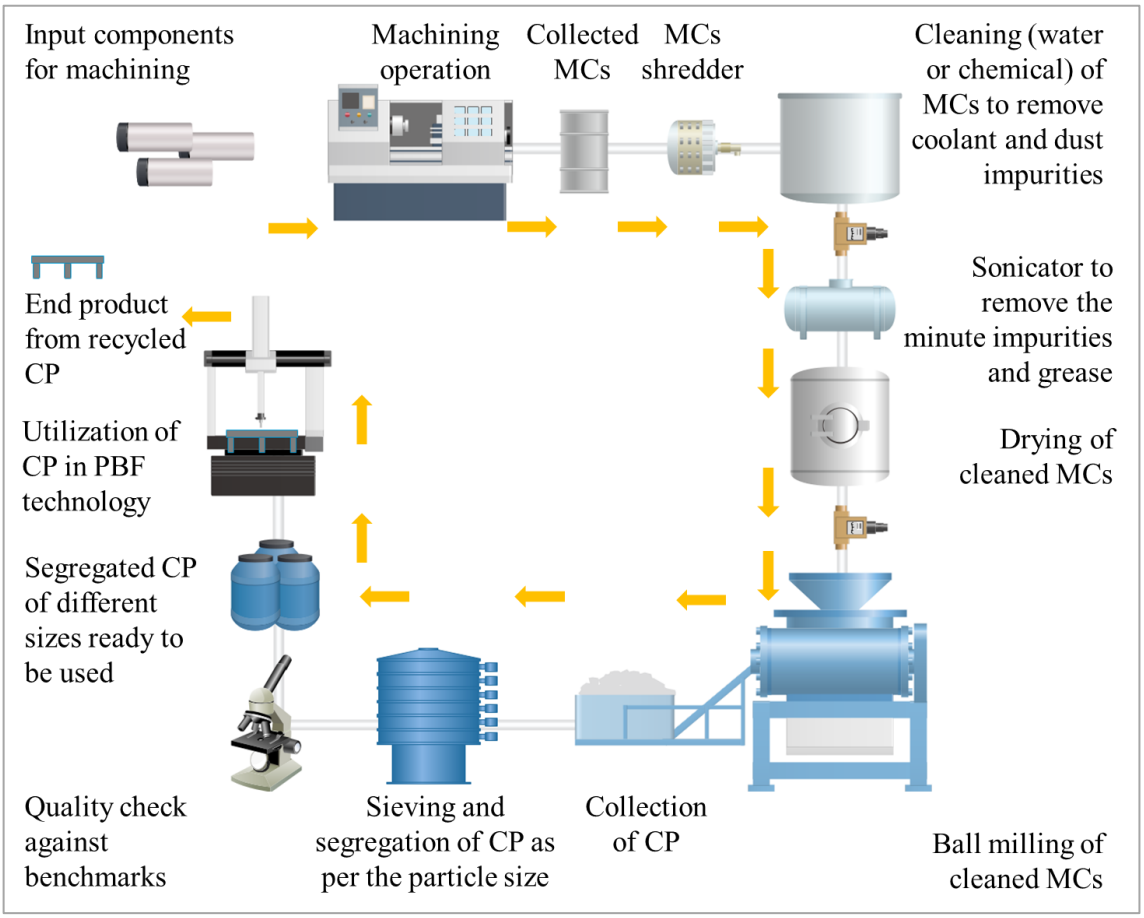

Fig. 3.1 *Proposed process flow for the sustainable conversion of machining chips into powder feedstock for metal-additive manufacturing.*

In addition, in the actual metal cutting work environment, there is no dedicated framework that collects MCs based upon their material, size, and type of operation. So, there is a large possibility of contamination of MCs with traces/chips of other material [197]. Accordingly, there is a need to remove both kinds of impurities before planning the recycling methodology. Thus, it is required to sort this scrap at the initial stage of its production. The below-shown flowchart (**Fig. 3.2**) provides a methodology to prepare MCs for recycling by removing coolant and other impurities.

MCs can be sorted during the production stage i.e., within the factory. This initial sorting saves time and effort and hence is the desired method. On the other hand, if there is no such infrastructure available within the factory, these can be segregated after the production by sorters. Sorters classify content composition using optical sensors through infrared cameras and then organize the scrap with mechanical sorters such as blowers or automated actuators.

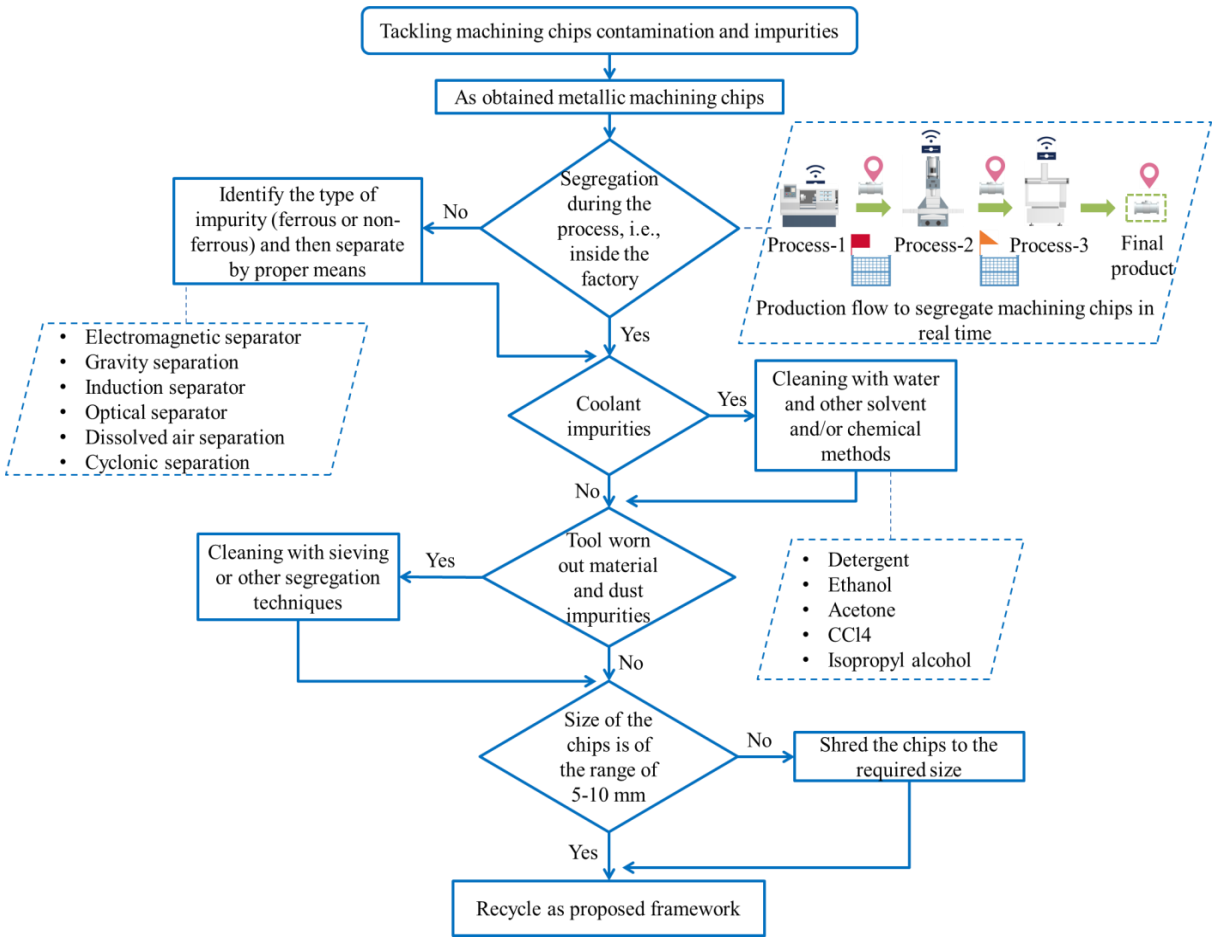

Fig. 3.2 *Methodology to clean and prepare machining chips for recycling by removing coolant and other impurities.*

In the view of same, [198] developed a method for automated sorting of metal scrap and the results show that the system developed is a greatly feasible solution that could substitute traditional dense medium segregation and conventional sorting. [199] used an electro-magnetic sensor to show a system for characterizing and sorting metals. [200] developed a system for evaluating the distribution of magnetic elements in an inventory sample of titanium minerals. [201] suggested a novel automatic scrap metal sorting system that uses an optical sensing system based on colour vision and an inductive array of sensors. [202] researched the recovery of fine non-ferrous metals from waste streams and found that non-ferrous metals varying from 2 to 6 mm can be clustered at high waste stream recovery by feeding them moderately wet to conventional eddy current separators built for larger particle sizes.

After the sorting stage, the MCs based on the type of material can be cleaned with water and/or chemicals to remove the impurity of dust and coolant. Specifically, if the impurity is hydrophobic, organic cleaners like CCl_4, acetone, or isopropyl can be used. Otherwise, water and detergent are suitable for the cleansing action. The segregated MCs then sent to the shredder for a reduction in size as explained in ***section 2.2***. Further, these cleaned MCs can be ball milled as per the suitable parameters following the sonicate bath and drying. It is important to mention here that the size of the BM unit can be adjusted as per the requirement. The tumbler BM apparatus can be redesigned and fabricated in-house to be retrofitted on a computer numeric control (CNC) lathe to eliminate the use of sophisticated BM apparatus in which the batch size is too small. Accordingly, the parameters can be regulated.

Finally, after size sorting and quality check, the CP is ready to fabricate components using PBF or blown powder metal AM technologies. PBF has evolved as the best alternative for the production of metallic parts from their respective powder feedstock [203]. PBF has been widely explored and currently being used for the manufacturing of parts with complex geometries from a variety of materials [204] such as titanium alloys [205], nickel-based super alloys [206], cobalt chrome alloys [207], steels [208], intermetallics [209], and metallic glasses [210]. With the development of PBF technologies, the manufacturing of components using DMLS [211], EBM [212], LENS [213], SLM [214], and selective laser sintering emerged as the most important and waste-free areas of metal-AM. Hence, there is the suitability of utilization of CP via this route for contributing to sustainability.

3.2. PREPARATION OF TI64 SWARF FOR BALL MILLING

Ti64 swarf obtained from cutting operation of billets using steel blade was acquired from Bhagyashali Metal Industries (Mumbai, India). It was cleaned and processed as per the schematic shown in **Fig. 3.3**.

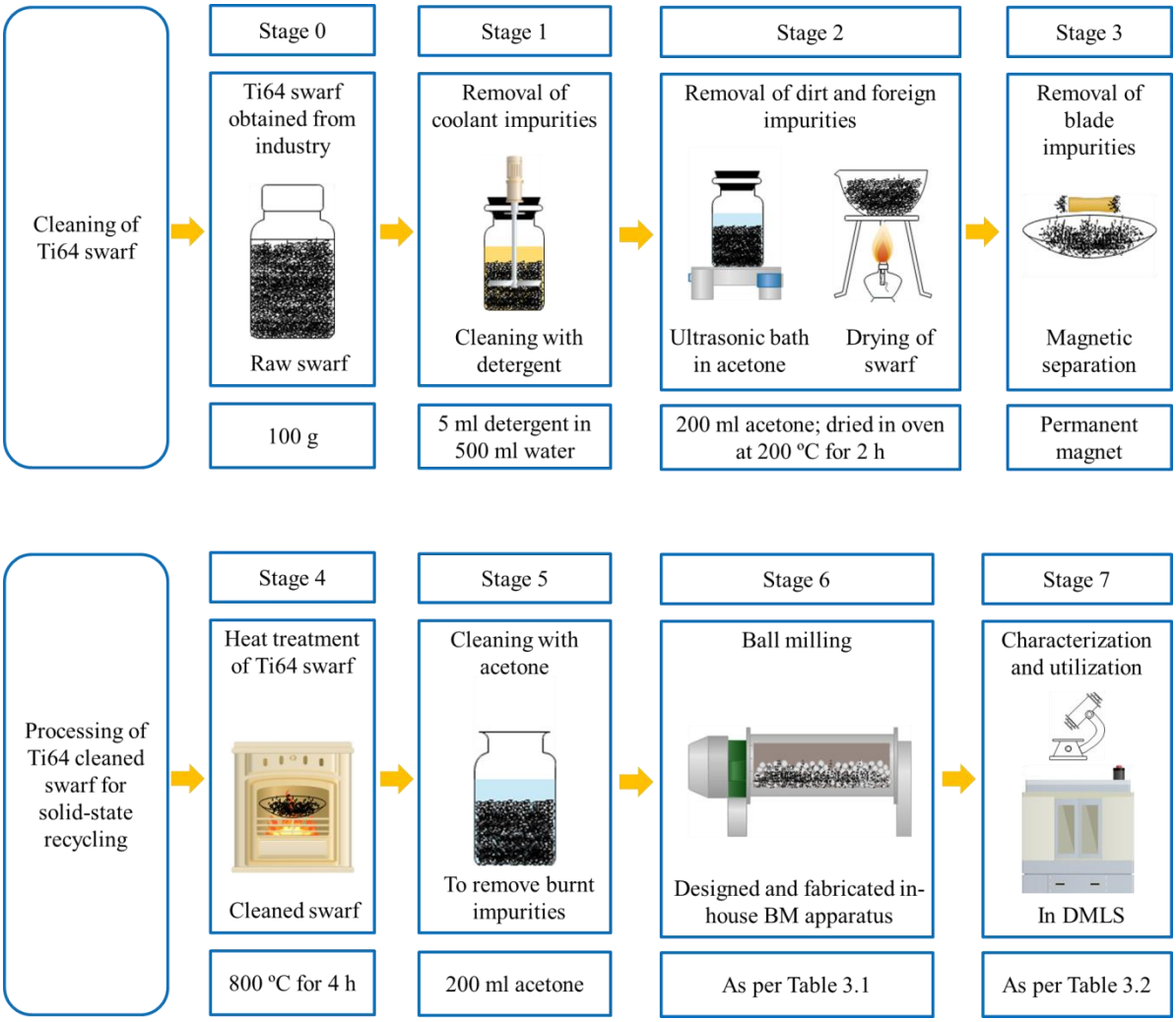

***Fig. 3.3** Steps followed to clean and process the Ti6Al4V swarf.*

To start with, the impurities of coolant were removed by cleaning with detergent followed by cleaning in the sonicator for 1 h. The cleaned swarf was then dried and sieved to eliminate very large particles (Size > 1000 µm) and foreign impurities which can interfere with the final results. Magnetic separation was carried out to eliminate the steel impurity of the cutting blade. Post this; heat treatment (4 h at 800 °C) in a vacuum furnace was performed to burn any leftover impurity. Finally, before BM, it was cleaned with acetone to remove any burned impurity.

3.3. BALL MILLING OF PREPARED SWARF

The cleaned Ti64 swarf was milled using an in-house fabricated tumbler ball mill driven by a CNC lathe (model: SANDS Precision SLT-135). The design specification of the BM apparatus is shown in **Fig. 3.4**. It constitutes stainless steel cylindrical jar having an internal diameter of 130 mm, wall thickness of 10 mm, and an inside volume of 12742.30 cm^3. Milling balls of stainless steel having diameter of 25 mm (Ø 25), 12.5 mm (Ø 12.5), and 6.25 mm (Ø 6.25) were used. The milling media with a consistent 20:1 BPR (weight ratio) was maintained throughout the BM operation. The cylindrical jar was sealed to avoid excessive oxidation of the powder. It was rotated at 73, 70, and 68 rpm (for Ø 25, Ø 12.5, and Ø 6.25 respectively as per the critical speed formula for tumbler ball mill, $S = 0.8\ \frac{1}{2\pi}\sqrt{\frac{g}{(R-r)}}$, where g is acceleration due to gravity, R is radius of BM cylinder, and r is radius of respective ball) with a 30 minutes pause after every 2 h of continuous rotation to avoid overheating the media and the associated system.

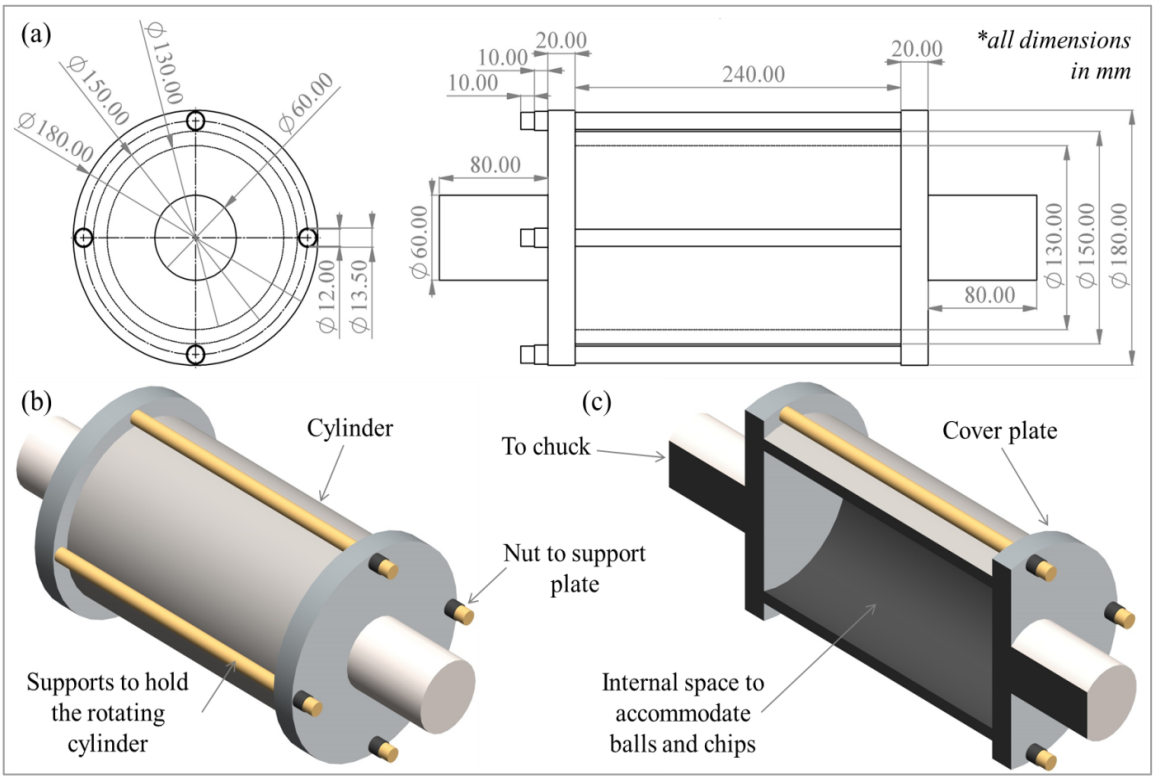

Fig. 3.4 *Specifications of In-house designed and fabricated tumbler ball milling apparatus.*

Two-stage BM was explored by [215] for steel and found promising results for the size reduction and morphology modification. For Ti64 alloy, the suitable BM parameters were selected from a study by [135]. Thus, in the current study, three BM conditions i.e., 1S-6H, 2S-12H, and 3S-18H (**Table 3.1)** were studied to investigate the effect of multi-stage BM on the size reduction and morphology modification of Ti64 swarf. The process starts with the BM of a fixed amount of cleaned swarf. After every stage of milling, the powder (generated from swarf) was sieved for 10 minutes to obtain the PSD and change in morphology. This process continued until the final stage of BM.

Table 3.1 *Ball milling parameters employed for the conversion of Ti6Al4V swarf into powder feedstock for additive manufacturing.*

S.No.	Sample code	Stage	Ball diameter (mm)	Milling time per stage (h)	Total Milling time (h)
1.	1S-6H	1st	Ø 25	6 (2-2-2)	6
2.	2S-12H	2nd	Ø 12.5	6 (2-2-2)	12
3.	3S-18H	3rd	Ø 6.25	6 (2-2-2)	18

3.4. CHARACTERIZATION OF BALL-MILLED POWDER

PSD was obtained by sieving and weighing the powder after every 2h of BM. The particles were separated as per different mesh sizes of sieve *viz.* #300, #200, #106, #80, #60, #44, #30, #22, and #16 corresponds to the pore size of 53, 75, 106, 150, 250, 400, 500, 710, and 1000 µm respectively. The powder in the range of 53-150 µm was considered for morphology inspection by scanning electron microscope (SEM) (model: JEOL6610LV) equipped with energy-dispersive X-ray spectroscopy (EDS) as shown in **Fig. 3.5**. After every stage, the powder was taken and mounted in epoxy for further characterization. The same was polished using a standard metallographic procedure. The hardness of the powder particles was measured using Vickers microhardness tester (**Fig. 3.5**) (model: Wilson 402MVD, US) at 100 gf load for 10 seconds.

Oxygen pickup was measured by EDS analysis after every stage. For both the hardness and oxygen pickup measurements, an average of three readings was taken to eliminate any inconsistency. The flowability of the bulk powder was examined using the angle of repose (α) measurement as per ASTM B964-16 (standard test technique for

metal powder flow rate using the Carney funnel). Spreadability was analysed using the method proposed in the study by [154].

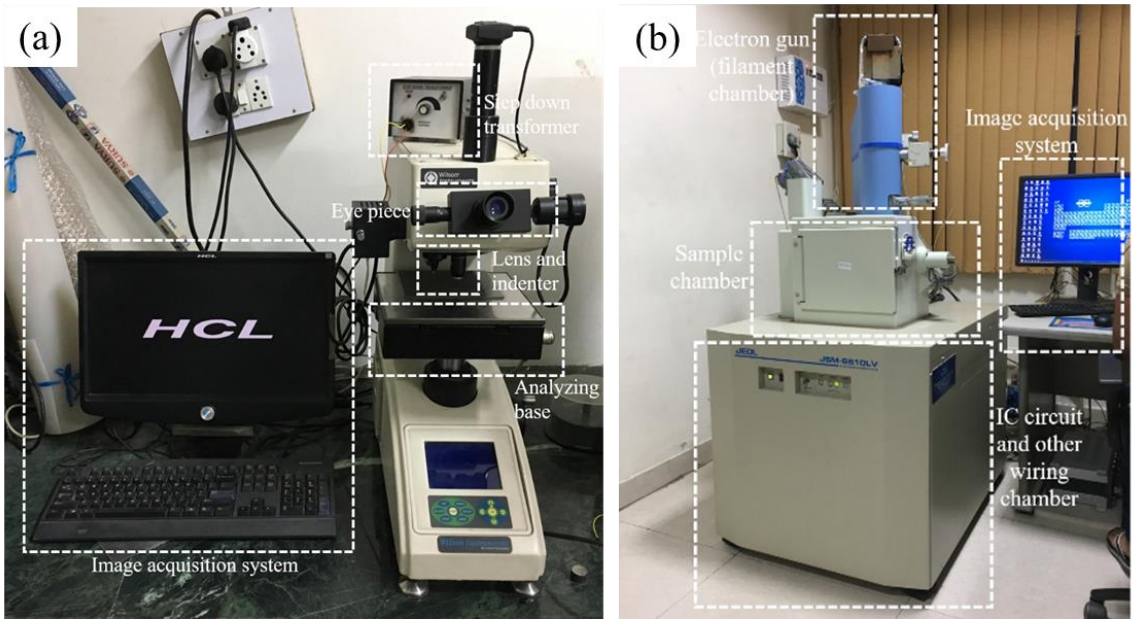

Fig. 3.5 *(a) setup for microhardness and (b) scanning electron microscope.*

3.5. UTILIZATION OF PRODUCED POWDER IN DMLS

The powder obtained after BM was used to fabricate single tracks (one layer of powder melted by laser beam) using the DMLS system (model: EOSINT M280). 3S-18H powder was used to generate single tracks as per the parametric design shown in **Table 3.2**. These are pre-optimized commercially used parameters for the Ti64 alloy for a particle size ranges from 50 - 150 µm having spherical morphology [178]. The constant parameters include a laser spot size of 80 µm and a layer thickness of 100 -140 µm.

Table 3.2 *Parametric design for the utilization of prepared powder by direct metal laser sintering.*

S. No.	Powder code	Laser power, LP (W)	Scanning speed, SS (mm/s)
1	3S-18H	250	1000
2	3S-18H	250	1300
3	3S-18H	310	1300
4	3S-18H	310	1000

3.6. EVALUATION OF SINGLE TRACKS FABRICATED BY DMLS

The powder in the range of 53 -100 µm was used for the fabrication of single tracks. The powder layer having a thickness of 100 -140 µm was spread manually on the Ti64 base plate. The laser then scanned a length of 1 cm to obtain single tracks as shown in **Fig. 3.6**. The single tracks were characterised in terms of continuity, track width, porosity, and defects using SEM. Also, the hardness of the single tracks was measured using nanoindenter (model: Hyistron TI 950) with a 5 mN load by taking an average of three readings as the final value.

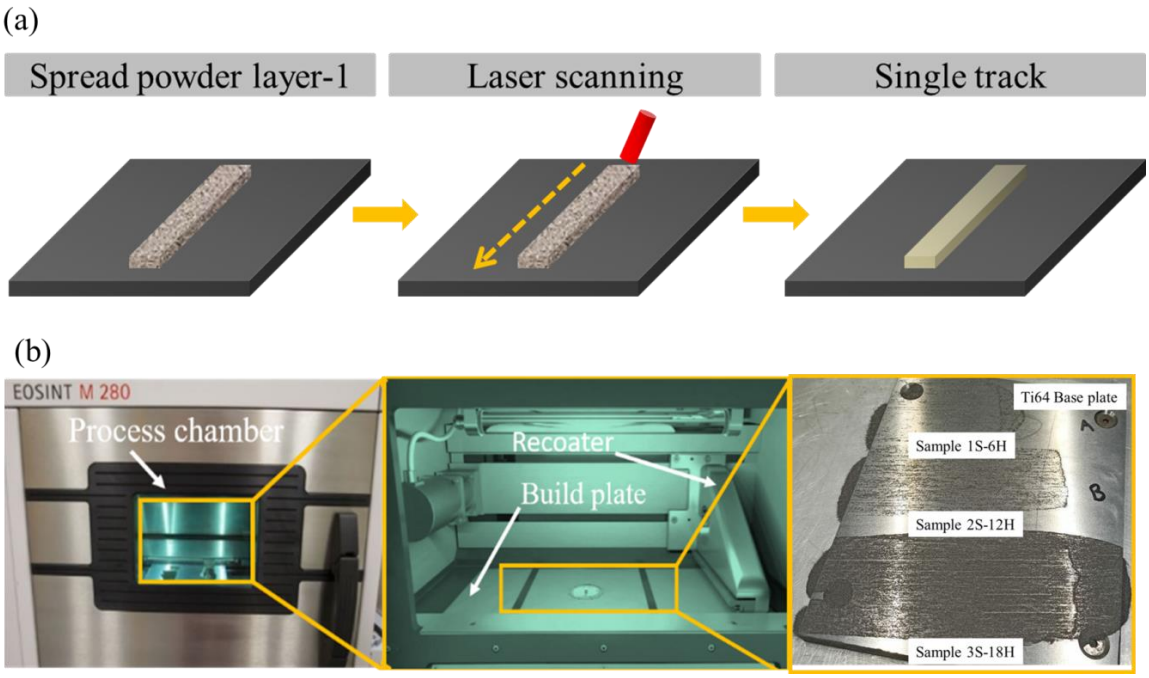

Fig. 3.6 *Steps to generate single tracks of the prepared powder using a laser in direct metal laser sintering, schematic (a) and actual process (b).*

CHAPTER 4

CONVERSION OF Ti64 SWARF TO POWDER

4.1. ANALYSIS OF Ti64 SWARF

To ascertain the quality of the received Ti64 swarf, characterization of the raw material was carried out. The morphology and composition of the freshly procured swarf is shown in **Fig. 4.1**. It can be seen from SEM micrograph that the chip size varies from 10 -1000 µm. The morphology of the chips is almost irregular, with a large percentage of long and thin chips. The variation in chip size and morphology is due to the different cutting cycles with the hacksaw blade. Initially, the blade erodes the Ti64 billet resulting in thin and small chips. Once the blade is fully inside the billet, long and big chips are generated. EDS mapping of Ti64 swarf reveals presence of small percentage of iron (Fe) impurity owing to wear of hacksaw blade. PSD result of swarf is shown in **Fig. 4.4**. It can be seen that the majority of the chip particles have a size in the range of 250 -475 µm.

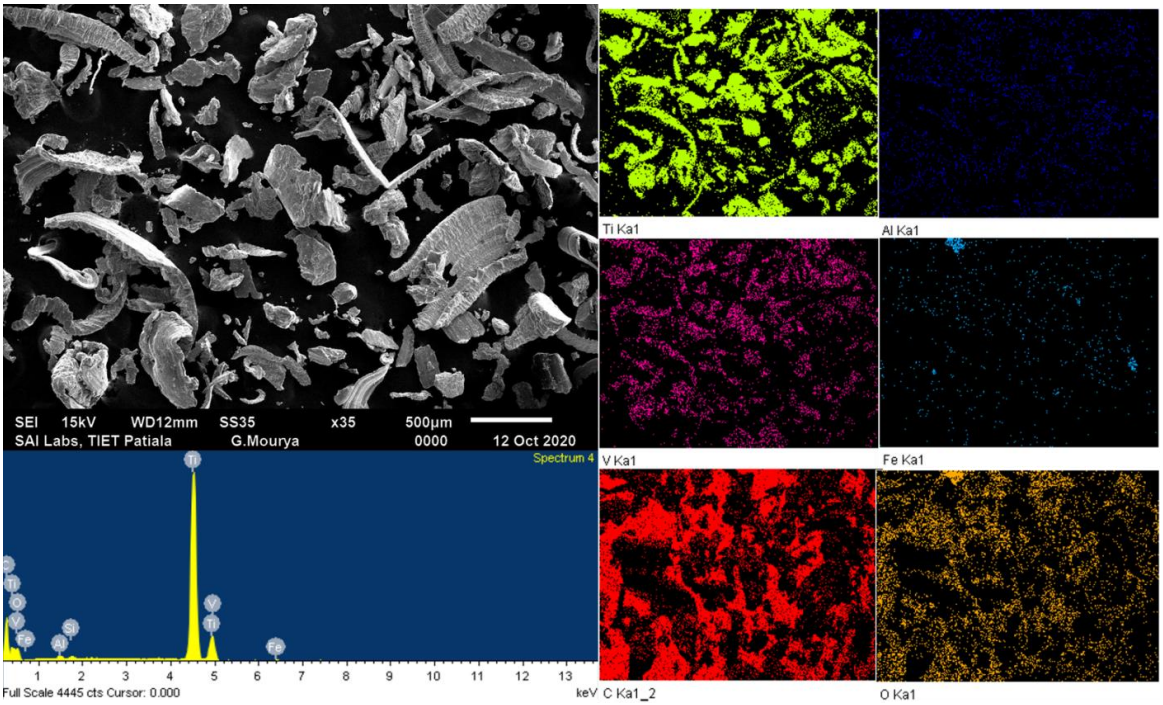

Fig. 4.1 *Result of scanning electron microscopy and energy-dispersive X-ray spectroscopy analyses representing morphology and composition of Ti6Al4V swarf respectively.*

4.2. CLEANING OF TI64 SWARF

Fig. 4.2 shows the elemental composition of the swarf after every cleaning stage. It can be observed that stage 1 cleaning leads to the removal of lubricant oil which was shown by a decreased value of carbon content (2.77 wt %). Also, a 0.18 wt % reduction in the share of Si is also observed. This is due to the soluble nature of Si and lubricant oil in detergent water and hence their removal. Stage 2 leads to the further removal of Si (0.78 wt %). Magnetic separation in the stage 3 leads to the removal of iron content from 1.93 to 0.06 wt %. Also, wt % of 85.55, 4.32, and 2.98 for Ti, Al, and V is achieved respectively.

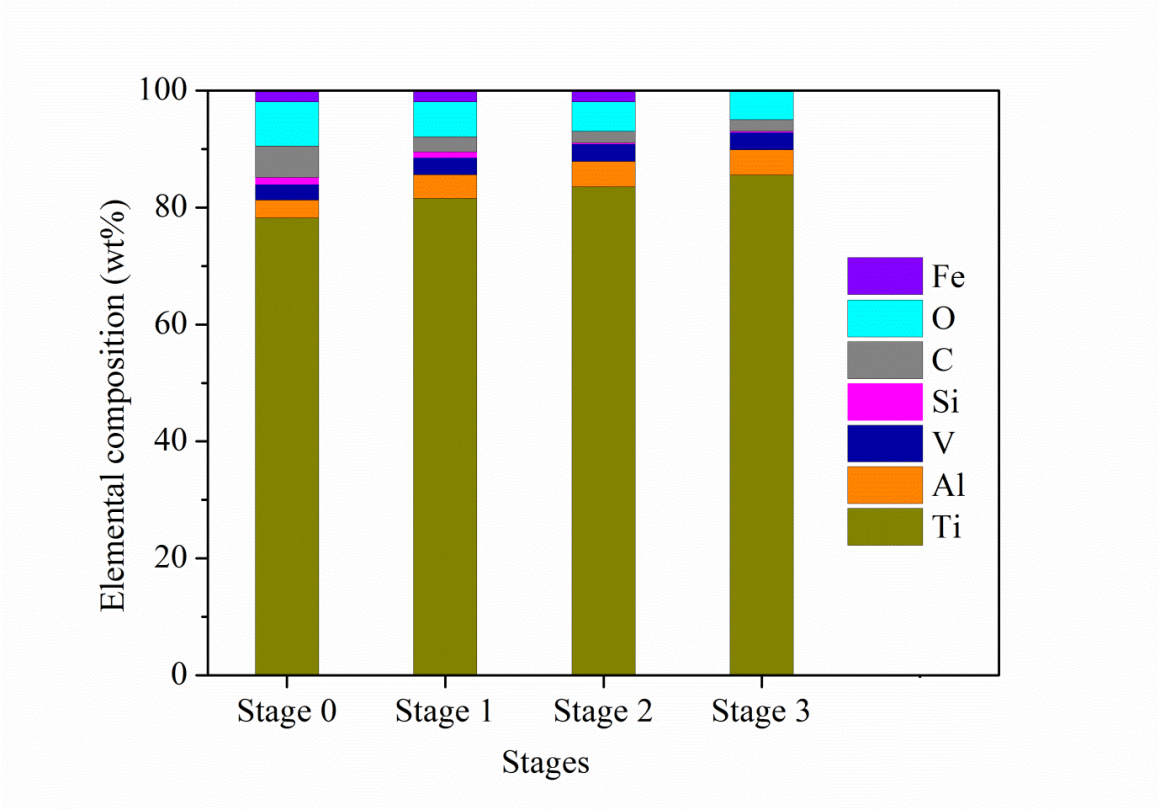

***Fig. 4.2** Elemental composition of Ti6Al4V swarf after various cleaning stages.*

The effect of no. of cleaning cycles on the final elemental composition was also evaluated and the results are shown in **Fig. 4.3**. No significant change is observed (85.55 to 85.91 of Ti). Thus, it can be said that only one cleaning cycle is enough for the removal of most of the impurities. The morphology and PSD of Ti64 cleaned swarf is shown in **Fig. 4.4**.

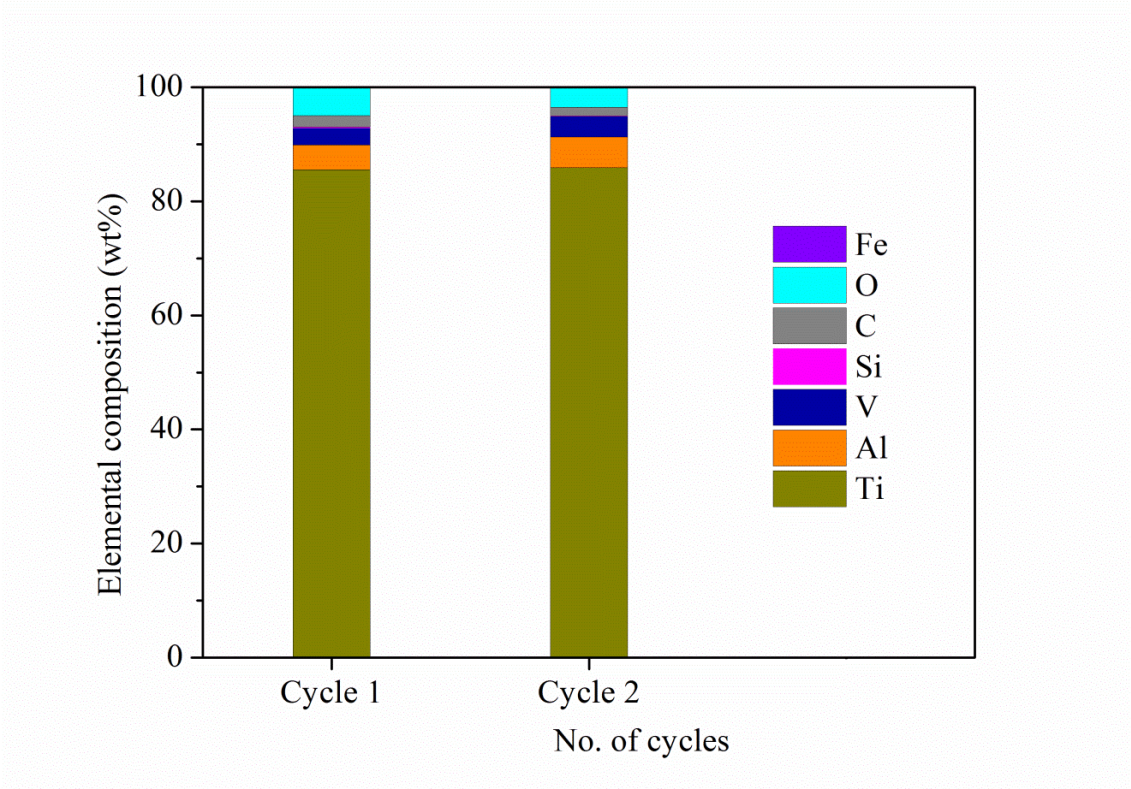

Fig. 4.3 *Elemental composition of Ti6Al4V swarf after number of cleaning cycles.*

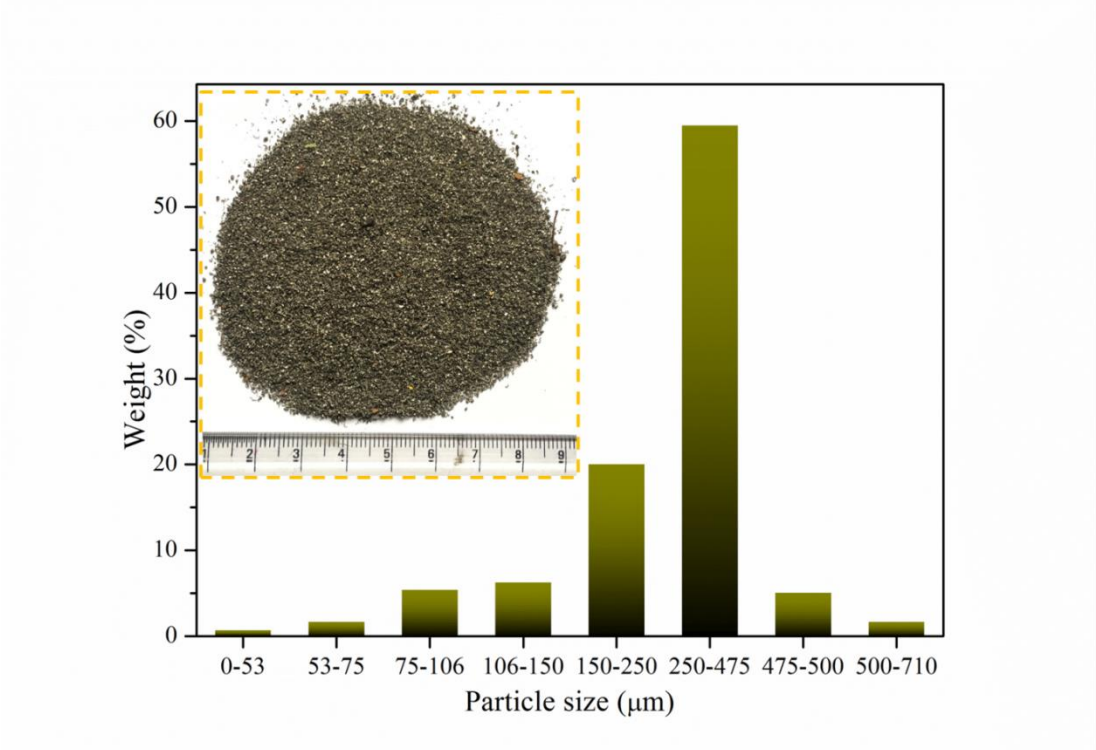

Fig. 4.4 *Particle size distribution of cleaned Ti6Al4V swarf.*

4.3. CHARACTERIZATION OF BALL-MILLED POWDER

4.3.1. Particle size and morphology

Fig. 4.5 shows the effect of BM time on the size of particles. It can be seen from the PSD graphs that the particle size gets substantially modified with Ø 25 balls followed by Ø 12.5 balls and Ø 6.25 balls.

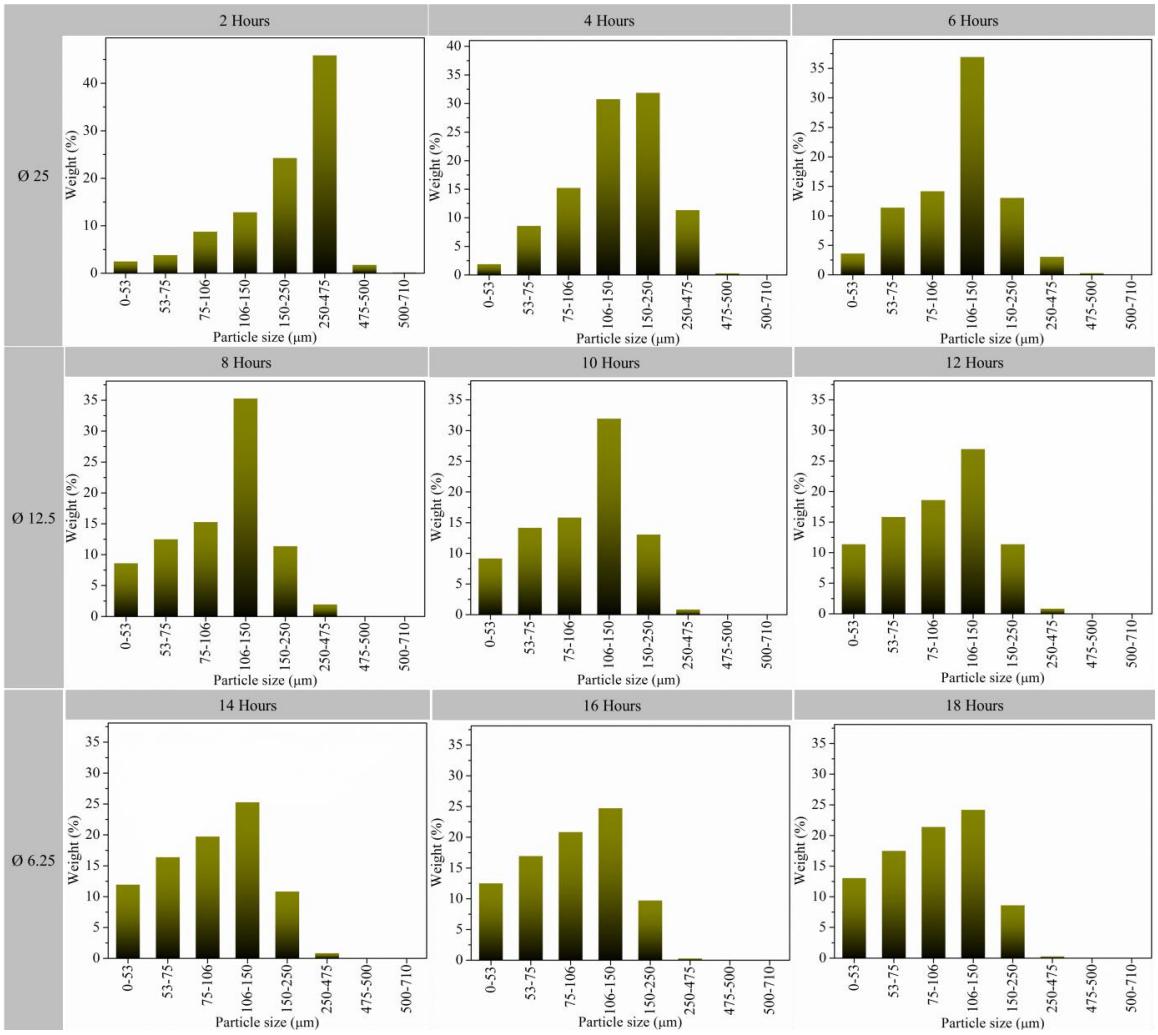

***Fig. 4.5** Particle size distribution graphs showing the effect of ball milling time and ball diameter on the particle size.*

This reduction in particle size is due to the high impact produced by balls dropping from near the top of the shell during rotation [215]. The impacts from large-sized balls induce micro-cracks. These micro-cracks become a site of crack propagation leading to the fracture of the particle with further milling (point 4 in **Fig. 4.6**). A schematic of the impact and abrasion phenomenon dominating morphological changes in

the BM process is shown in **Fig. 4.6**. The irregular morphology of the particles at the beginning is converted to angular and sharp-edged particles after stage 1 of BM. Further BM with Ø 12.5 balls does not reduce the size of particles very significantly but increased the percentage of powder size of lower values due to the alteration in their morphology. The morphology after stage 2 becomes slightly round from angular and sharp-edged as can be seen from **Fig. 4.7**. Abrasion phenomenon associated with Ø 12.5 balls may become a reason for the change in morphology of particles. Herein the balls revolve and rub hard against the wall along with the powder in between and hence modify the morphology (points 1, 2, and 3 in **Fig. 4.6**).

It can be observed from PSD graphs (**Fig. 4.5)** that for 3S-18H powder, the output is ~60% for particle size ranged between 53 -150 µm (size range for commercial GA powder used in DMLS). For the same powder range, however, the yield in GA is ~70% [216], but there are other issues related to cost and environmental impacts associated with the GA that makes the process unsustainable (further explained in *section 4*). Particles having a size >150 µm (~8 %) can further be milled to bring their size down to the desired range. On the contrary, the powder <50 µm (~13 %) can be employed in other applications such as cold spray based AM where a smaller size (< 38 µm) is required [217].

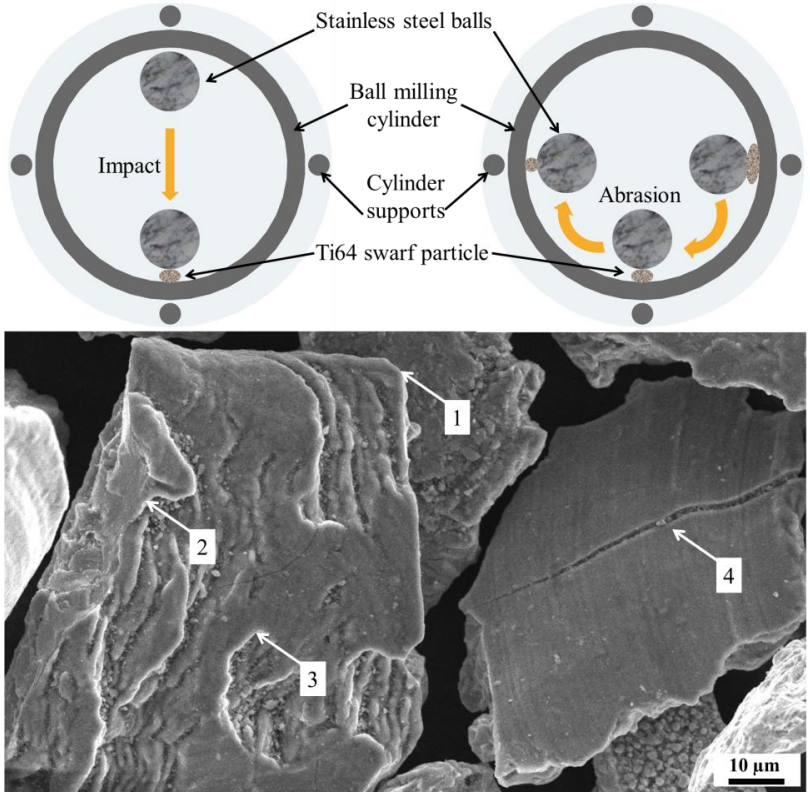

Fig. 4.6 *Impact and abrasion action during ball milling of Ti6Al4V swarf.*

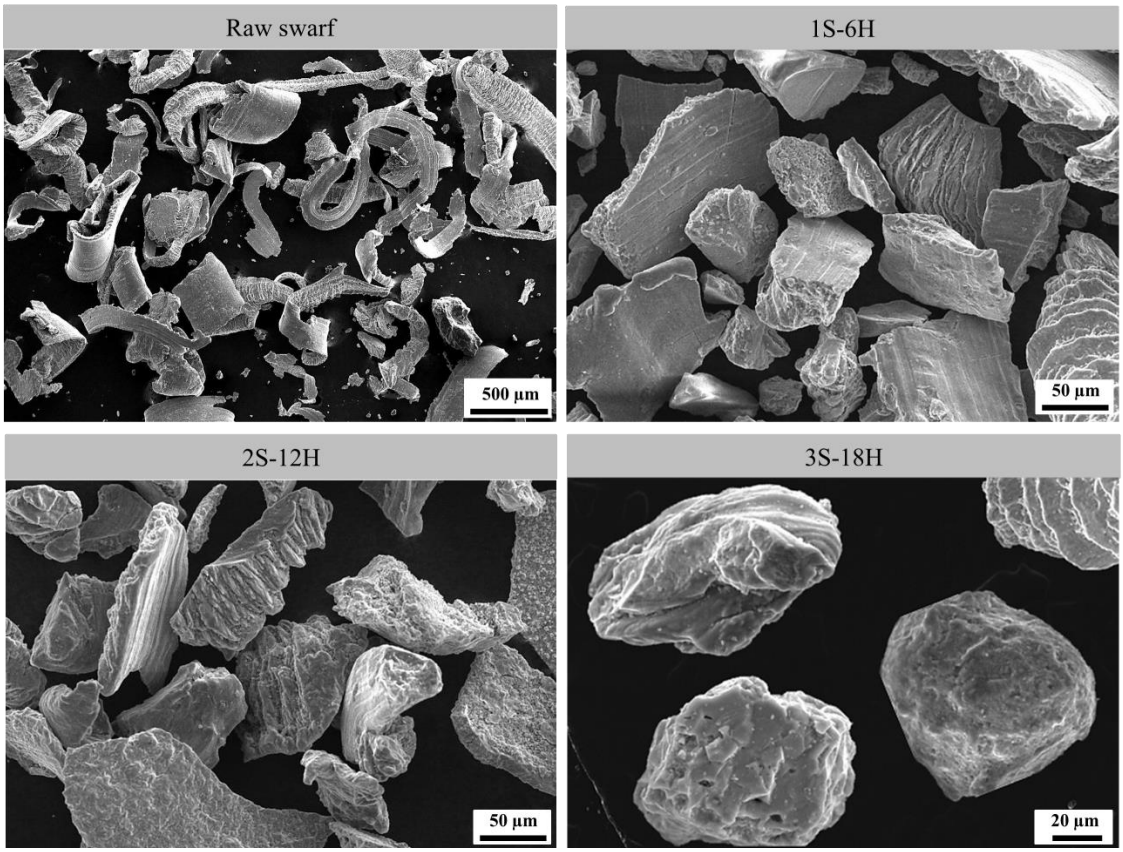

Fig. 4.7 *Modifications in the morphology of powder particles after different ball milling intervals.*

4.3.2. Hardness and XRD analysis

Fig. 4.8 shows the variation of Ti64 powder hardness with milling time. Raw swarf of Ti64 (represented by 0 on the abscissa in **Fig. 4.8**) was found to have a hardness of 390±4 HV. It can be seen that the hardness value increases linearly with an increase in milling time up to 440±2 HV. This increase in hardness is attributed to the enhanced dislocation density and reduced grain size by work hardening due to the constant hammering action on trapped particles between balls and BM cylinder [218]. Constant hammering leads to grain refinement as per the Hall–Petch relationship, which states that grain refinement is also a significant strengthening mechanism [219].

After a saturation state (~440 HV), no further strain gets developed in the particles due to the increase in resistance to plastic deformation. The particles at this stage cease to deform plastically and hence the hardness curve gets flattens with a change in morphology to near-spherical. Beyond the expected strain hardening due to BM, the oxygen pickup by Ti64 also has an effect on increased hardness value [220]. Ti (commercially pure) has a high affinity towards oxygen, but its alloy Ti64 picks up comparatively less oxygen during mechanical deformation [221]. An increased oxygen

content (from 0.5±0.09 (wt %) to 1.1±0.08 (wt %) till last stage) with milling time can be seen in **Fig. 4.8**. A steep curve can be observed after 12 h because after this stage, particle size cannot be reduced further except the modification in morphology which exposes a high surface area [222].

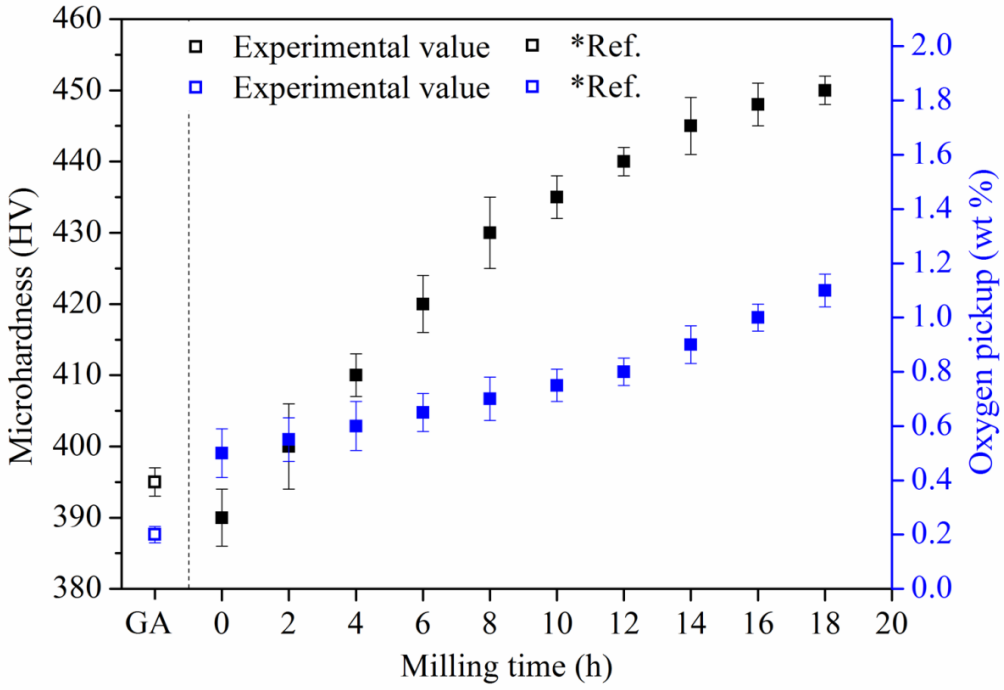

Fig. 4.8 *Variation of hardness and oxygen pickup of ball-milled powder with milling time (*hardness* [223]*, *oxygen pickup* [224]*).*

Fig. 4.9 shows the X-ray diffraction (XRD) patterns of raw swarf, final BM powder (3S-18H), and GA powder for comparison purposes. The XRD pattern of 3S-18H powder does not reveal any extra peak for Fe due to the removal of Fe impurity during the cleaning stage. For the same powder, after the BM for 18 h, the intensity of the peaks reduced as compared to the GA powder. This loss in intensity is due to the refining of coherent scattering regions and internal strain accumulation [219].

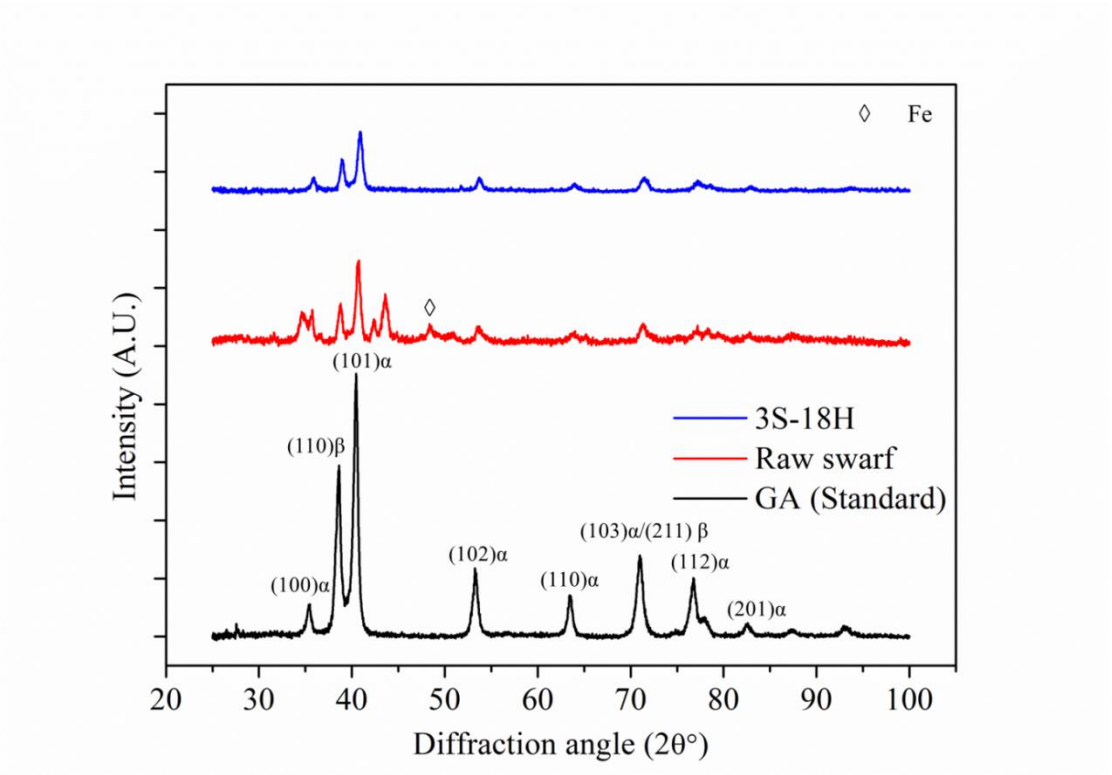

Fig. 4.9 *X-ray diffraction patterns of Ti6Al4V raw swarf, ball-milled powder (3S-18H), and commercially available gas atomized powder.*

4.3.3. Powder flowability and spreadability

The measurement of α gives a general idea about the cohesiveness between powder particles and thus the flowability. Values fewer than 30º suggest lower cohesiveness or high flowability. Higher values up to 55º suggest an increase in cohesiveness or a decrease in flowability. Over 55º, the cohesiveness is so large that it makes powder difficult to flow properly [225]. It can be seen from **Fig. 4.10** that the value of α for 3S-18H powder is closer to that of GA powder. This is due to the near-spherical morphology of the 3S-18H powder particles that enhances its flowability. The particle with such morphology does not resist flow due to the presence of very little friction between them at the microscopic level. This reduction in friction is due to the absence of surface asperities [156]. Low flowability of the 1S-6H and 2S-12H particles is because of angular sharp-edged morphology of particles as they oppose each other's motion during the flow (**Fig. 4.7)**.

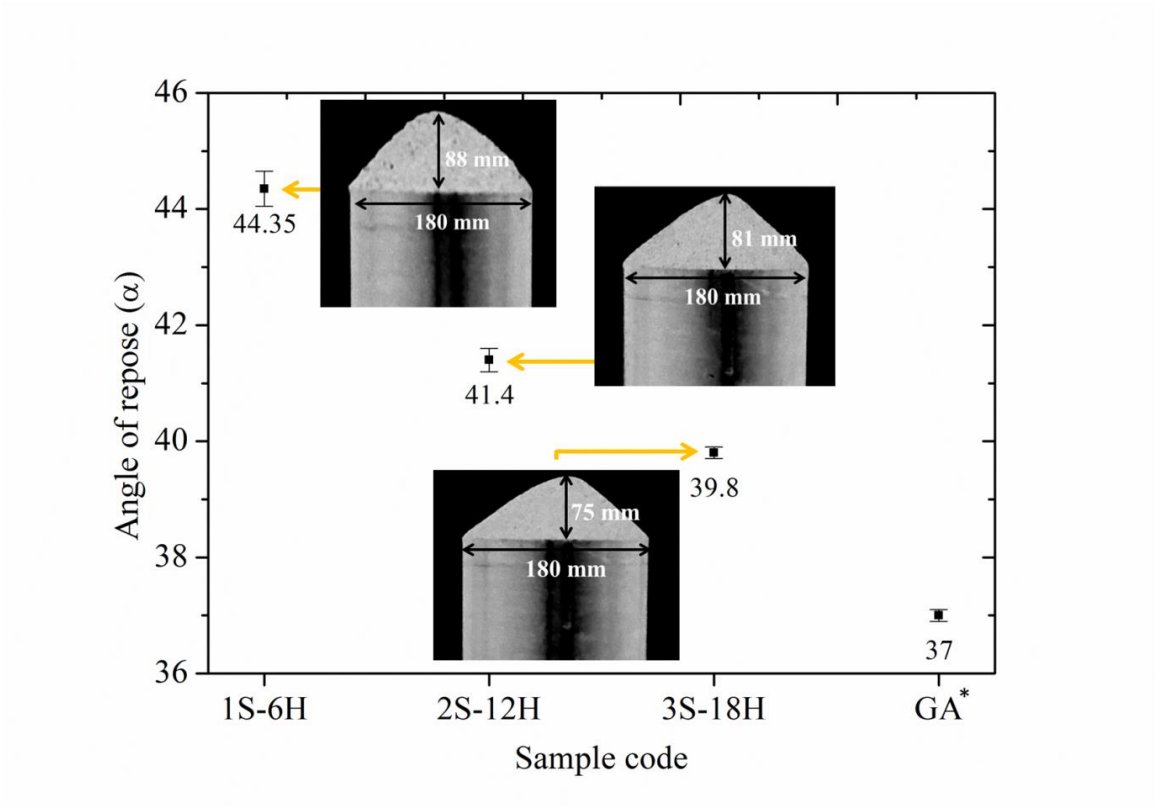

Fig. 4.10 *Flowability results of ball-milled powders using Carney funnel (*GA* [67]*).*

Spreadability deals with the flow of powder in the narrow clearances with a very small shearing zone [154]. The powder is usually spread on the base plate using either roller or blade with very small gaps in the range of 50-150 µm depending upon the system. In the present case, due to the large size range of particles as compared to GA powder, the layer thickness varies with particle size and morphology. Patchy coverage of the powder affects the particle bonding during the melting and hence affects the part quality [226]. **Fig. 4.11** shows the spreadability analysis of the different powders produced using BM. It can be observed from the analysis that 3S-18H powder shows better spreadability in terms of the homogeneous spread of layer without patchy coverage. This is due to the near-spherical and more homogeneous morphology than 2S-12H followed by 1S-6H. The spread is inconsistent and patchy for 1S-6H due to the presence of sharp-edged particles (point 1 in **Fig. 4.11**). Moreover, the layer height is not the same throughout (points 2 and 3 in **Fig. 4.11**) because in 3S-18H powder, the share of smaller particles i.e., 0-106 µm is large as compared to 1S-6H. Thus, due to this, the particle accumulates in two layers (one over another). On the other hand, for 1S-6H, a high share of larger particles hinders the formation of the double layer.

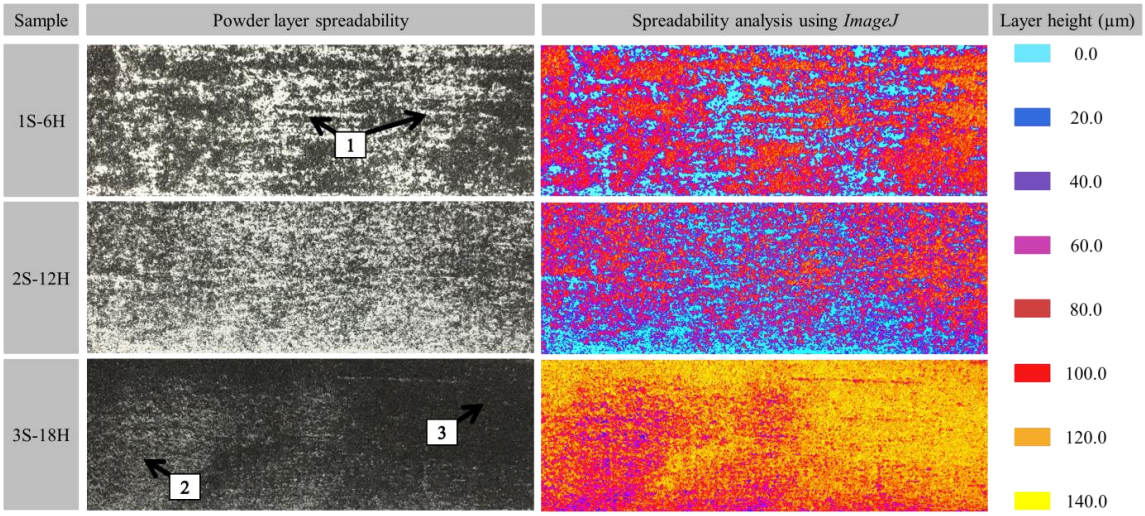

Fig. 4.11 *Spreadability analysis of powder obtained after different stages of ball milling.*

4.4. EVALUATION OF FABRICATED SINGLE TRACKS

4.4.1. Effects of laser parameters

It can be observed from **Fig. 4.11** that the spread of 3S-18H powder is homogeneous due to the near-spherical morphology and can generate a single layer in the DMLS system, in which only one layer per scan is melted. Thus, based on the morphological, mechanical, and spreadability analyses, the only 3S-18H powder is considered suitable for further processing with the DMLS system. The results of the parametric investigation of the single tracks are shown in **Fig. 4.12**. It can be seen from **Fig. 4.12** that both the parameters *viz.*, laser power (LP), and scanning speed (SS) are crucial to study the melting behaviour of metal powder using lasers.

It is evident from trials no. 1 and 2 that at high SS, the powder does not melt properly due to the insufficient laser exposure time. With a high SS, a huge fluctuation in melt pool length leads to improper melting. The effect of LP can be observed by comparing trials no. 1 and 4. The increased width of the single track can be seen with a high LP due to the large melt pool. This effect is attributed to more melting at the same SS. Due to the formation of keyholes in the melt pool caused by the non-spherical morphology of the powder, the melt pool becomes unstable that prevents the good development of single tracks [227]. However, on comparing, an overall uniformity in the single track can be observed in the trial no. 4. Thus, process parameters in the trial no. 4 become suitable for 3S-18H powder while processing using DMLS.

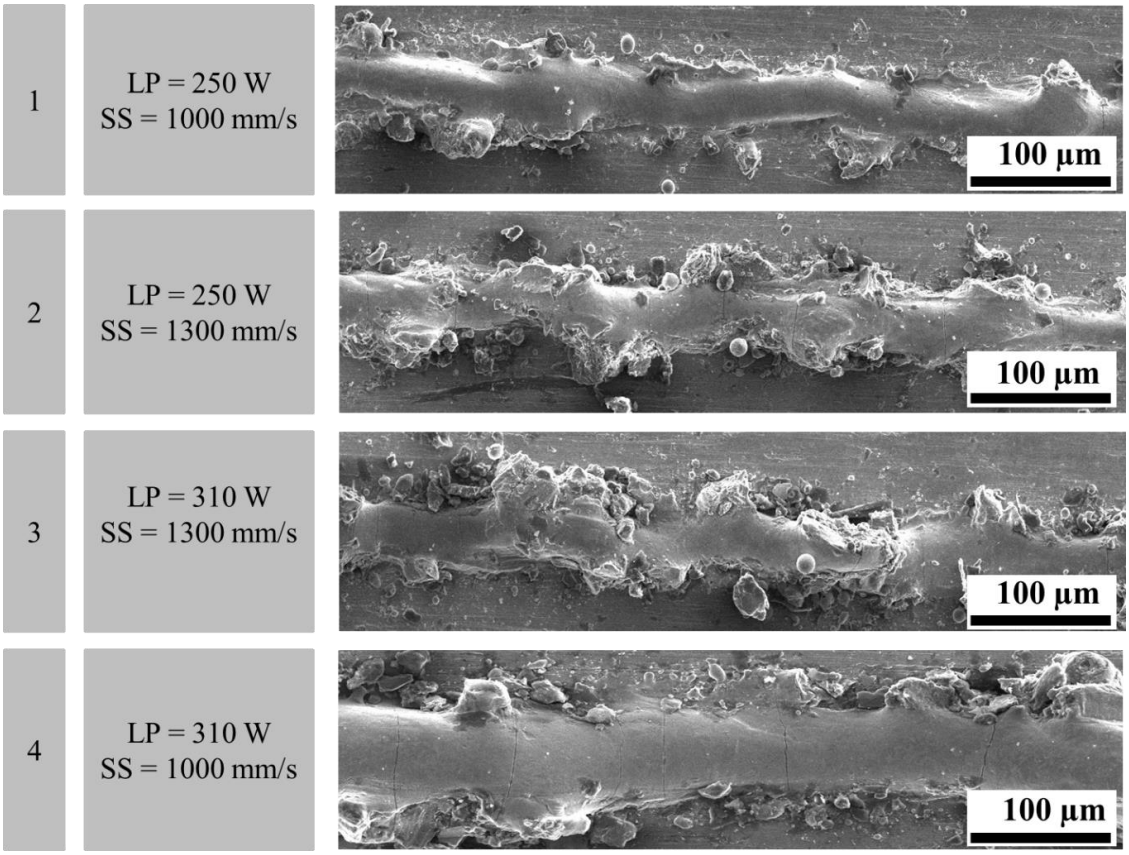

Fig. 4.12 *Utilization of ball-milled powder (3S-18H) to fabricate single tracks by direct metal laser sintering.*

4.4.2. Porosity and defects

Porosity and defect information of the single tracks shows that along the length of the single track, the powder is not melted properly leading to a disturbed melt pool and hence non-uniform build (**Fig. 4.12**). Also, transverse cracks are identified along the length of single tracks (**Fig. 4.13**, fabricated at SS of 1000 mm/s and an LP of 310 W, pre-optimised parameters for spherical GA powder in the same size range). This is due to the formation of a complex stress field by uneven heating and cooling process caused by the non-spherical 3S-18H powder in the DMLS process [228]. Thus, as also suggested by [229], inadequate melting along the length and transverse cracks can be prevented by preheating the base plate (to avoid the sudden temperature variation during melting) and optimizing the total energy density required to melt 3S-18H powder.

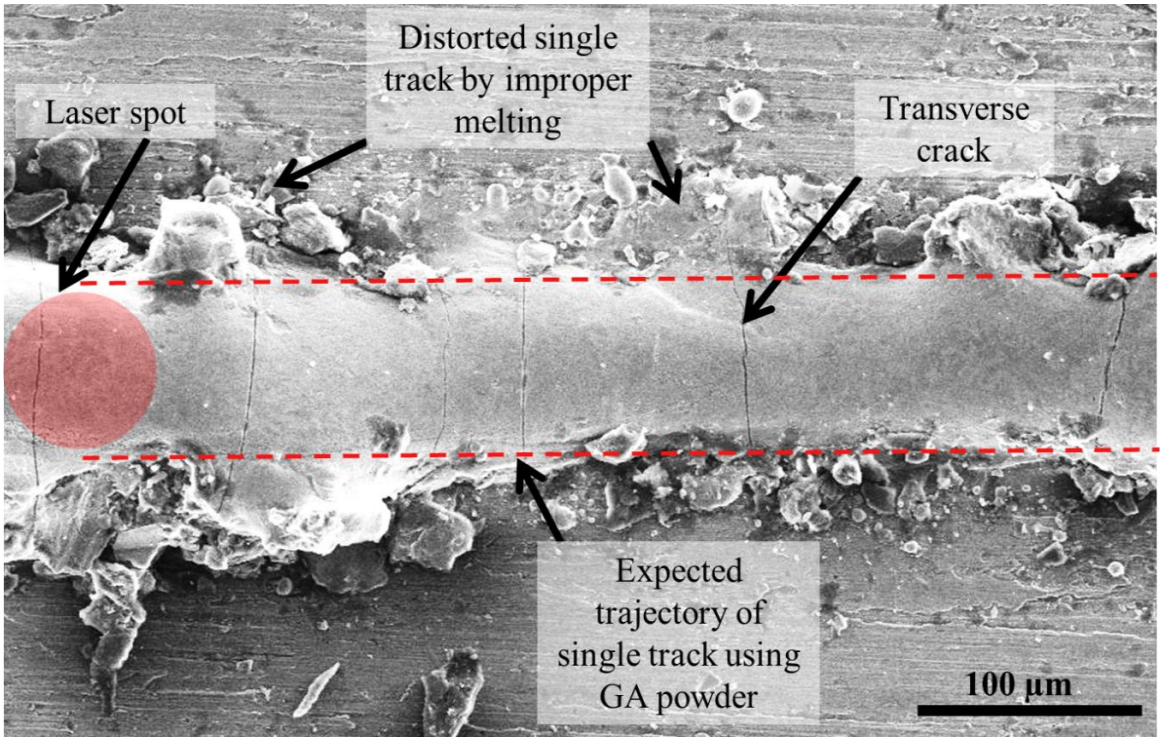

Fig. 4.13 *Porosity and defects information in single tracks fabricated by direct metal laser sintering (red dotted lines shows single tracks width made using GA powder at same parameters* [178]*).*

4.4.3. Track width

Fig. 4.14 shows a comparative analysis of single tracks based on their physical and mechanical properties fabricated with 3S-18H and GA powder. For 3S-18H powder, It can be observed that with an increase in SS (trial 1 and 2), the track width decreases (~ 4 %) but with an increase in LP (trial 2 and 3), track width increases (~ 10 %). At the same parameters, on the other hand with GA powder, a similar trend can be observed but with a 5-25 % difference in track width in comparison to the experimental values. Conversely, the overall hardness of single track build with 3S-18H powder is better (~ 4-7 %) as compared to the same generated with GA powder at the same parameters. But there is no particular trend in hardness values in different trials that suggests its dependency on the used parameters during DMLS.

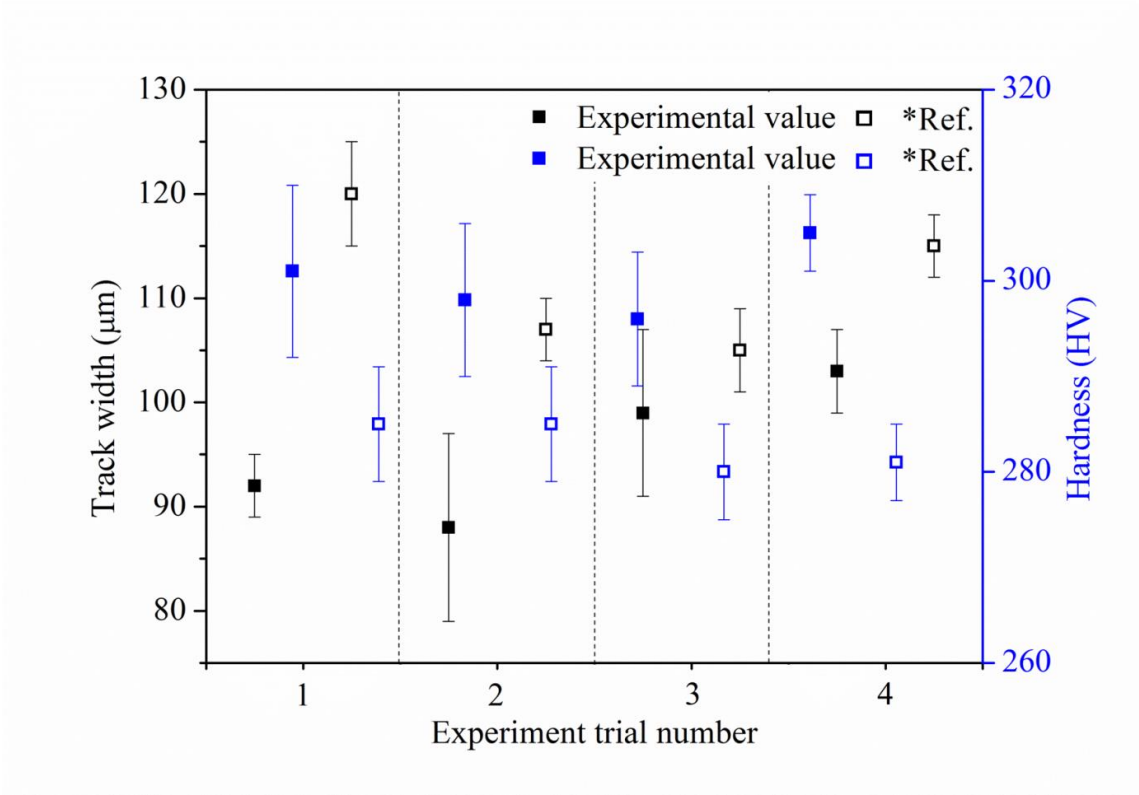

Fig. 4.14 *Track width and hardness results varying laser parameters for 3S-18H powder (*track width and hardness data of single tracks generated using gas atomized powder at same parameters* [178]*).*

CHAPTER 5

SUSTAINABILITY ANALYSIS

5.1. COMPARATIVE LIFE CYCLE ASSESSMENT

Sustainability analysis is an important strategy that defines the success factor of a process by comprehending its impact on the environment and cost to the industry [230]. For the current study, LCA is used as the tool to measure the environmental impact. The associated cost of the process is also presented to provide an in-depth comparison with the GA process.

5.1.1. Goal and scope

The goal of the present LCA study is to understand and compare the environmental impact of the proposed powder production framework with its conventional counterpart, GA. The scope of the study is limited to the production of powder via these two different routes. There are general assumptions made for the present LCA study such as:

1. Both the processes were considered to be in continuous operation i.e. neglecting the initial material and energy wastage.
2. Electricity used for both processes was produced from black coal [231].
3. The GWP and eco-cost of Ti64 swarf were taken as zero because it is a by-product generated during the preparation of Ti64 billets.
4. Both the processes were considered to be operated at the optimised set of parameters for the chosen raw material.
5. The study does not include the transportation share of raw and produced materials.
6. It also does not include the establishment cost of equipment and systems.

5.1.2. Functional unit and system boundary

The functional unit for the present study was defined as the total powder produced from 0.1 Kg total weight of raw material (Ti64) [232]. This small amount of raw material was chosen due to the capability of designed BM equipment used in the present study that processes a small amount of powder in a single batch. For both the processes, the system

boundaries were defined as per the cradle-to-gate variant of LCA and the same is shown in **Fig. 5.1**. The rationale for choosing the cradle-to-gate variant is due to the nature of the assessment, which is a partial product life cycle from the resource extraction (cradle) to the factory gate, just before it is transported to the consumers (gate).

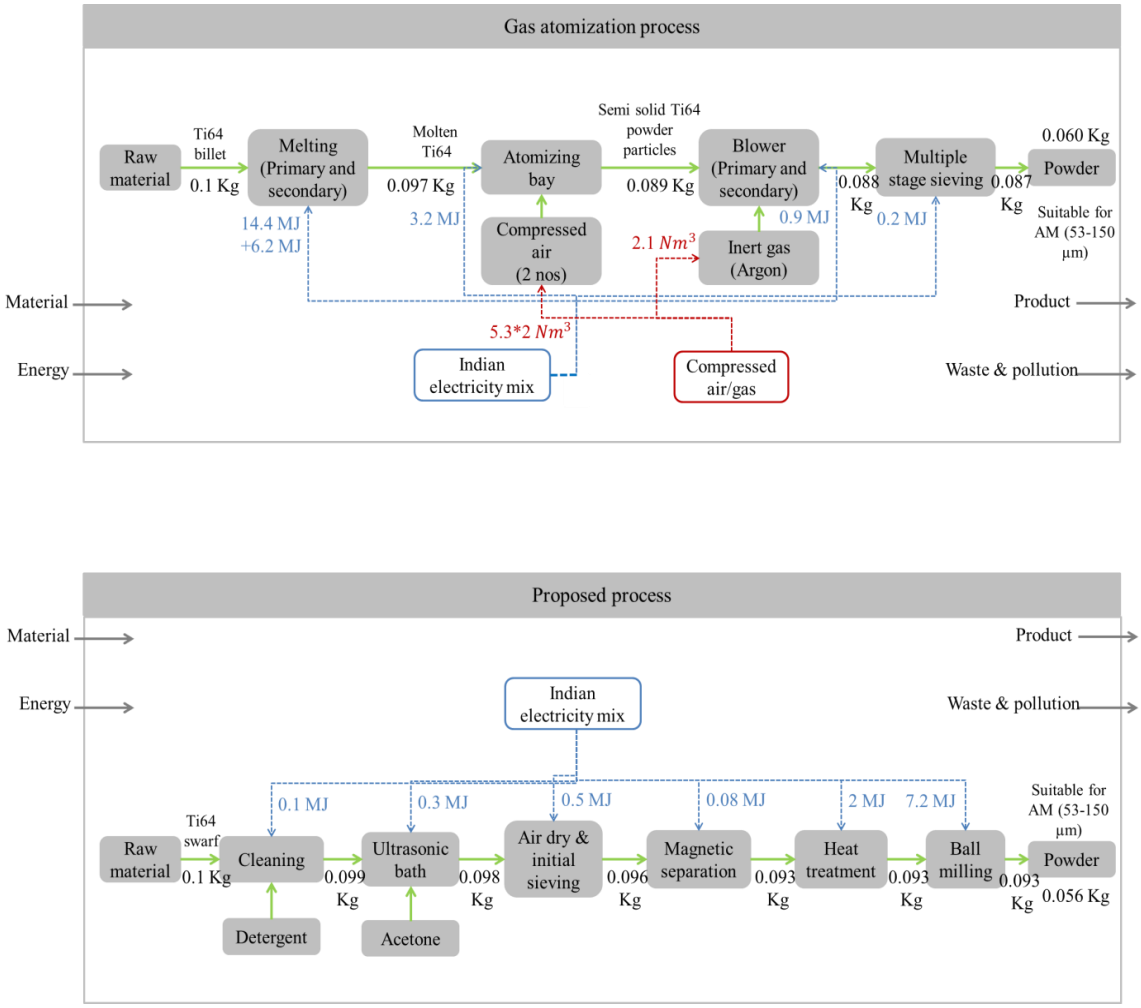

Fig. 5.1 *System boundaries for gas atomization and proposed process.*

5.1.3. Life cycle inventory analysis

For the inventory analysis, the primary data (BM, heat treatment, and cleaning) was collected using real-time observation during the powder production. Also, the secondary data (mostly the energy sources for GA sub-processes) was taken from reports, data product catalogs, and existing literature in journals and reference books. The inventory data for both processes is shown in **Table 5.1**.

Table 5.1 *Inventory data used in comparative life cycle assessment study.*

Gas atomization process				
S.No.	**Energy/material**	**Unit**	**Quantity**	**Ref.**
1	Ti64 billet	Kg	0.1	Kept fixed
2	Electrical energy for Ti64 melting (primary and secondary)	MJ/0.1 Kg Ti64 billet	(11.4+6.2) = 20.60	[233]
3	Electrical energy for other processes	MJ/0.1 Kg Ti64 billet	4.31	[234]
4	Compressed air (>10 bar)	Nm^3/0.1 Kg Ti64 billet	5.3*2 = 10.62	[235] [236]
5	Inert gas (argon)	Nm^3/0.1 Kg Ti64 billet	2.10	[233]
Proposed method				
1	Ti64 swarf	Kg	0.1	Kept fixed
2	Electrical energy for BM of Ti alloys (size reduction from 400 to 10 µm)	MJ/0.1 Kg Ti64 swarf	7.22	Calculated and adjusted with [237]
3	Electrical energy for other processes	MJ/0.1 Kg Ti64 swarf	2.98	Calculated
4	Acetone	l/0.1 Kg Ti64 swarf	0.2	Calculated
5	Detergent (liquid)	l/0.1 Kg Ti64 swarf	0.005	Calculated
6	Water for cleaning	l/0.1 Kg Ti64 swarf	0.5	Calculated

5.1.4. Life cycle impact assessment

The final and last stage of LCA is life cycle impact assessment. Environmental impact was assessed using GWP and associated eco-cost. GWP was quantified by measuring the total amount of CO_2 equivalents emitted into the atmosphere. Eco-cost gives the preventive cost of the aggregate effects of human toxicity, eco-toxicity, and resource

depletion [238]. The respective data for CO_2 equivalents and eco-cost was accessed from the open-source database Idemat by [234] and is shown in **Table 5.2**.

Table 5.2 *Environmental impact assessment (data taken from open-source database Idemat* [234]*).*

S.No.	Energy/material	GWP (Kg CO_2 equivalent)	Eco-cost (external cost includes the preventive cost of human toxicity, resource depletion, and eco-toxicity)
1	Ti64 billet	4.46/Kg	84.30 INR/Kg
2	Indian electricity mix	0.93 kg/kWh	214.80 INR/100MJ
3	Compressed air	0.176 Kg/Kg	3.30 INR/Kg
4	Inert gas (argon)	0.18 Kg/Kg	3.98 INR/Kg
5	Acetone	1.40 Kg/l	17.82 INR/l
6	Detergent	10.1 Kg/l	103.01 INR/l

5.1.5. Results of life cycle assessment

The results for the endpoint assessment are shown in **Fig. 5.2**. It can be observed from the figure that for 0.1 Kg raw material, GER (Gross Energy Requirement) for the GA process is 59% more as compared to the proposed process. This huge difference in GER is primarily due to the energy-intensive melting stage (20.60 MJ/ 0.1 Kg Ti64) in the GA process. Metallurgical smoke generated during this stage contains minute particles of metal powders and toxic substances (NO_2, silica, magnesia, calcium oxide, and alkali oxides) which are highly dangerous for living beings and its continuous exposure can cause severe health issues in a long run [239]. Besides, the atomization bay also consumes a significant amount of energy (3.2 MJ/0.1 Kg Ti64) in the form of electricity. These stages are thus a major contributor to the GWP and total eco-cost associated with the GA process. In another LCA study on metal powders, the GWP due to energy consumption was found to be substantially higher than any of the other associated sub-process [240]. A high-pressure jet of extremely pure inert gases like argon and helium is used to atomize the melted metal in the GA process [73]. A high value of associated GWP (0.176 Kg/Kg) and eco-cost (3.98 INR/Kg) proved its deteriorating impact on the

environment. Prolonged work in an environment having a high concentration of such gases is not safe for onsite workers [241]. However, the leftover grey-acetone in the proposed process is not a hazardous air pollutant, and it is broken down by microorganisms in soil and water (eco-cost: 17.82 INR/l). But, the phosphates in detergents can cause freshwater algal blooms, which emit toxins and reduce oxygen levels in waterways thus, leads to its high associated eco-cost (103.01 INR/l) [242]. Thus, the consumption of these consumables should be minimized and some better alternatives can be explored.

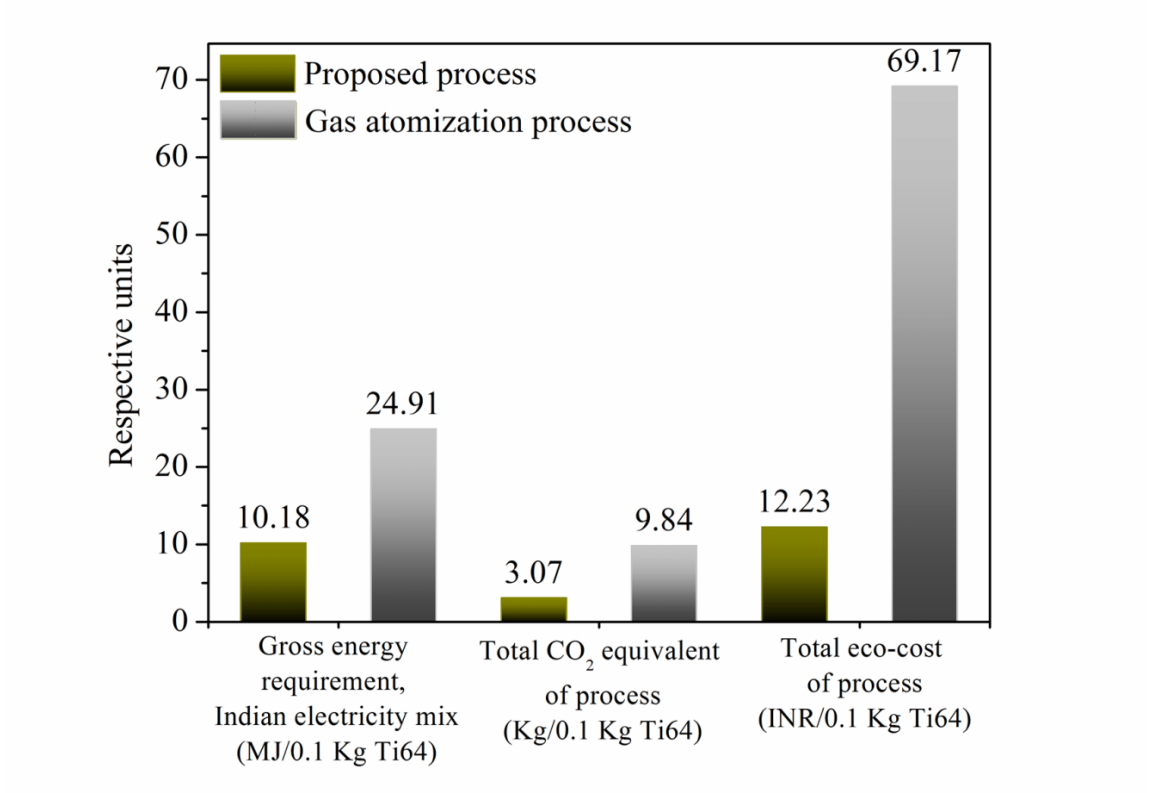

Fig. 5.2 *Life cycle assessment results for Ti6Al4V powder produced from gas atomization and the proposed method.*

5.2. ASSOCIATED COST

Large scale and continuous operation of the GA process is very difficult to maintain due to the high expenditure of consumables, thus the total cost of the process is increased by the yield loss factor [74]. As the yields can vary from 20-90 % depending upon the scale of operation, issues such as tundish skull losses and dust losses to filters further reduce the overall yield. This leads to the high cost (25-45 k INR for Ti64) of commercial powder feedstock for AM, which is not economical for the manufacturing of products on

a large scale [243]. The total equipment cost of the GA process (1000-2000 k INR) is very high due to the presence of complex sub-systems like atomization bay and the availability of highly controlled environment chambers [244]. Highly skilled labour is vital to run and monitor the sophisticated GA system.

Contrarily, in the proposed process, the cost of the final powder can further be reduced by shifting the processing mode from batch to continuous due to the non-utilization of expensive consumables (**Fig. 5.3**). The yield of the proposed process is directly dependent on the size of the BM apparatus i.e., for a fixed time interval, the output can be regulated by varying the cylinder diameter. Raw material in the form of swarf (pre-sorted in the industry) comes at a very cheap price contrary to high purity billets used in GA. Also, the absence of the melting stage which changes the physical state of the raw material (solid to liquid), and the absence of consumables like inert gases contribute to the sustainability based on the total GWP and associated eco-cost. Plant safety is high in the case of the proposed method due to the harmless action of the BM process. More technical and scientific interventions in the proposed process will further reduce the environmental footprint of the known hotspots.

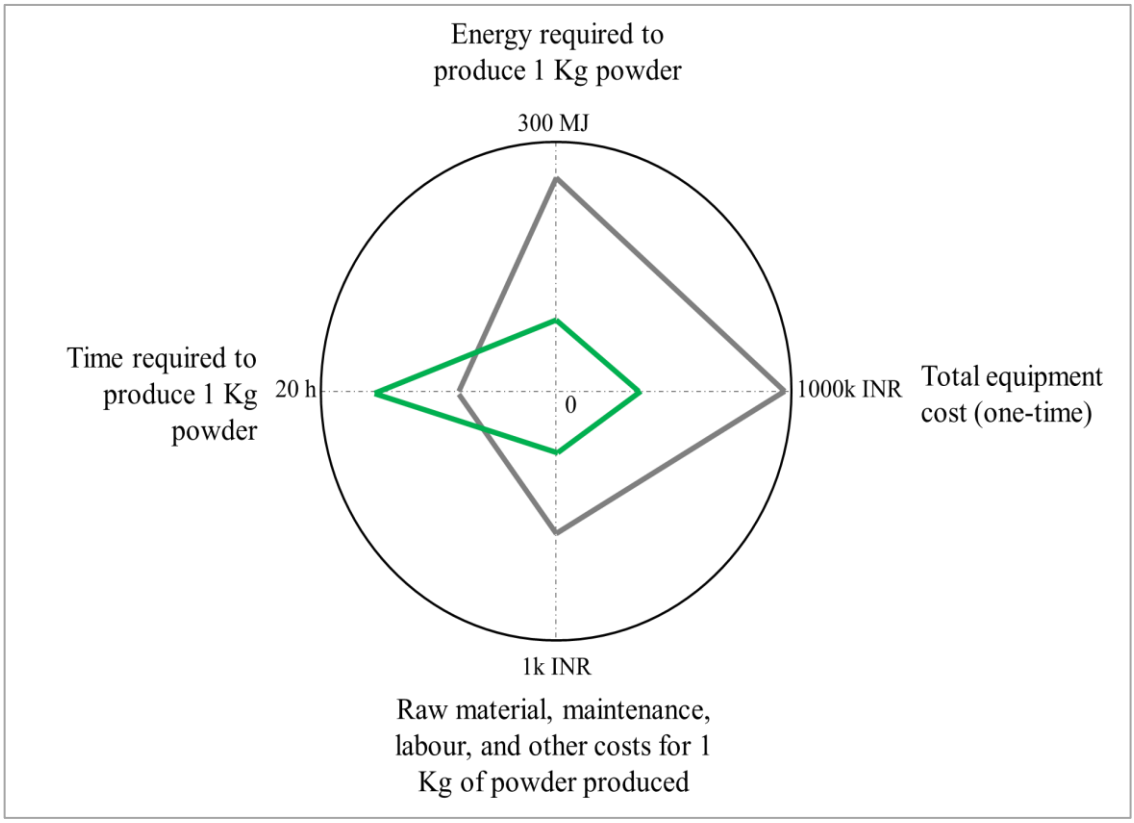

Fig. 5.3 *Associated cost and time for both gas atomization and proposed process.*

CHAPTER 6

CONCLUSIONS AND FUTURE SCOPE

6.1. CONCLUSIONS

This study examines the clean conversion of Ti64 cutting swarf to powder feedstock for AM. Such powder is important to investigate various factors before being qualified as a feedstock. Based on such investigations, the following conclusions are made:

1. Particle size reduces largely with Ø 25 balls (~ 40%) followed by Ø 12.5 balls (~ 12%) and Ø 6.25 balls (~ 5%) due to impact force by balls of bigger diameter. Morphology modifies largely with Ø 6.25 balls due to the abrasion phenomenon.
2. The hardness value of powder increases linearly with an increase in milling time up to 430 HV. This increase in hardness is attributed to the work hardening and oxygen pickup by Ti64 powder.
3. The value of α for 3S-18H powder is closer to that of GA powder due to the enhanced flowability of the particles with near-spherical morphology. It also shows better spreadability due to the more homogeneous morphology as compared to 2S-12H and 1S-6H powder.
4. Comparative suitable parameters for melting of 3S-18H powder are a scanning speed of 1000 mm/s and laser power of 310 W. Inadequate melting and transverse cracks along the length of single tracks are also observed.
5. In DMLS, with an increase in SS, the width of single tracks decreases (~ 4 %), and with an increase in LP, it increases (~ 10 %). The overall hardness of single track builds with 3S-18H powder is better (~ 4-7 %) as compared to the same generated with GA powder at the same parameters.
6. The proposed method consumes less energy (~ 59 %), has low eco-cost (~ 82 %), and has less GWP (~ 68 %) as compared to the GA and thus, has the potential to produce powders with regulated characteristics from Ti64 swarf.

6.2. FUTURE SCOPE

Metal waste is a type of waste that can be recycled based on the type of material and impurity involved. In the present study, a framework has been proposed for the clean conversion of Ti64 swarf into powder using multi-stage ball milling without the energy-intensive HDH process. The developed framework has been shown advantageous as compared to other recycling techniques on environmental impact, cost, and quality basis. Despite the constructive and favourable results, the use of such feedstock powder in the actual industrious environment has not been observed on a large scale.

Thus, the present study has raised a gap related to the industrial use of this recycled powder feedstock. The research gap found in this study is the cost generation model for recycled metal powders, health hazards, availability of standards, and government policies for its use. Thus, the future study will attempt to bridge the gap between industry and academia by identifying the non-technical barriers to the use of recycled powders of Ti64.

REFERENCES

[1] Rusinko C. Green manufacturing: an evaluation of environmentally sustainable manufacturing practices and their impact on competitive outcomes. IEEE Trans Eng Manag 2007;54:445–54.

[2] Doaemo W, Dhiman S, Borovskis A, Zhang W, Bhat S, Jaipuria S, et al. Assessment of municipal solid waste management system in Lae City, Papua New Guinea in the context of sustainable development. Environ Dev Sustain 2021. https://doi.org/10.1007/s10668-021-01465-2.

[3] Mauthoor S, Mohee R, Kowlesser P. An assessment on the recycling opportunities of wastes emanating from scrap metal processing in Mauritius. Waste Manag 2014;34:1800–5. https://doi.org/https://doi.org/10.1016/j.wasman.2013.12.014.

[4] Newman ST, Zhu Z, Dhokia V, Shokrani A. Process planning for additive and subtractive manufacturing technologies. CIRP Ann 2015;64:467–70.

[5] Pusavec F, Kramar D, Krajnik P, Kopac J. Transitioning to sustainable production–part II: evaluation of sustainable machining technologies. J Clean Prod 2010;18:1211–21.

[6] Carmignani G. Scrap value stream mapping (S-VSM): a new approach to improve the supply scrap management process. Int J Prod Res 2017;55:3559–76. https://doi.org/10.1080/00207543.2017.1308574.

[7] Singh S, Ramakrishna S, Gupta MK. Towards zero waste manufacturing: A multidisciplinary review. J Clean Prod 2017;168:1230–43. https://doi.org/https://doi.org/10.1016/j.jclepro.2017.09.108.

[8] Haider J, Hashmi M s. J. Health and Environmental Impacts in Metal Machining Processes. Compr Mater Process 2014;8:7–33. https://doi.org/10.1016/B978-0-08-096532-1.00804-9.

[9] Jordon JB, Allison PG, Phillips BJ, Avery DZ, Kinser RP, Brewer LN, et al. Direct recycling of machine chips through a novel solid-state additive manufacturing process. Mater Des 2020:108850. https://doi.org/https://doi.org/10.1016/j.matdes.2020.108850.

[10] He P, Feng H, Hu G, Hewage K, Achari G, Wang C, et al. Life cycle cost analysis for recycling high-tech minerals from waste mobile phones in China. J Clean Prod 2020;251:119498. https://doi.org/https://doi.org/10.1016/j.jclepro.2019.119498.

[11] Cooper DR, Song J, Gerard R. Metal recovery during melting of extruded machining chips. J Clean Prod 2018;200:282–92. https://doi.org/https://doi.org/10.1016/j.jclepro.2018.07.246.

[12] Zhang J, Pang X, Chen H, Shi G, Deng W. Process and forming performance of ploughing extrusion cutting for recycling of metal chips. J Mater Process Technol 2019;274:116283. https://doi.org/https://doi.org/10.1016/j.jmatprotec.2019.116283.

[13] Wędrychowicz M, Wzorek Ł, Tokarski T, Noga P, Wiewióra J. Recycling without melting: an alternative approach to aluminum scrap recovery. Key Eng. Mater., vol. 682, Trans Tech Publ; 2016, p. 284–9.

[14] Macintosh WH. Induction furnaces for melting secondary aluminium. Conserv Recycl 1983;6:41–8. https://doi.org/https://doi.org/10.1016/0361-3658(83)90015-2.

[15] Shamsudin S, Lajis MA, Zhong ZW. Evolutionary in Solid State Recycling Techniques of Aluminium: A review. Procedia CIRP 2016;40:256–61. https://doi.org/https://doi.org/10.1016/j.procir.2016.01.117.

[16] Castro MM, Pereira PHR, Isaac A, Figueiredo RB, Langdon TG. Development of a magnesium-alumina composite through cold consolidation of machining chips by high-pressure torsion. J Alloys Compd 2019;780:422–7. https://doi.org/https://doi.org/10.1016/j.jallcom.2018.11.357.

[17] Mahmood K, Stevens N, Pinkerton AJ. Laser surface modification using Inconel 617 machining swarf as coating material. J Mater Process Technol 2012;212:1271–80. https://doi.org/https://doi.org/10.1016/j.jmatprotec.2012.01.014.

[18] Johansson J, Ivarsson L, Ståhl J-E, Bushlya V, Schultheiss F. Hot Forging Operations of Brass Chips for Material Reclamation after Machining Operations. Procedia Manuf 2017;11:584–92. https://doi.org/https://doi.org/10.1016/j.promfg.2017.07.152.

[19] Paraskevas D, Vanmeensel K, Vleugels J, Dewulf W, Deng Y, Duflou JR. Spark Plasma Sintering As a Solid-State Recycling Technique: The Case of Aluminum Alloy Scrap Consolidation. Mater (Basel, Switzerland) 2014;7:5664–87. https://doi.org/10.3390/ma7085664.

[20] Tekkaya AE, Schikorra M, Becker D, Biermann D, Hammer N, Pantke K. Hot profile extrusion of AA-6060 aluminum chips. J Mater Process Technol 2009;209:3343–50. https://doi.org/https://doi.org/10.1016/j.jmatprotec.2008.07.047.

[21] Baffari D, Buffa G, Ingarao G, Masnata A, Fratini L. Aluminium sheet metal scrap recycling through friction consolidation. Procedia Manuf 2019;29:560–6. https://doi.org/https://doi.org/10.1016/j.promfg.2019.02.134.

[22] Luo P, McDonald DT, Zhu SM, Palanisamy S, Dargusch MS, Xia K. Analysis of microstructure and strengthening in pure titanium recycled from machining chips by equal channel angular pressing using electron backscatter diffraction. Mater Sci Eng A 2012;538:252–8. https://doi.org/https://doi.org/10.1016/j.msea.2012.01.039.

[23] HU M, JI Z, CHEN X, WANG Q, DING W. Solid-state recycling of AZ91D magnesium alloy chips. Trans Nonferrous Met Soc China 2012;22:s68–73. https://doi.org/https://doi.org/10.1016/S1003-6326(12)61685-9.

[24] Mahmood K, Syed WUH, Pinkerton AJ. Innovative reconsolidation of carbon steel machining swarf by laser metal deposition. Opt Lasers Eng 2011;49:240–7. https://doi.org/https://doi.org/10.1016/j.optlaseng.2010.09.014.

[25] Rane KK, Date PP. Sustainable recycling of ferrous metallic scrap using powder metallurgy process. J Sustain Metall 2017;3:251–64.

[26] Chiba R, Yoshimura M. Solid-state recycling of aluminium alloy swarf into c-channel by hot extrusion. J Manuf Process 2015;17:1–8. https://doi.org/https://doi.org/10.1016/j.jmapro.2014.10.002.

[27] Misiolek W, Haase M, Ben Khalifa N, Tekkaya A, Kleiner M. High quality extrudates from aluminum chips by new billet compaction and deformation routes. CIRP Ann - Manuf Technol 2012;61:239–42. https://doi.org/10.1016/j.cirp.2012.03.113.

[28] Vartak VR, Shanker A, Nath D, Sharma CS. Compacting Characteristics of Cast Iron Powder Prepared from Machining Swarf BT - Proceedings of the Twenty-Sixth International Machine Tool Design and Research Conference: held in Manchester 17th–18th September 1986. In: Davies BJ, editor., London: Macmillan Education UK; 1986, p. 437–42. https://doi.org/10.1007/978-1-349-08114-1_56.

[29] Cullen JM, Allwood JM. Mapping the Global Flow of Aluminum: From Liquid Aluminum to End-Use Goods. Environ Sci Technol 2013;47:3057–64. https://doi.org/10.1021/es304256s.

[30] Goonan TG. Titanium Recycling in the United States in 2004. Flow Stud Recycl Met Commod United States 2004:1–16.

[31] Kumar S, Kumar R, Bandopadhyay A. Innovative methodologies for the utilisation of wastes from metallurgical and allied industries. Resour Conserv Recycl 2006;48:301–14. https://doi.org/https://doi.org/10.1016/j.resconrec.2006.03.003.

[32] RUF Briquetting systems 2020. https://www.briquetting.com/ (accessed October 20, 2020).

[33] PALLMANN Industries 2019. http://www.pallmannindustries.com/ (accessed October 20, 2020).

[34] WEIMA 2019. https://weima.com/us/ (accessed October 20, 2020).

[35] NEDERMAN n.d. https://www.nederman.com/en/ (accessed October 20, 2020).

[36] Stansz Environment Systems 2020. https://www.stansz.nl/en/ (accessed October 20, 2020).

[37] SIMOLIN WATER & ENERGY LTD 2020. http://www.simolingroup.com/wordpress/recycling/briquetting/ (accessed October 20, 2020).

[38] CO.MA.FER MACCHINE 2020. https://www.comafer.it/en/product-category/metal (accessed October 20, 2020).

[39] Metso 2020. https://www.metso.com/ (accessed October 20, 2020).

[40] Equipment Manufacturers International (EMI) 2019. https://www.emi-inc.com/about-us/ (accessed October 20, 2020).

[41] Applied Recovery Systems 2019. https://ars-inc.com/ (accessed October 20, 2020).

[42] JOHN HART Advanced Manufacturing Technologies 2020. https://johnhart.com.au/ (accessed October 20, 2020).

[43] PRAB A Global Company 2020. https://www.prab.com/ (accessed October 20, 2020).

[44] POSSTECH 2019. http://posstech.co.kr/?page_id=491&ckattempt=1 (accessed October 20, 2020).

[45] Anyang Forging Press (Group) Machinery Industry Co., Ltd. 2019. http://www.chinesehammers.com/EngLish/channels/metal-briquetter.html (accessed October 20, 2020).

[46] AMADA Machinery 2020. https://www.amc.amada.co.jp/en/english/products/cutting/other/scp100h_10/ (accessed October 20, 2020).

[47] Baffari D, Buffa G, Campanella D, Fratini L. Design of continuous Friction Stir Extrusion machines for metal chip recycling: issues and difficulties. Procedia Manuf 2018;15:280–6. https://doi.org/https://doi.org/10.1016/j.promfg.2018.07.220.

[48] Aboussouan L, Russo P, Pons M-N, Thomas D, Birat JP, Leclerc D. Steel scrap fragmentation by shredders. Powder Technol 1999;105:288–94.

[49] Fullenwider B, Kiani P, Schoenung JM, Ma K. Two-stage ball milling of recycled machining chips to create an alternative feedstock powder for metal additive manufacturing. Powder Technol 2019;342:562–71. https://doi.org/10.1016/J.POWTEC.2018.10.023.

[50] Chen G, Zhao SY, Tan P, Wang J, Xiang CS, Tang HP. A comparative study of Ti-6Al-4V powders for additive manufacturing by gas atomization, plasma rotating electrode process and plasma atomization. Powder Technol 2018;333:38–46. https://doi.org/https://doi.org/10.1016/j.powtec.2018.04.013.

[51] Dunkley JJ. Metal Powder Atomisation Methods for Modern Manufacturing. Johnson Matthey Technol Rev 2019;63:226–32. https://doi.org/10.1595/205651319x15583434137356.

[52] Hausnerova B, Mukund BN, Sanetrnik D. Rheological properties of gas and water atomized 17-4PH stainless steel MIM feedstocks: Effect of powder shape and size. Powder Technol 2017;312:152–8. https://doi.org/https://doi.org/10.1016/j.powtec.2017.02.023.

[53] Beckers D, Ellendt N, Fritsching U, Uhlenwinkel V. Impact of process flow conditions on particle morphology in metal powder production via gas atomization. Adv Powder Technol 2019. https://doi.org/https://doi.org/10.1016/j.apt.2019.10.022.

[54] León GP de, Lamberti VE, Seals RD, Abu-Lebdeh TM, Hamoush SA. Gas atomization of molten metal: PartI. Numerical modeling conception. Am J Eng Appl Sci 2016;9:303–22. https://doi.org/10.3844/ajeassp.2016.303.322.

[55] Chen Y. Chapter 3 - Solid-state formation of carbon nanotubes. In: Dai LBT-CN, editor., Amsterdam: Elsevier; 2006, p. 53–80. https://doi.org/https://doi.org/10.1016/B978-044451855-2/50006-1.

[56] Gou J, Zhuge J, Liang F. 4 - Processing of polymer nanocomposites. In: Advani SG, Hsiao K-TBT-MT for PMC (PMCs), editors. Woodhead Publ. Ser. Compos. Sci. Eng., Woodhead Publishing; 2012, p. 95–119. https://doi.org/https://doi.org/10.1533/9780857096258.1.95.

[57] Senkov O, Srisukhumbowornchai N, Öveçoğlu L, Froes F. High-temperature stability of nanocrystalline structure in a TiAl alloy prepared by mechanical alloying and hot isostatic pressing. J Mater Res 1998;13:3399–410. https://doi.org/10.1557/JMR.1998.0463.

[58] Li R, Shi Y, Wang Z, Wang L, Liu J, Jiang W. Densification behavior of gas and water atomized 316L stainless steel powder during selective laser melting. Appl Surf Sci 2010;256:4350–6. https://doi.org/https://doi.org/10.1016/j.apsusc.2010.02.030.

[59] Popovich A, Sufiiarov V. Metal Powder Additive Manufacturing, 2016, p. 215–36. https://doi.org/10.5772/63337.

[60] Samuel M. A new technique for recycling aluminium scrap. J Mater Process Technol 2003;135:117–24. https://doi.org/https://doi.org/10.1016/S0924-0136(02)01133-0.

[61] Dhiman S, Sidhu SS, Bains PS, Bahraminasab M. Mechanobiological assessment of Ti-6Al-4V fabricated via selective laser melting technique: a review. Rapid Prototyp J 2019;25:1266–84. https://doi.org/10.1108/RPJ-03-2019-0057.

[62] Zhang Y, Lu W, Sun P, Fang ZZ, Qiao S, Zhang Y, et al. Deoxygenation of Ti metal: A review of processes in literature. Int J Refract Met Hard Mater 2020;91:105270. https://doi.org/https://doi.org/10.1016/j.ijrmhm.2020.105270.

[63] Bomberger HB, Froes FH. The Melting of Titanium. JOM 1984;36:39–47. https://doi.org/10.1007/BF03339212.

[64] Martchek KJ. The importance of recycling to the environmental profile of metal products. Proc TMS Fall Extr Process Conf 2000;4th Intern:19–28. https://doi.org/10.1002/9781118788073.ch2.

[65] Cirtina D, Ionescu N, Cirtina LM. Environmental impact assessement related to metallurgical industry activities. Metalurgija 2016;55:481–4.

[66] Rotmann B, Friedrich B, Lochbichler C. Challenges in titanium recycling - Do we need a new specification for secondary alloys? Proc - Eur Metall Conf EMC 2011 2011;4:1465–80.

[67] Gökelma M, Celik D, Tazegul O, Cimenoglu H, Friedrich B. Characteristics of TI6AL4V powders recycled from turnings via the HDH technique. Metals (Basel) 2018;8. https://doi.org/10.3390/met8050336.

[68] Umeda J, Mimoto T, Imai H, Kondoh K. Powder Forming Process from Machined Titanium Chips via Heat Treatment in Hydrogen Atmosphere. Mater Trans 2017;58:1702–7. https://doi.org/10.2320/matertrans.Y-M2017833.

[69] Hamayun MH, Hussain M, Maafa IM, Aslam R. Integration of hydrogenation and dehydrogenation system for hydrogen storage and electricity generation – simulation study. Int J Hydrogen Energy 2019;44:20213–22. https://doi.org/https://doi.org/10.1016/j.ijhydene.2019.06.053.

[70] Fedina T, Sundqvist J, Powell J, Kaplan AFH. A comparative study of water and gas atomized low alloy steel powders for additive manufacturing. Addit Manuf 2020;36:101675. https://doi.org/https://doi.org/10.1016/j.addma.2020.101675.

[71] Abu-Lebdeh TM, Leon GP, Hamoush SA, Seals RD, Lamberti VE. Gas atomization of molten metal: part II. Applications. Am J Eng Appl Sci 2016;9.

[72] Lagutkin S, Achelis L, Sheikhaliev S, Uhlenwinkel V, Srivastava V. Atomization process for metal powder. Mater Sci Eng A 2004;383:1–6.

[73] Tsirlis M, Michailidis N. Low-pressure gas atomization of aluminum through a Venturi nozzle. Adv Powder Technol 2020;31:1720–7. https://doi.org/https://doi.org/10.1016/j.apt.2020.02.011.

[74] Dunkley JJ. 1 - Advances in atomisation techniques for the formation of metal powders. In: Chang I, Zhao YBT-A in PM, editors. Woodhead Publ. Ser. Met. Surf. Eng., Woodhead Publishing; 2013, p. 3–18. https://doi.org/https://doi.org/10.1533/9780857098900.1.3.

[75] Neikov OD. Chapter 3 - Mechanical Alloying. In: Neikov OD, Naboychenko SS, Yefimov NABT-H of N-FMP (Second E, editors., Oxford: Elsevier; 2019, p. 91–124. https://doi.org/https://doi.org/10.1016/B978-0-08-100543-9.00003-8.

[76] Goncharov IS, Razumov NG, Silin AO, Ozerskoi NE, Shamshurin AI, Kim A, et al. Synthesis of Nb-based powder alloy by mechanical alloying and plasma spheroidization processes for additive manufacturing. Mater Lett 2019;245:188–91. https://doi.org/https://doi.org/10.1016/j.matlet.2019.03.014.

[77] Suryanarayana C. Mechanical Alloying: A Novel Technique to Synthesize Advanced Materials. Research 2019;2019:1–17. https://doi.org/10.34133/2019/4219812.

[78] Hong S-H, Kim B-K. Effects of lifter bars on the ball motion and aluminum foil milling in tumbler ball mill. Mater Lett 2002;57:275–9. https://doi.org/https://doi.org/10.1016/S0167-577X(02)00778-4.

[79] Krycer I, Hersey JA. Grinding and granulation in a vibratory ball mill. Powder Technol 1981;28:91–5. https://doi.org/https://doi.org/10.1016/0032-5910(81)87015-5.

[80] Rosenkranz S, Breitung-Faes S, Kwade A. Experimental investigations and modelling of the ball motion in planetary ball mills. Powder Technol 2011;212:224–30. https://doi.org/https://doi.org/10.1016/j.powtec.2011.05.021.

[81] Bulgakov V, Pascuzzi S, Ivanovs S, Kaletnik G, Yanovich V. Angular oscillation model to predict the performance of a vibratory ball mill for the fine grinding of grain. Biosyst Eng 2018;171:155–64. https://doi.org/https://doi.org/10.1016/j.biosystemseng.2018.04.021.

[82] Guzzo PL, Marinho de Barros FB, Soares BR, Santos JB. Evaluation of particle size reduction and agglomeration in dry grinding of natural quartz in a planetary ball mill. Powder Technol 2020;368:149–59. https://doi.org/https://doi.org/10.1016/j.powtec.2020.04.052.

[83] Piras CC, Fernández-Prieto S, De Borggraeve WM. Ball milling: A green technology for the preparation and functionalisation of nanocellulose derivatives. Nanoscale Adv 2019;1:937–47. https://doi.org/10.1039/c8na00238j.

[84] Alex TC, Kumar R, Roy SK, Mehrotra SP. Mechanically induced reactivity of gibbsite: Part 2. Attrition milling. Powder Technol 2014;264:229–35. https://doi.org/https://doi.org/10.1016/j.powtec.2014.05.029.

[85] Liang Y, Wu Z, Fu E, Du J, Wang P, Zhao Y, et al. Refinement process and mechanisms of tungsten powder by high energy ball milling. Int J Refract Met Hard Mater 2017;67. https://doi.org/10.1016/j.ijrmhm.2017.04.006.

[86] Almotairy SM, Alharthi NH, Abdo HS. Regulating Mechanical Properties of Al/SiC by Utilizing Different Ball Milling Speeds. Cryst 2020;10. https://doi.org/10.3390/cryst10040332.

[87] Hadef F, Otmani A, Djekoun A, Grenèche JM. Nanocrystalline FeAl intermetallics obtained in mechanically alloyed Fe50Al40Ni10 powder. Superlattices Microstruct 2011;49:654–65. https://doi.org/https://doi.org/10.1016/j.spmi.2011.04.003.

[88] Wu ZM, Liang YX, Fan Y, Wang PP, Du JL, Zhao YB, et al. The ball to powder ratio (BPR) dependent morphology and microstructure of tungsten powder refined by ball milling. Powder Technol 2018;339:256–63. https://doi.org/https://doi.org/10.1016/j.powtec.2018.07.094.

[89] Amini Mashhadi H, Moloodi A, Golestanipour M, Karimi EZ V. Recycling of aluminium alloy turning scrap via cold pressing and melting with salt flux. J Mater Process Technol 2009;209:3138–42. https://doi.org/https://doi.org/10.1016/j.jmatprotec.2008.07.020.

[90] Joshi RS, Singh H. AN INVESTIGATION ON FLANK WEAR MECHANISM OF TUNGSTEN CARBIDE DRILLS DURING CONVENTIONAL AND MODULATION ASSISTED DRILLING. Mach Sci Technol 2014;18:99–119. https://doi.org/10.1080/10910344.2014.863647.

[91] Lengyel B, Tan CL, Teh GG. Hot Re-pressing of Powder Made from Mild Steel Machining Swarf. Powder Metall 1976;19:134–40. https://doi.org/10.1179/pom.1976.19.3.134.

[92] Rojas-Díaz LM, Verano-Jiménez LE, Muñoz-García E, Esguerra-Arce J, Esguerra-Arce A. Production and characterization of aluminum powder derived from mechanical saw chips and its processing through powder metallurgy. Powder Technol 2020;360:301–11. https://doi.org/https://doi.org/10.1016/j.powtec.2019.10.028.

[93] Souza J, Motta C, Machado T, Giacomin A, Arabi H. Analysis of Metallic Waste from Laser Cutting for Utilization in Parts Manufactured by Conventional Powder Metallurgy. Int J Res Eng Sci 2320-9356 2016;4:1.

[94] Daymi A, Boujelbene M, Ben Salem S, Sassi B, S T. Effect of the cutting speed on the chip morphology and the cutting forces. Arch Comput Mater Sci Surf Eng 2009;1.

[95] Yasir M, Ginta T, Ariwahjoedi B, Danish M, Alkali A. Evaluation of chips formation of AISI 316L SS using precision end-milling. J Eng Appl Sci 2016;11:12903.

[96] Morehead MD, Huang Y, Luo J. Chip morphology characterization and modeling in machining hardened 52100 steels. Mach Sci Technol 2007;11:335–54. https://doi.org/10.1080/10910340701567289.

[97] Su Y, Jia Z, Niu B, Bi G. Size effect of depth of cut on chip formation mechanism in machining of CFRP. Compos Struct 2017;164:316–27. https://doi.org/https://doi.org/10.1016/j.compstruct.2016.11.044.

[98] von Turkovich BF. Cutting Theory and Chip Morphology BT - Handbook of High-Speed Machining Technology. In: King RI, editor., Boston, MA: Springer US; 1985, p. 27–47. https://doi.org/10.1007/978-1-4684-6421-4_2.

[99] Iyengar HSR, Salmon R, Rice WB. Some Effects of Cutting Fluids on Chip Formation in Metal Cutting. J Eng Ind 1965;87:36–8. https://doi.org/10.1115/1.3670754.

[100] Garg S, Dornfeld D, Berger K. Formulation of the Chip Cleanability Mechanics from Fluid Transport BT - Burrs - Analysis, Control and Removal. In: Aurich JC, Dornfeld D, editors., Berlin, Heidelberg: Springer Berlin Heidelberg; 2010, p. 229–35.

[101] Yılmaz B, Karabulut Ş, Güllü A. Performance analysis of new external chip breaker for efficient machining of Inconel 718 and optimization of the cutting parameters. J Manuf Process 2018;32:553–63. https://doi.org/https://doi.org/10.1016/j.jmapro.2018.03.025.

[102] Singh M, Dhiman S, Singh H, Berndt CC. Optimization of modulation-assisted drilling of Ti-6Al-4V aerospace alloy via response surface method. Mater Manuf Process 2020:1–17. https://doi.org/10.1080/10426914.2020.1772487.

[103] Timmel G, Sander S, Schubert G. Comminution of scrap and metals in shredders with horizontally and vertically mounted rotor. In: Massacci PBT-D in MP, editor. Oral Sess., vol. 13, Elsevier; 2000, p. C12a-1-C12a-8. https://doi.org/https://doi.org/10.1016/S0167-4528(00)80091-5.

[104] Abdollahi H, Mahdavinejad R, Ghambari M, Moradi M. Investigation of green properties of iron/jet-milled grey cast iron compacts by response surface method. Proc Inst Mech Eng Part B J Eng Manuf 2013;228:493–503. https://doi.org/10.1177/0954405413502023.

[105] Fullenwider B, Kiani P, Schoenung JM, Ma K. From Recycled Machining Waste to Useful Powders for Metal Additive Manufacturing BT - REWAS 2019. In: Gaustad G, Fleuriault C, Gökelma M, Howarter JA, Kirchain R, Ma K, et al., editors., Cham: Springer International Publishing; 2019, p. 3–7.

[106] Wu S, Ji Z, Zhang T. Microstructure and mechanical properties of AZ31B magnesium alloy recycled by solid-state process from different size chips. J Mater Process Technol 2009;209:5319–24. https://doi.org/https://doi.org/10.1016/j.jmatprotec.2009.04.002.

[107] Qi Y, Timokhina IB, Shekhter A, Sharp K, Lapovok R. Optimization of upcycling of Ti-6Al-4V swarf. J Mater Process Technol 2018;255:853–64. https://doi.org/https://doi.org/10.1016/j.jmatprotec.2018.01.036.

[108] Afshari E, Ghambari M, Abdolmalek H. Production of CuSn10 bronze powder from machining chips using jet milling. Int J Adv Manuf Technol 2017;92:663–72. https://doi.org/10.1007/s00170-017-0126-3.

[109] Yılmaz B, Karabulut Ş, Güllü A. A review of the chip breaking methods for continuous chips in turning. J Manuf Process 2020;49:50–69. https://doi.org/https://doi.org/10.1016/j.jmapro.2019.10.026.

[110] Chiba R, Nakamura T, Kuroda M. Solid-state recycling of aluminium alloy swarf through cold profile extrusion and cold rolling. J Mater Process Technol 2011;211:1878–87. https://doi.org/https://doi.org/10.1016/j.jmatprotec.2011.06.010.

[111] de Martini Fernandes L, Lopes JC, Ribeiro FSF, Gallo R, Razuk HC, de Angelo Sanchez LE, et al. Thermal model for surface grinding application. Int J Adv Manuf Technol 2019;104:2783–93. https://doi.org/10.1007/s00170-019-04101-6.

[112] Dewanjee D, Kundu P, Sikder B, Biswas D, Mandal B, Das S. Comparison of Grinding Performance Under Different Eco-Friendly Environment BT - CAD/CAM, Robotics and Factories of the Future. In: Mandal DK, Syan CS, editors., New Delhi: Springer India; 2016, p. 33–41.

[113] Ito Y, Matsumura T. Raw Materials for Work, Engineering Materials and Swarf Discharge BT - Theory and Practice in Machining Systems. In: Ito Y, Matsumura T, editors., Cham: Springer International Publishing; 2017, p. 71–89. https://doi.org/10.1007/978-3-319-53901-0_3.

[114] Fang XD, Jawahir IS. An Analytical Model for Cyclic Chip Formation in 2-D Machining with Chip Breaking. CIRP Ann 1996;45:53–8. https://doi.org/https://doi.org/10.1016/S0007-8506(07)63016-9.

[115] Fang N, Jawahir IS, Oxley PLB. A universal slip-line model with non-unique solutions for machining with curled chip formation and a restricted contact tool. Int J Mech Sci 2001;43:557–80. https://doi.org/https://doi.org/10.1016/S0020-7403(99)00117-4.

[116] Capuzzi S, Timelli G. Preparation and Melting of Scrap in Aluminum Recycling: A Review. Met 2018;8. https://doi.org/10.3390/met8040249.

[117] Sander S, Schubert G, Jäckel H-G. The fundamentals of the comminution of metals in shredders of the swing-hammer type. Int J Miner Process 2004;74:S385–93. https://doi.org/https://doi.org/10.1016/j.minpro.2004.07.038.

[118] Li Q, Zhang L, Chen X, Wei D, Zhang P, Chen Y, et al. Characterization of plasma rotating electrode atomized Nb-Ti based alloy powder. Met Powder Rep 2020;75:82–91. https://doi.org/https://doi.org/10.1016/j.mprp.2019.04.064.

[119] Canakci A, Varol T. A novel method for the production of metal powders without conventional atomization process. J Clean Prod 2015:1–8. https://doi.org/10.1016/j.jclepro.2015.02.090.

[120] Dobbelstein H, Gurevich EL, George EP, Ostendorf A, Laplanche G. Laser metal deposition of compositionally graded TiZrNbTa refractory high-entropy alloys using elemental powder blends. Addit Manuf 2019;25:252–62. https://doi.org/https://doi.org/10.1016/j.addma.2018.10.042.

[121] Azevedo JMC, Serrenho AC, Allwood JM. The deformation of metal powder particles: hardness and microstructure. Procedia Eng 2017;207:1200–5. https://doi.org/https://doi.org/10.1016/j.proeng.2017.10.870.

[122] Fernández H, Ordoñez S, Pesenti H, González RE, Leoni M. Microstructure homogeneity of milled aluminum A356–Si3N4 metal matrix composite powders. J Mater Res Technol 2019;8:2969–77. https://doi.org/https://doi.org/10.1016/j.jmrt.2019.05.004.

[123] Guo W, Han Y, Li Y, Tang Z. Impact of ball filling rate and stirrer tip speed on milling iron ore by wet stirred mill: Analysis and prediction of the particle size distribution. Powder Technol 2021;378:12–8. https://doi.org/https://doi.org/10.1016/j.powtec.2020.09.052.

[124] Higashi M, Ozaki T. Powder property, microstructure, and creep behavior of a P/M Mo-Si-B based alloy. Mater Des 2020:109351. https://doi.org/https://doi.org/10.1016/j.matdes.2020.109351.

[125] Muñiz-Lerma JA, Nommeots-Nomm A, Waters KE, Brochu M. A comprehensive approach to powder feedstock characterization for powder bed fusion additive manufacturing: A case study on AlSi7Mg. Materials (Basel) 2018;11. https://doi.org/10.3390/ma11122386.

[126] Cooke A, Slotwinski J. Properties of metal powders for additive manufacturing: A review of the state of the art of metal powder property testing. Addit Manuf Mater Stand Test Appl 2015:21–48.

[127] Choudhary A, Ramavath P, Biswas P, Ravi N, Johnson R. Experimental Investigation on Flowability and Compaction Behavior of Spray Granulated Submicron Alumina Granules. ISRN Ceram 2013;2013:264194. https://doi.org/10.1155/2013/264194.

[128] Crouter A, Briens L. The effect of moisture on the flowability of pharmaceutical excipients. AAPS PharmSciTech 2014;15:65–74. https://doi.org/10.1208/s12249-013-0036-0.

[129] Shekunov B, Chattopadhyay P, Tong H, Chow A. Particle Size Analysis in Pharmaceutics: Principles, Methods and Applications. Pharm Res 2007;24:203–27. https://doi.org/10.1007/s11095-006-9146-7.

[130] A.B. S, N. H, G. L. Influence of the particle size distribution on surface quality and mechanical properties in AM steel parts. Rapid Prototyp J 2011;17:195–202. https://doi.org/10.1108/13552541111124770.

[131] Brika SE, Letenneur M, Dion CA, Brailovski V. Influence of particle morphology and size distribution on the powder flowability and laser powder bed fusion manufacturability of Ti-6Al-4V alloy. Addit Manuf 2020;31:100929. https://doi.org/https://doi.org/10.1016/j.addma.2019.100929.

[132] Landauer J, Kuhn M, Nasato DS, Foerst P, Briesen H. Particle shape matters – Using 3D printed particles to investigate fundamental particle and packing properties. Powder Technol 2020;361:711–8. https://doi.org/https://doi.org/10.1016/j.powtec.2019.11.051.

[133] Rosso M, Suśniak M, Dutkiewicz J, Karwan-Baczewska J, Actis Grande M. Structure Investigation of Ball Milled Composite Powder Based on AlSi5Cu2 Alloy Chips Modified by Sic Particles. Arch Metall Mater 2013.

[134] Prem G, Ragu M, Sivakumar R, Sasidharan S. Characterization of Cu Chips Producing Through High Energy Ball Milling 2015:1675–9.

[135] Mahboubi Soufiani A, Enayati MH, Karimzadeh F. Fabrication and characterization of nanostructured Ti6Al4V powder from machining scraps. Adv Powder Technol 2010;21:336–40. https://doi.org/https://doi.org/10.1016/j.apt.2009.12.018.

[136] Hadef F. Synthesis and disordering of B2 TM-Al (TM=Fe, Ni, Co) intermetallic alloys by high energy ball milling: A review. Powder Technol 2017;311:556–78. https://doi.org/https://doi.org/10.1016/j.powtec.2017.01.082.

[137] Azzaza S, Alleg S, Moumeni H, Nemamcha AR, Rehspringer JL, Greneche JM. Magnetic properties of nanostructured ball-milled Fe and Fe50Co50alloy. J Phys Condens Matter 2006;18:7257–72. https://doi.org/10.1088/0953-8984/18/31/020.

[138] Suryanarayana C. Mechanical alloying and milling. Prog Mater Sci 2001;46:1–184. https://doi.org/https://doi.org/10.1016/S0079-6425(99)00010-9.

[139] Li H, He J, Sun Q, Wang S. Effect of the environment on the morphology of Ni powder during high-energy ball milling. Mater Today Commun 2020;25:101288. https://doi.org/https://doi.org/10.1016/j.mtcomm.2020.101288.

[140] Mendonça C, Capellato P, Bayraktar E, Gatamorta F, Gomes J, Oliveira A, et al. Recycling Chips of Stainless Steel Using a Full Factorial Design. Met 2019;9. https://doi.org/10.3390/met9080842.

[141] Enayati MH, Bafandeh MR, Nosohian S. Ball milling of stainless steel scrap chips to produce nanocrystalline powder. J Mater Sci 2007;42:2844–8. https://doi.org/10.1007/s10853-006-1371-2.

[142] Afshari E, Ghambari M. Characterization of pre-alloyed tin bronze powder prepared by recycling machining chips using jet milling. Mater Des 2016;103:201–8. https://doi.org/https://doi.org/10.1016/j.matdes.2016.04.064.

[143] Shaibani ME, Ghambari M. Characterization and comparison of gray cast iron powder produced by target jet milling and high energy ball milling of machining scraps. Powder Technol 2011;212:278–83. https://doi.org/https://doi.org/10.1016/j.powtec.2011.06.002.

[144] Hong S-H, Lee D-W, Kim B-K. Manufacturing of Aluminum Flake Powder From Foil Scrap by Dry Ball Milling Process. J Mater Process Technol 2000;100:105–9. https://doi.org/10.1016/S0924-0136(99)00469-0.

[145] Canakci A, Varol T. A novel method for the production of metal powders without conventional atomization process. J Clean Prod 2015;99:312–9. https://doi.org/https://doi.org/10.1016/j.jclepro.2015.02.090.

[146] Afshari E, Ghambari M, Abdolmalek H. Production of CuSn10 bronze powder from machining chips using jet milling. Int J Adv Manuf Technol 2017:663–72. https://doi.org/10.1007/s00170-017-0126-3.

[147] Rubinstein MH, Gould P. Praticle Size Reduction in the Ball Mill. Drug Dev Ind Pharm 1987;13:81–92. https://doi.org/10.3109/03639048709040157.

[148] Fuziana YF, Warikh ARM, Lajis MA, Azam MA, Muhammad NS. Recycling aluminium (Al 6061) chip through powder metallurgy route. Mater Res Innov 2014;18:S6-354-S6-358. https://doi.org/10.1179/1432891714Z.000000000981.

[149] de Sales Pereira Mendonça C, dos Santos Ribeiro VA, Junqueira MM, Sachs D, Oliveira LA, Melo M de LNM, et al. Recycling Chips of Stainless Steel by High Energy Ball Milling. Mater Sci Forum 2018;930:454–9. https://doi.org/10.4028/www.scientific.net/MSF.930.454.

[150] Mendonça C de SP, Oliveira AF, Oliveira LA, Silva MR da, Melo M de LNM, Silva G. Structural and Magnetic Properties of Duplex Stainless steel (UNS S31803) Powders Obtained by high Energy Milling of Chips with Additions of NbC . Mater Res 2018;21.

[151] Lui EW, Palanisamy S, Dargusch MS, Xia K. Effects of chip conditions on the solid state recycling of Ti-6Al-4V machining chips. J Mater Process Technol 2016;238:297–304. https://doi.org/https://doi.org/10.1016/j.jmatprotec.2016.07.028.

[152] Liang JM, Jia MT, Guo XQ, Zhang DL. Microstructural evolution and microhardness change of Al–7wt%Si–0.3wt%Mg alloy granules/powder particles during high energy ball milling. Mater Sci Eng A 2014;590:307–13. https://doi.org/https://doi.org/10.1016/j.msea.2013.10.050.

[153] Roshan MR, Soltanpour M, Jahromi SAJ. Microstructural evolution of nanocrystalline chips particles produced via large strain machining during ball milling. Powder Technol 2013;249:134–9. https://doi.org/https://doi.org/10.1016/j.powtec.2013.07.028.

[154] Ahmed M, Pasha M, Nan W, Ghadiri M. A simple method for assessing powder spreadability for additive manufacturing. Powder Technol 2020;367:671–9. https://doi.org/https://doi.org/10.1016/j.powtec.2020.04.033.

[155] Hryha E, Riabov DBT-RM in MS and ME. Metal Powder Production for Additive Manufacturing, Elsevier; 2021. https://doi.org/https://doi.org/10.1016/B978-0-12-819726-4.00089-2.

[156] Zegzulka J, Gelnar D, Jezerska L, Ramirez-Gomez A, Necas J, Rozbroj J. Internal friction angle of metal powders. Metals (Basel) 2018;8:1–12. https://doi.org/10.3390/met8040255.

[157] Mehrabi M, Hassanpour A, Bayly A. An X-ray microtomography study of particle morphology and the packing behaviour of metal powders during filling, compaction and ball indentation processes. Powder Technol 2021;385:250–63. https://doi.org/https://doi.org/10.1016/j.powtec.2021.02.069.

[158] Zhang J, Gu D, Yang Y, Zhang H, Chen H, Dai D, et al. Influence of Particle Size on Laser Absorption and Scanning Track Formation Mechanisms of Pure Tungsten Powder During Selective Laser Melting. Engineering 2019;5:736–45. https://doi.org/https://doi.org/10.1016/j.eng.2019.07.003.

[159] Shaw L, Villegas J, Luo H, Zawrah M, Miracle D. Effects of process-control agents on mechanical alloying of nanostructured aluminum alloys. Metall Mater Trans A 2003;34:159–70. https://doi.org/10.1007/s11661-003-0217-7.

[160] Yang L. Effect of particle size on oxygen content and porosity of sintered Ti-6Al-4V 2015.

[161] Alamolhoda S, Heshmati-Manesh S, Ataie A, Badiei A. Role of Process Control Agents on Milling Behavior of Al and TiO2 Powder Mixture to Synthesize TiAl/Al2O3 Nano Composite. Int J Mod Phys Conf Ser 2012;05:638–45. https://doi.org/10.1142/S2010194512002577.

[162] Rocha CJ, Leal Neto RM, Gonçalves VS, Carvalho LL, Ambrozio Filho F. An investigation of the use of stearic acid as a process control agent in high energy ball milling of Nb-Al and Ni-Al powder mixtures. Mater Sci Forum 2003;416–418:144–9. https://doi.org/10.4028/www.scientific.net/msf.416-418.144.

[163] Kazantseva N, Krakhmalev P, Yadroitsev I, Fefelov A, Merkushev A, Ilyinikh M, et al. Oxygen and nitrogen concentrations in the Ti-6Al-4V alloy manufactured by direct metal laser sintering (DMLS) process. Mater Lett 2017;209:311–4. https://doi.org/https://doi.org/10.1016/j.matlet.2017.08.037.

[164] Pauzon C, Hryha E, Forêt P, Nyborg L. Effect of argon and nitrogen atmospheres on the properties of stainless steel 316 L parts produced by laser-powder bed fusion. Mater Des 2019;179:107873. https://doi.org/https://doi.org/10.1016/j.matdes.2019.107873.

[165] Babu NK, Kallip K, Leparoux M, Talari MK, AlOgab KA, Alqahtani NM. Phase Evolution during High Energy Cube Milling of Ti–6Al–4V–0.5 vol% TiC Powders Using Heptane and Tin as Process Control Agents (PCAs). Adv Eng Mater 2017;19:1600662. https://doi.org/https://doi.org/10.1002/adem.201600662.

[166] Kishore Babu N, Kallip K, Leparoux M, AlOgab KA, Talari MK, Alqahtani NM. High strength Ti-6Al-4V alloy fabricated by high-energy cube milling using calcium as process control agent (PCA) and spark plasma sintering. Int J Adv Manuf Technol 2017;93:445–53. https://doi.org/10.1007/s00170-017-9994-9.

[167] Nath AK, Jiten C, Singh KC. Influence of ball milling parameters on the particle size of barium titanate nanocrystalline powders. Phys B Condens Matter 2010;405:430–4. https://doi.org/https://doi.org/10.1016/j.physb.2009.08.299.

[168] Wu Z, Liang Y, Fu E, Du J, Wang P, Fan Y, et al. Effect of Ball Milling Parameters on the Refinement of Tungsten Powder. Met 2018;8. https://doi.org/10.3390/met8040281.

[169] Zhang F, Zhu M, Chengyong W. Parameters optimization in the planetary ball milling of nanostructured tungsten carbide/cobalt powder. Int J Refract Met Hard Mater 2008;26:329–33. https://doi.org/10.1016/j.ijrmhm.2007.08.005.

[170] Fogagnolo JB, Velasco F, Robert MH, Torralba JM. Effect of mechanical alloying on the morphology, microstructure and properties of aluminium matrix composite powders. Mater Sci Eng A 2003;342:131–43. https://doi.org/https://doi.org/10.1016/S0921-5093(02)00246-0.

[171] Saleem IY, Smyth HDC. Micronization of a soft material: air-jet and micro-ball milling. AAPS PharmSciTech 2010;11:1642–9. https://doi.org/10.1208/s12249-010-9542-5.

[172] Cacace S, Furlan V, Sorci R, Semeraro Q, Boccadoro M. Using recycled material to produce gas-atomized metal powders for additive manufacturing processes. J Clean Prod 2020;268:122218. https://doi.org/https://doi.org/10.1016/j.jclepro.2020.122218.

[173] Mahboubi Soufiani A, Enayati MH, Karimzadeh F. Fabrication and characterization of nanostructured Ti6Al4V powder from machining scraps. Adv Powder Technol 2010;21:336–40. https://doi.org/10.1016/j.apt.2009.12.018.

[174] Chen Q, Guillemot G, Gandin C-A, Bellet M. Numerical modelling of the impact of energy distribution and Marangoni surface tension on track shape in selective laser melting of ceramic material. Addit Manuf 2018;21:713–23. https://doi.org/https://doi.org/10.1016/j.addma.2018.03.003.

[175] Narra SP, Wu Z, Patel R, Capone J, Paliwal M, Beuth J, et al. Use of Non-Spherical Hydride-Dehydride (HDH) Powder in Powder Bed Fusion Additive Manufacturing. Addit Manuf 2020;34:101188. https://doi.org/https://doi.org/10.1016/j.addma.2020.101188.

[176] GUO Y, JIA L, KONG B, WANG N, ZHANG H. Single track and single layer formation in selective laser melting of niobium solid solution alloy. Chinese J Aeronaut 2018;31:860–6. https://doi.org/https://doi.org/10.1016/j.cja.2017.08.019.

[177] Yadroitsev I, Yadroitsava I, Bertrand P, Smurov I. Factor analysis of selective laser melting process parameters and geometrical characteristics of synthesized

single tracks. Rapid Prototyp J 2012;18:201–8. https://doi.org/10.1108/13552541211218117.

[178] Vaglio E, De Monte T, Lanzutti A, Totis G, Sortino M, Fedrizzi L. Single tracks data obtained by selective laser melting of Ti6Al4V with a small laser spot diameter. Data Br 2020;33:106443. https://doi.org/https://doi.org/10.1016/j.dib.2020.106443.

[179] Doubenskaia M, Domashenkov A, Smurov I, Petrovskiy P. Study of Selective Laser Melting of intermetallic TiAl powder using integral analysis. Int J Mach Tools Manuf 2018;129. https://doi.org/10.1016/j.ijmachtools.2018.02.003.

[180] Gunenthiram V, Peyre P, Schneider M, Dal M, Coste F, Fabbro R. Analysis of laser–melt pool–powder bed interaction during the selective laser melting of a stainless steel. J Laser Appl 2017;29:22303. https://doi.org/10.2351/1.4983259.

[181] Beese AM, Carroll BE. Review of mechanical properties of Ti-6Al-4V made by laser-based additive manufacturing using powder feedstock. Jom 2016;68:724–34.

[182] Slotwinski JA, Garboczi EJ, Stutzman PE, Ferraris CF, Watson SS, Peltz MA. Characterization of metal powders used for additive manufacturing. J Res Natl Inst Stand Technol 2014;119:460.

[183] Rausch AM, Küng VE, Pobel C, Markl M, Körner C. Predictive Simulation of Process Windows for Powder Bed Fusion Additive Manufacturing: Influence of the Powder Bulk Density. Mater 2017;10. https://doi.org/10.3390/ma10101117.

[184] Yuan L. Solidification Defects in Additive Manufactured Materials. JOM 2019;71:3221–2. https://doi.org/10.1007/s11837-019-03662-x.

[185] Lewandowski J, Seifi M. Metal Additive Manufacturing: A Review of Mechanical Properties. Annu Rev Mater Res 2016;46:151–86. https://doi.org/10.1146/annurev-matsci-070115-032024.

[186] Koutiri I, Pessard E, Peyre P, Amlou O, De Terris T. Influence of SLM process parameters on the surface finish, porosity rate and fatigue behavior of as-built Inconel 625 parts. J Mater Process Technol 2018;255:536–46. https://doi.org/https://doi.org/10.1016/j.jmatprotec.2017.12.043.

[187] AlMangour B, Grzesiak D, Yang J-M. In situ formation of TiC-particle-reinforced stainless steel matrix nanocomposites during ball milling: Feedstock powder preparation for selective laser melting at various energy densities. Powder Technol 2018;326:467–78. https://doi.org/https://doi.org/10.1016/j.powtec.2017.11.064.

[188] da Costa CE, Zapata WC, Parucker ML. Characterization of casting iron powder from recycled swarf. J Mater Process Technol 2003;143–144:138–43. https://doi.org/https://doi.org/10.1016/S0924-0136(03)00394-7.

[189] Yadroitsev I, Gusarov A, Yadroitsava I, Smurov I. Single track formation in selective laser melting of metal powders. J Mater Process Technol 2010;210:1624–31. https://doi.org/https://doi.org/10.1016/j.jmatprotec.2010.05.010.

[190] Calka A, Radlinski AP. Universal high performance ball-milling device and its application for mechanical alloying. Mater Sci Eng A 1991;134:1350–3.

[191] Geissdoerfer M, Savaget P, Bocken NMP, Hultink EJ. The Circular Economy–A new sustainability paradigm? J Clean Prod 2017;143:757–68.

[192] Alibaba. Avimetal Powder Metallurgy Technology Co., Ltd 2020. https://avimetalpm.en.alibaba.com/ (accessed October 21, 2020).

[193] Carpentar Technology n.d. https://www.carpentertechnology.com/ (accessed October 21, 2020).

[194] Unal A. Production of metal powders by gas atomization. Ulus Toz Met Konf Natl Powder Metall Conf 1996:111–57.

[195] Bhushan RK. Impact of nose radius and machining parameters on surface roughness, tool wear and tool life during turning of AA7075/SiC composites for green manufacturing. Mech Adv Mater Mod Process 2020;6:1. https://doi.org/10.1186/s40759-020-00045-7.

[196] Sun J, Wong YS, Rahman M, Wang ZG, Neo KS, Tan CH, et al. EFFECTS OF COOLANT SUPPLY METHODS AND CUTTING CONDITIONS ON TOOL LIFE IN END MILLING TITANIUM ALLOY. Mach Sci Technol 2006;10:355–70. https://doi.org/10.1080/10910340600902181.

[197] Feil A, Pretz T, Julius J, Go N, Bosling M, Johnen K. Chapter 10 - Metal Waste. In: Letcher TM, Vallero DABT-W (Second E, editors., Academic Press; 2019, p. 211–23. https://doi.org/https://doi.org/10.1016/B978-0-12-815060-3.00010-4.

[198] Koyanaka S, Kobayashi K. Automatic sorting of lightweight metal scrap by sensing apparent density and three-dimensional shape. Resour Conserv Recycl 2010;54:571–8. https://doi.org/https://doi.org/10.1016/j.resconrec.2009.10.014.

[199] Mesina MB, Dalmijn WL. Non-ferrous scrap metals using an electromagnetic sensor 2013;12:87–101. https://doi.org/10.1080/1478647031000139079.

[200] Cavanough G, Holtham PN. Rapid characterization of magnetic separator feed stocks in titanium 2014;13:141–52. https://doi.org/10.1080/14786470412331308033.

[201] Kutila M, Viitanen J, Vattulainen A. Scrap Metal Sorting with Colour Vision and Inductive Sensor Array. Int. Conf. Comput. Intell. Model. Control Autom. Int. Conf. Intell. Agents, Web Technol. Internet Commer., vol. 2, 2015, p. 725–9. https://doi.org/10.1109/CIMCA.2005.1631554.

[202] Rem P. Eddy current separation of fine non-ferrous particles from bulk streams 2014;13:15–23. https://doi.org/10.1080/00207390410001710726.

[203] Harun WSW, Kamariah MSIN, Muhamad N, Ghani SAC, Ahmad F, Mohamed Z. A review of powder additive manufacturing processes for metallic biomaterials. Powder Technol 2018;327:128–51. https://doi.org/https://doi.org/10.1016/j.powtec.2017.12.058.

[204] Balachandramurthi AR, Olsson J, Ålgårdh J, Snis A, Moverare J, Pederson R. Microstructure tailoring in Electron Beam Powder Bed Fusion additive manufacturing and its potential consequences. Results Mater 2019;1:100017. https://doi.org/https://doi.org/10.1016/j.rinma.2019.100017.

[205] Yang W, He X, Li H, Dong J, Chen W, Xin H, et al. A tribological investigation of SLM fabricated TC4 titanium alloy with carburization pre-treatment. Ceram Int 2020;46:3043–50. https://doi.org/https://doi.org/10.1016/j.ceramint.2019.10.004.

[206] Periane S, Duchosal A, Vaudreuil S, Chibane H, Morandeau A, Cormier J, et al. Machining influence on the fatigue resistance of Inconel 718 fabricated by Selective Laser Melting (SLM). Procedia Struct Integr 2019;19:415–22. https://doi.org/https://doi.org/10.1016/j.prostr.2019.12.045.

[207] Fox P, Pogson S, Sutcliffe CJ, Jones E. Interface interactions between porous titanium/tantalum coatings, produced by Selective Laser Melting (SLM), on a cobalt–chromium alloy. Surf Coatings Technol 2008;202:5001–7. https://doi.org/https://doi.org/10.1016/j.surfcoat.2008.05.003.

[208] Kale AB, Kim B-K, Kim D-I, Castle EG, Reece M, Choi S-H. An investigation of the corrosion behavior of 316L stainless steel fabricated by SLM and SPS techniques. Mater Charact 2020;163:110204. https://doi.org/https://doi.org/10.1016/j.matchar.2020.110204.

[209] Khomutov M, Potapkin P, Cheverikin V, Petrovskiy P, Travyanov A, Logachev I, et al. Effect of hot isostatic pressing on structure and properties of intermetallic NiAl–Cr–Mo alloy produced by selective laser melting. Intermetallics 2020;120:106766. https://doi.org/https://doi.org/10.1016/j.intermet.2020.106766.

[210] Gao X, Lin X, Yu J, Li Y, Hu Y, Fan W, et al. Selective Laser Melting (SLM) of in-situ beta phase reinforced Ti/Zr-based bulk metallic glass matrix composite. Scr Mater 2019;171:21–5. https://doi.org/https://doi.org/10.1016/j.scriptamat.2019.06.007.

[211] Tezel T, Topal ES, Kovan V. Characterising the wear behaviour of DMLS-manufactured gears under certain operating conditions. Wear 2019;440–441:203106. https://doi.org/https://doi.org/10.1016/j.wear.2019.203106.

[212] Milton S, Duchosal A, Chalon F, Leroy R, Morandeau A. Thermal study during milling of Ti6Al4V produced by Electron Beam Melting (EBM) process. J Manuf Process 2019;38:256–65. https://doi.org/https://doi.org/10.1016/j.jmapro.2018.12.027.

[213] Shu Z, Chen Z, Wang L, Wei X, Li W, Zheng Z. Microstructure evolution and formation mechanism of a crack-free nickel-based superalloy fabricated by laser engineered net shaping. Opt Laser Technol 2020;128:106222. https://doi.org/https://doi.org/10.1016/j.optlastec.2020.106222.

[214] Maconachie T, Leary M, Lozanovski B, Zhang X, Qian M, Faruque O, et al. SLM lattice structures: Properties, performance, applications and challenges. Mater Des 2019;183:108137. https://doi.org/https://doi.org/10.1016/j.matdes.2019.108137.

[215] Fullenwider B, Kiani P, Schoenung JM, Ma K. Two-stage ball milling of recycled machining chips to create an alternative feedstock powder for metal additive manufacturing. Powder Technol 2019;342:562–71. https://doi.org/https://doi.org/10.1016/j.powtec.2018.10.023.

[216] Malỳ M, Höller C, Skalon M, Meier B, Koutnỳ D, Pichler R, et al. Effect of process parameters and high-temperature preheating on residual stress and relative density of Ti6Al4V processed by selective laser melting. Materials (Basel) 2019;16. https://doi.org/10.3390/ma12060930.

[217] Singh S, Chaudhary S, Singh H. Effect of electroplated interlayers on properties of cold-sprayed copper coatings on SS316L steel. Surf Coatings Technol 2019;375:54–65. https://doi.org/https://doi.org/10.1016/j.surfcoat.2019.07.015.

[218] Xu H, Zou N, Li Q. Effect of Ball Milling Time on Microstructure and Hardness of Porous Magnesium/Carbon Nanofiber Composites. JOM 2017;69:1236–43. https://doi.org/10.1007/s11837-017-2361-3.

[219] Naik SN, Walley SM. The Hall–Petch and inverse Hall–Petch relations and the hardness of nanocrystalline metals. J Mater Sci 2020;55:2661–81. https://doi.org/10.1007/s10853-019-04160-w.

[220] Donachie MJ. Titanium: a technical guide. ASM international; 2000.

[221] Oh J-M, Lee B-G, Cho S-W, Lee S-W, Choi G-S, Lim J-W. Oxygen effects on the mechanical properties and lattice strain of Ti and Ti-6Al-4V. Met Mater Int 2011;17:733–6. https://doi.org/10.1007/s12540-011-1006-2.

[222] Velasco-Castro M, Hernández-Nava E, Figueroa IA, Todd I, Goodall R. The effect of oxygen pickup during selective laser melting on the microstructure and mechanical properties of Ti–6Al–4V lattices. Heliyon 2019;5. https://doi.org/10.1016/j.heliyon.2019.e02813.

[223] Murr LE, Esquivel E V., Quinones SA, Gaytan SM, Lopez MI, Martinez EY, et al. Microstructures and mechanical properties of electron beam-rapid manufactured Ti-6Al-4V biomedical prototypes compared to wrought Ti-6Al-4V. Mater Charact 2009;60:96–105. https://doi.org/10.1016/j.matchar.2008.07.006.

[224] Konečná R, Medvecká D, Nicoletto G. Structure, Texture and Tensile Properties of Ti6Al4V Produced by Selective Laser Melting. Prod Eng Arch 2019;25:60–5. https://doi.org/10.30657/pea.2019.25.12.

[225] Carr RL. EVALUATING FLOW PROPERTIES OF SOLIDS. Chem Eng 1965;72:163–8.

[226] Townsend A, Senin N, Blunt L, Leach RK, Taylor JS. Surface texture metrology for metal additive manufacturing: a review. Precis Eng 2016;46:34–47. https://doi.org/https://doi.org/10.1016/j.precisioneng.2016.06.001.

[227] Shrestha S, Chou K. Single track scanning experiment in laser powder bed fusion process. Procedia Manuf 2018;26:857–64. https://doi.org/10.1016/j.promfg.2018.07.110.

[228] Wang D-Z, Li K-L, Yu C-F, Ma J, Liu W, Shen Z-J. Cracking behavior in additively manufactured pure tungsten. Acta Metall Sin (English Lett 2019;32:127–35.

[229] Gao P, Wang Z, Zeng X. Effect of process parameters on morphology, sectional characteristics and crack sensitivity of Ti-40Al-9V-0.5Y alloy single tracks produced by selective laser melting. Int J Light Mater Manuf 2019;2:355–61. https://doi.org/https://doi.org/10.1016/j.ijlmm.2019.04.001.

[230] Dimian AC, Bildea CS, Kiss AA. Chapter 17 - Sustainability Analysis. In: Dimian AC, Bildea CS, Kiss AABT-CACE, editors. Integr. Des. Simul. Chem. Process., vol. 35, Elsevier; 2014, p. 679–702. https://doi.org/https://doi.org/10.1016/B978-0-444-62700-1.00017-6.

[231] Mittal ML. Estimates of Emissions from Coal Fired Thermal Power Plants in India 2010;39:1–22.

[232] Wilson BP, Lavery NP, Jarvis DJ, Anttila T, Rantanen J, Brown SGR, et al. Life cycle assessment of gas atomised sponge nickel for use in alkaline hydrogen fuel cell applications. J Power Sources 2013;243:242–52. https://doi.org/10.1016/j.jpowsour.2013.05.186.

[233] Norgate TE, Rajakumar V, Trang S. Titanium and other light metals - Technology pathways to sustainable development. Australas Inst Min Metall Publ Ser 2004:105–12.

[234] TU Delft. Indicator systeem ecocost 2020. https://www.ecocostsvalue.com/ (accessed May 8, 2021).

[235] Sharma RK, Sodhi GPS, Bhakar V, Kaur R, Pallakonda S, Sarkar P, et al. Sustainability in manufacturing processes: Finding the environmental impacts of friction stir processing of pure magnesium. CIRP J Manuf Sci Technol 2020;30:25–35. https://doi.org/https://doi.org/10.1016/j.cirpj.2020.03.007.

[236] Ünal A. Production of rapidly solidified aluminium alloy powders by gas atomisation and their applications. Powder Metall 1990;33:53–64. https://doi.org/10.1179/pom.1990.33.1.53.

[237] Pourghahramani P. Effects of grinding variables on structural changes and energy conversion during mechanical activation using Line Profile Analysis (LPA) 2006:163.

[238] Vogtlander J. LCA-based assessment of sustainability: the Eco-costs/Value Ratio EVR. 2010.

[239] Weber HJ. Air pollution problems of the foundry industry. J Air Pollut Control Assoc 1961;11:157–72. https://doi.org/10.1080/00022470.1961.10467985.

[240] Tengzelius J, Ab H, Höganäs S-. Life cycle assessment (LCA) of powder metallurgy Resources. Press Sinter 2000:6.

[241] Mohankumar S, Senthilkumar P. Particulate matter formation and its control methodologies for diesel engine: A comprehensive review. Renew Sustain Energy Rev 2017;80:1227–38. https://doi.org/https://doi.org/10.1016/j.rser.2017.05.133.

[242] Giagnorio M, Amelio A, Grüttner H, Tiraferri A. Environmental impacts of detergents and benefits of their recovery in the laundering industry. J Clean Prod 2017;154:593–601. https://doi.org/https://doi.org/10.1016/j.jclepro.2017.04.012.

[243] Dong YP, Li YL, Zhou SY, Zhou YH, Dargusch MS, Peng HX, et al. Cost-affordable Ti-6Al-4V for additive manufacturing: Powder modification, compositional modulation and laser in-situ alloying. Addit Manuf 2021;37:101699. https://doi.org/https://doi.org/10.1016/j.addma.2020.101699.

[244] Kassym K, Perveen A. Atomization processes of metal powders for 3D printing. Mater Today Proc 2020;26:1727–33. https://doi.org/https://doi.org/10.1016/j.matpr.2020.02.364.

BRIEF BIODATA

Sahil Dhiman
Master of Engineering
Mechanical Engineering (Production)
Department of Mechanical Engineering
Thapar Institute of Engineering and Technology, Patiala-147004, Punjab India
Email:sdhiman_me19@thapar.edu;
sahildhiman943@gmail.com
Date of Birth & Sex: 28 April 1996, Male
Google Scholar: https://rb.gy/bpwsjr
ResearchGate: https://rb.gy/zpu6rs
ORCID: https://orcid.org/0000-0002-4961-0569